UNIVERSITÄT HAMBURG

Insights into the palaeovegetation and palaeoclimate evolution of the New Jersey hinterland (eastern North America) during the Oligocene and Miocene

-a palynological study-

vorgelegt von
Sabine Prader

Dissertation zur Erlangung des Doktorgrades
an der

Fakultät für Mathematik, Informatik und Naturwissenschaften
Fachbereich Geowissenschaften der Universität Hamburg
Hamburg, Januar 2018

Tag der Disputation: 18.04.2018

Folgende Gutachter empfehlen die Annahme der Dissertation:

Dr. Ulrich Kotthoff

Prof. Dr. Gerhard Schmiedl

Zusammenfassung

Das Oligozän und Miozän gehören zu den spannendsten erdgeschichtlichen Zeitepochen sind von starken globalen Klimaschwankungen geprägt, welche ihrerseits erheblichen Einfluss auf Lebensraumveränderungen und Neuorganisationen in der jeweiligen Paläovegetation nahmen. Änderungen in der Paläovegetation während dieser Epochen sind gut bekannt und für verschiedene Regionen in Europa umfassend dokumentiert. Vergleichbare Studien, die sich mit den regionalen paläoökologischen Evolutionsprozessen im Kontext globaler Klimaveränderungen im östlichen Nordamerikanischen Raum befassen, sind hingegen bisher lückenhaft und die zugrunde liegenden Prozesse gelten als unzureichend verstanden.

Im Zuge dieser Dissertationsschrift wurden 206 Sedimentproben, welche im Rahmen der Integrated Ocean Drilling Program (IODP) Expedition (Exp.) 313 vom flachen Schelf von New Jersey (NJSS) gewonnen wurden, auf ihren Pollengehalt hin untersucht.

Das Ziel dieser Arbeit ist es, Einblicke in die Evolution der langzeitlichen Paläovegetation und des Paläoklimas im Hinterland von New Jersey zu gewinnen. Für die Pollenkornanalysen wurde eine Kombination aus Licht- (LM) und Rasterelektronenmikroskopie (REM) herangezogen. Taphonomisch bedingte Transportprozesse wurden über das Verhältnis von Pollenkörnern zu Dinoflagellatenzysten ermittelt. Um Rückschlüsse auf regional bedingte Klimaveränderungen ziehen zu können, wurde eine bioklimatische Analyse angewandt, aus der im Wesentlichen vier Standardparameter (Durchschnittliche Jahrestemperatur und Jahresniederschlag sowie durchschnittliche Temperatur des kältesten sowie des wärmsten Monats) berechnet wurden. Für die Abschätzung, ob Änderungen in den Paläoökosystemen orbital gesteuert worden sind, wurden Spektralanalysen für ein zeitlich hochaufgelöstes kurzes Zeitinterval während des Burdigaliums durchgeführt.

Die vorliegende Arbeit demonstriert, dass es innerhalb der untersuchten oligozänen und miozänen Zeiträume zu kleinen floristischen Veränderungen kam und zeigt, dass das floristische Diversität umfangreicher war als bisher angenommen. Während der gesamten untersuchten Zeitintervalle führte das vorherrschende humid warm-temperierte Klima dazu, dass mesophytische Wälder das Landschaftsbild dominierten. Allerdings reflektiert die mikrofloristische Zusammensetzung eine komplexe topographische Festlandvegetation. Wanderungsprozesse einzelner Paläovegetationseinheiten sind entweder durch globale Klimaereignisse oder durch regionale landschaftliche Veränderungen ausgelöst worden. Außerdem wurden durch Obliquität und Exzentrizität bedingte Modifikationen von Umweltparametern identifiziert, die zu erheblichen Wanderungsbewegungen von Vegetationseinheiten während des Burdigaliums führten.

Zusammenfassend zeigt die vorliegende Dissertation, dass die Paläovegetationen des Hinterlandes von New Jersey mit geringen und signifikanten Verhaltensweisen in Bezug auf dynamisch verändernde Umweltfaktoren reagieren. Diese Studie präsentiert, dass nicht nur der Einsatz des REM für die Bestimmbarkeit von fossilen Pollenkornmaterial unverzichtbar ist, sondern auch, dass die Analyse hochauflösender Sedimentproben eine besondere Wichtigkeit hat, um die evolutionäre Entwicklung von Ökosystemen und die dabei zugrundeliegenden Prozesse nachvollziehen zu können.

Abstract

The vegetation of the Oligocene and Miocene witnessed shifts and reorganisations responding to changes in global and regional climate. While these palaeovegetation shifts are well examined for Europe and various other regions, the regional terrestrial ecosystem evolution of eastern North America and its relation to climate changes is only poorly understood.

In the framework of the present thesis 206 sediment core samples from the Integrated Ocean Drilling Program (IODP) Expedition (Exp.) 313 to the New Jersey shallow shelf (NJSS) were studied. The aim was to reconstruct the long-term palaeovegetation and palaeoclimate evolution in the New Jersey hinterland. Pollen grain analyses were performed using a combination of light microscopy (LM) and scanning electron microscopy (SEM).

Transport-caused bias was identified via analysis of the terrestrial/marine palynomorph ratio. In order to infer regional climate changes, four standard climatic parameters (mean annual temperature, mean annual precipitation, and mean annual temperature of the coldest month and warmest month) were calculated using the bioclimatic analysis approach. Spectral analysis was performed to identify orbital-driven alternations within the palaeovegetation units during a short time interval of the Burdigalian. The present thesis demonstrates that small changes in the floristic composition occurred during the Oligocene and Miocene and that the floristic composition in hinterland was more divers than previously thought. Throughout the entire analysed time intervals, the mesophytic forest was the most widespread palaeovegetation unit in the hinterland, flourishing under a generally humid and warm-temperate climate. However, the microfloristic assemblages reflect a complex vertical onshore vegetation. Possible topographic palaeovegetation movements are either regulated by global climate events or by regional landscape changes. In addition, strong orbital signatures of obliquity and eccentricity drove palaeoenvironmental changes, leading to associated vegetation responses in the New Jersey hinterland. In conclusion, the palaeovegetation shows small but characteristic modes of responses in respect to the climatic and environmental dynamics. This study shows that both high-resolution pollen grain identification via SEM and high temporal resolution are important for the understanding of evolutionary processes that control the interaction between biotic an abiotic environments.

Table of Contents

General Introduction

This present thesis deals with fossil pollen grains originating from the hinterland of the middle Atlantic east coast of North America to infer terrestrial ecosystem evolution during selected time intervals of the Oligocene and Miocene. The aim of the present thesis is to give new insights into the response of the vegetation to climate changes in the New Jersey hinterland through the selected time intervals.

1.2 Plant fossils and their relationship with and contribution to ecosystem reconstructions

Land plants are almost immobile and their distribution is strongly connected to certain soil types, water availability and temperature, which in turn are often dependent on the climatic conditions under which they are developing (Prentice et al., 1992). Thus, fossil plant remains provide a powerful tool for inferring terrestrial palaeoecosystems. The almost ubiquitous occurrence of pollen and spores (Frasen et al., 2012) makes them one of the best plant proxies for reconstructing the spatiotemporal distribution of environmental variation at local, regional or global scale (Huntley and Webb, 1989; Pross and Klotz, 2002).
Pollen grains represent the highly reduced (two or three cells) male gametophyte of seed plants (Hesse et al., 2009). They are able to persist stressful situations during dispersal (Hesse et al., 2009). The outer pollen wall (sporoderm) is mainly composed of sporopollenin, one of the most recalcitrant biomacromolecules (Alexander, 1973; Fraser et al., 2012). Its intrinsic resistance makes sporopollenin one of the most important organic components in sedimentary records (Zonneveld et al., 2010) and allows pollen and spores to be nearly omnipresent in the fossil record (Fraser et al., 2012). The characteristic morphological features of the pollen wall such as the shape and size, the number of apertures and their position, and particularly their enormously variable pollen wall ornamentation (sculpture) and stratification (structure: Fig. 1.1) provide the basics characters in the comparative pollen morphology and are, in addition, important in plant systematics (Hesse et al., 2009; Hesse and Blackmore, 2013).

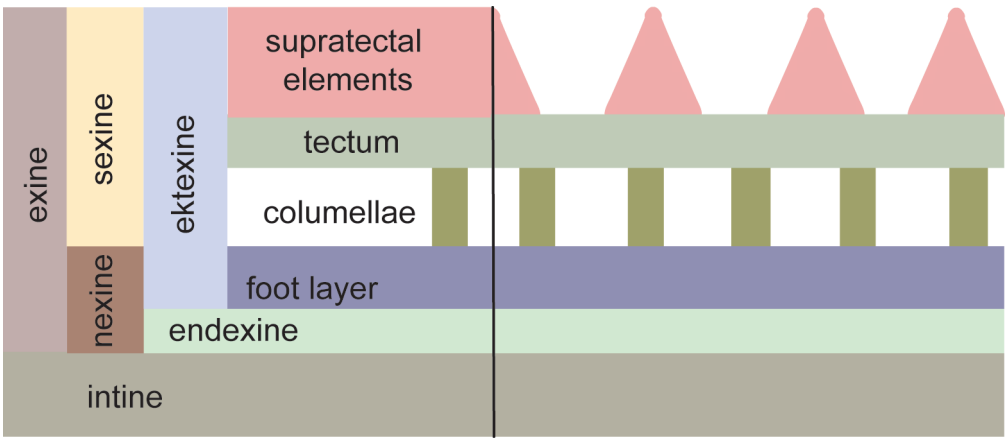

Figure 1.1 General pollen wall structure, exine consists mainly of sporopollenin (modified after Hesse et al., 2009).

For an understanding of the evolution of the landscape in the past, information about modern requirements of taxa, their morphology and physiology are of importance (Chaloner and Creber, 1990; Boyce and Jung-Eun, 2017). One of the most commonly used method for inferring ancient terrestrial climates is based on the assumption that requirements of fossil plant taxa are presumably similar to those of their nearest living relatives (NLR-method: Chaloner and Creber, 1990; Spicer, 1990) or potential modern analogues (Denk et al., 2013). The climatic interval, which is formed via the overlap of a maximum of climatic signatures of identified taxa, can be considered as the best possible palaeoclimatic description under which the fossil flora probably flourished (Mosbrugger and Utescher, 1997; Greenwood et al., 2003, 2005; Utescher et al., 2014).

1.3 Overview of the global climatic conditions during the Cenozoic

The Cenozoic climate (Fig. 2.4) is a dynamic system of alternating short- and long-term cooler and warmer time intervals (Mudelsee et al., 2014; Zachos et al., 2001a). The increases and decreases of global temperatures drive strong and weak turnovers in marine (Lourens et al., 2005) and terrestrial (Huntly and Webb, 1989; van Dam et al., 2006) ecosystems. In the first order, however, the Cenozoic climate evolution reflects an overall long-term cooling trend from the late Eocene (Zachos et al., 2001a; Mudelsee et al., 2014).

During the early Cenozoic (Palaeocene and Eocene), extraordinary high concentrations of greenhouse gases in the atmosphere already contributed to much warmer global temperatures (Lourens et al., 2005; Zachos et al., 2008) than today. But short intervals of extreme carbon injection, referred to as hyperthermals (Zachos et al., 2008) like the Palaeocene-Eocene thermal maximum (PETM), pushed global conditions into particularly extreme warm phases (Zachos et al., 2001a; Lourens et al., 2005; Zachos et al., 2008). Since the last hyperthermal event, the Early Eocene Climatic Optimum (EECO at ~51 to 53 Ma: Zachos et al., 2001a; 2008; Wright et al., 1992, Mudelsee et al., 2014) of the early Cenozoic, global temperatures gradually declined, terminating at 33.7 Ma into a large cooling event at the Eocene-Oligocene boundary (Miller et al., 1998; Zachos et al., 2001a; Coxall et al., 2005). Antarctica became glaciated for the first time in the Cenozoic history as indicated by the first major oxygen isotopic event (increased values of $\delta^{18}O$ in foraminifers; Miller et al., 1998; Zachos et al., 2001a; Coxall et al., 2005). Climate variability marked the entire Oligocene epoch (~33.7 to 23 Ma: Pälike et al., 2006; Chapter 4). During this time, a series of global cooling led to unipolar glacial periods, which in turn produced sea-level falls (Miller et al., 1991; Pekar et al., 2002; Wade and Pälike, 2004; Pälike et al., 2006; Pekar et al., 2006).

The Mi-1 event (Miocene isotope event) at 23.03 Ma (Liebrand et al., 2011) terminated the Oligocene, and in the following seven Mi events characterized the entire Miocene epoch (Miller et al., 1991). During these events, climatic oscillations pushed the retreat and expansion of Antarctic ice sheets at different magnitudes (Zachos et al., 2001a; Mudelsee et al., 2014). Between ~17 to ~14.5 Ma, a global warming trend in Earth's climate culminated into the Mid-Miocene Climatic Optimum (MMCO; Flower and Kennet, 1994; Zachos et al., 2001a; 2008; Shevenell et al., 2004, 2008; Mudelsee et al., 2014: Chapter 3). This warm period coincides with the "Monterey" carbon isotope excursion, a period of strong marine carbonate dissolution as indicated by decreased values of $\delta^{13}C$ in foraminifers (Holbourn et al., 2015). Subsequently, a global gradual cooling phase began (Wright et al., 1992; Flower and Kennett, 1994; Zachos et

al., 2001a; Shevenell et al., 2004; Abels et al., 2005; Zachos et al., 2008), resulting in bipolar ice caps (Moran et al., 2006).

1.4 Vegetation and climatic evolution along the middle Atlantic coastal plain of North America during the Cenozoic

At present the hinterland of the Mid-Atlantic coast of North America is considered to be a warm-temperate region with moderate winters, mild summers and with no consistent dry phases (Box, 2015; Fig. 1.2). The threshold value of absolute minima winter temperatures at about -15°C (Woodward, 1990) prevents evergreen broad-leaved forest from dominating the Mid-Atlantic coast (Woodward, 1990). The climax community under these climatic circumstances

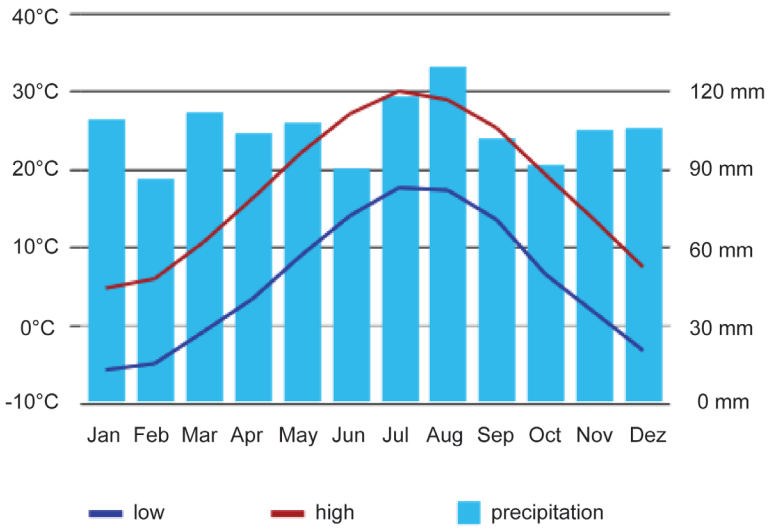

Figure 1.2 Climate graph for a modern New Jersey area (Toms River) showing a temperate Climate with precipitation through the year. Average temperatue 11.7°C; annual high temperature: 17.7°C; annual low temperature 5.7°C; average annual 1239mm (after US Climate Data, 2018)

is a deciduous broad-leaved forest mainly dominated by *Quercus*, *Fagus*, *Liquidambar* or *Nyssa* (Box, 2015; Fig. 1.3).

During the Cenozoic the vegetation of North America underwent significant modifications in response to reformations of the continent and global climatic variations (Wing, 1998). However, main information about Cenozoic terrestrial ecosystems derives from floristic assemblages of western and the interior of North America, and from the higher latitudes (Wing, 1998, Graham, 1999). There are just a few palaeobotanical reconstructions of eastern North America ecosystem evolution available, due to a very poor fossil record, and the existing palaeobotanical records are only fragmentary (Wing, 1998; Graham, 1999).

Information about the Oligocene epoch concerning the Mid-Atlantic coast is very rare. The existing information (e.g., in the marine Piney Point Formation; New Jersey coastal plain) suggest that the landscape during the Oligocene was already occupied by a warm-temperate flora (Owens et al., 1988). This includes common taxa, which are already distributed in the Cenozoic in the Northern Hemisphere, of which Owens et al. (1988) mentioned *Nyssa*, *Ulmus*,

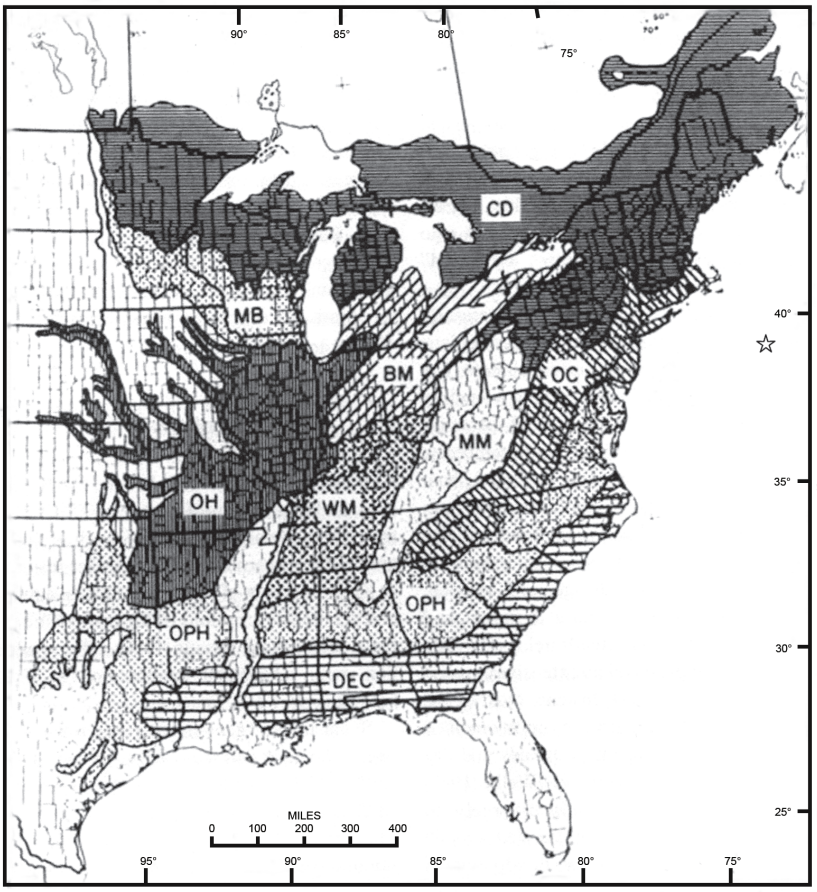

Figure 1.3 Modern forest types growing in eastern North America. Except of Conifer-Deciduous Forest (CD) and Deciduous-Evergreen-Conifer Forest (DEC), all types represent deciduous forests. Appalachian Oak-Chestnut Forest (OC): at higher elevation, *Quercus* and *Castanea* dominated; Mixed Mesophytic Forest (MM): high diversity, without dominant species; Western Mesophytic forest (WM): *Quercus* dominated plus other species; Beech-Maple Forest (BM): *Fagus grandifolia*, *Acer saccharum*; Maple-Basswood Forest (MB) *Acer saccharum*, *Tilia* spp.; Oak-Hickory Forest (OH) *Quercus* spp., *Carya* spp.; Oak-Hickory-Pine Forest (OPH): *Pinus* successional. After Box,(2015); taken from Braun (1950) modified by Greller (1988). Star: location of IODP Site M0027.

Tilia, *Carya*, *Castanea*-type, Taxodiaceae-type, *Podocarpus*, *Pinus*, *Momipites* (form-genus of *Engelhardia-Alfaroa*), Sapotaceae and Ericales. The increased input of *Quercus* and *Quercus*-like pollen grains together with the general influence of temperate taxa in the microfloristic assemblage, was probably the result of the Eocene-Oligocene climate cooling in the southern North American region (Owens et al., 1988; Oboh and Reeves Morris, 1994; Oboh, et al., 1996). A similar floristic and vegetation arrangement and accordant climate changes are reported from South Carolina and the eastern Gulf coast (Frederiksen, 1991b).

Miocene micro- and macro-plant fossil-bearing sediments along the east coast of North America are also rare and often cover only short time intervals (e.g., Rachele, 1976; Greller and Rachele, 1984; Frederiksen, 1984; Owens et al., 1988; Groot, 1991, 1992; Traverse, 1994; Pazzaglia et al., 1997; Ochoa et al., 2012; McCartan et al., 1990; Tiffney, 1994). The floristic assemblages were largely dominated by *Quercus* (e.g., Owens et al., 1988; Pazzaglia et al., 1997; Ochoa et al., 2012; Groot, 1991, 1992). In addition, all floras share a broad mixture of plant elements that were

typical for the Northern Hemisphere during that time interval. The assemblages were mainly represented by deciduous broad-leaved trees such as *Pterocarya*, *Liquidambar*, *Symplocos*, *Fagus*, *Carya*, *Engelhardia*-type, *Quercus*, *Alangium*, *Ulmus*, and *Zelkova* (Brandywine deposit, Maryland: McCartan et al., 1990), which flourished under warm-temperate (e.g., McCartan et al., 1990) to subtropical climatic conditions (Groot et al., 1991, Pazzaglia et al., 1997).

Plant-based interpretations of climate warming or cooling during the Cenozoic were mostly determined by the presence or absence of taxa. Taxa like *Engelhardia*, *Sciadopitys*, *Cyrilla*, *Taxodium* (Groot et al., 1991), *Podocarpus* or *Cyathea* (Greller and Rachele, 1984), acted as good climatic indicators (Groot et al., 1991). The subtropical climatic character within the floristic assemblages is therefore suggested by the occurrence of single "exotic" elements such as *Symplocos*, *Gordonia*, *Cyrilla*, *Engelhardia*, as present in the Bryn Mawr Formation, Maryland (Pazzaglia et al., 1997; Groot et al., 1991), or *Sciadopitys* (Groot et al., 1991). Winter temperatures were probably higher than at present (Legler Lignite: Cohansey Formation, New Jersey; Rachele et al., 1976). However, cooler environmental condition presumably occurred as well and are explained by findings of *Tsuga*, *Pinus* or *Picea* pollen grains (Pazzaglia et al., 1997), or by the loss of *Podocarpus* or *Cyathea* (Greller and Rachele, 1984). In addition, the occurrence of genera like *Tsuga*, *Pinus* or *Picea* were interpreted as an altitudinal shallow climatic gradient (Groot, 1991).

All palaeobotanical investigations of scarce Cenozoic deposits of eastern North America suffer from imprecise age models. The lack of well-dated and continuous palaeovegetation records make the regional floristic variabilities incomplete. In addition, inferring vegetation respond to Cenozoic climatic key intervals and to bring them into a global context is difficult.

1.5 The New Jersey margin and the IODP Exp. 313

The New Jersey margin (Fig. 1.4) is a perfect location for studying the history of global sea level change ("The New Jersey Sea-level Transect" after Miller and Mountain, 1994) from the late Cretaceous to the Holocene for various reasons: (1) The rate of rapid sedimentation is important for a suitable temporal resolution, (2) the area is tectonically stable and thus factors like thermal subsidence or isostatic compensation which influence eustatic changes are minimized, (3) very well-preserved cosmopolitan microfossils can contribute to an excellent chronostratigraphy, (4) and clear seismic expressions necessary to identify sequence boundaries and definitive ages are present (Miller and Mountain, 1994).
Since previous drilling campaigns to the New Jersey margin (coastal plain drilling: Ocean Drilling Program: ODP Leg 150X and continental slope drilling: ODP Leg 174X) did not capture the full range of Oligo-Miocene sea level change, the evaluation of amplitudes of extreme sea level variations was insufficient (Miller and Mountain, 1996). IODP Exp. 313 was designed to study the full range of sea level variation during the Oligocene and Miocene (Mountain et al., 2010a). Studies of the full range of sea level variation can best be performed between the palaeo-shoreline and the palaeo-inner-to-middle shelf region, which is the most sensitive region for sea level oscillations (Mountain et al., 2010a). Three IODP Exp. 313 boreholes (M0027A, M0028A, M0029A) were drilled between April 30th and July 17th 2009 in a transect in this sensitive setting (Expedition Scientists, 2010a), and from the three boreholes continuous sediment cores were successfully retrieved using an ECORD "mission-specific" jack-up platform (Fig.1.5; Expedition Scientists, 2010a).

Figure 1.5 ECORD "mission-specific" jack-up platform (after Mountain et al., 2010a).

In this thesis, palynomorph analyses are based on core sediments from Site M0027. Site M0027 is the most landward direct site and was drilled into the New Jersey shallow shelf (Fig. 1.4) at 39°38.046'N and 73°37.301'W at 33.5 m water depth and a site-shoreline distance of 45 km (Expedition Scientists, 2010b). In total 547 m of sediment was recovered, with a total penetration of 613 meter below seafloor (mbsf; Expedition Scientists, 2010b). Site M0027 was selected to minimize taphonomic transport effects, which increase farther offshore and especially behind the shelf break (Heusser, 1983; Mudie and McCarthy, 1994; Montade et al., 2011, Chapters 2, 3).

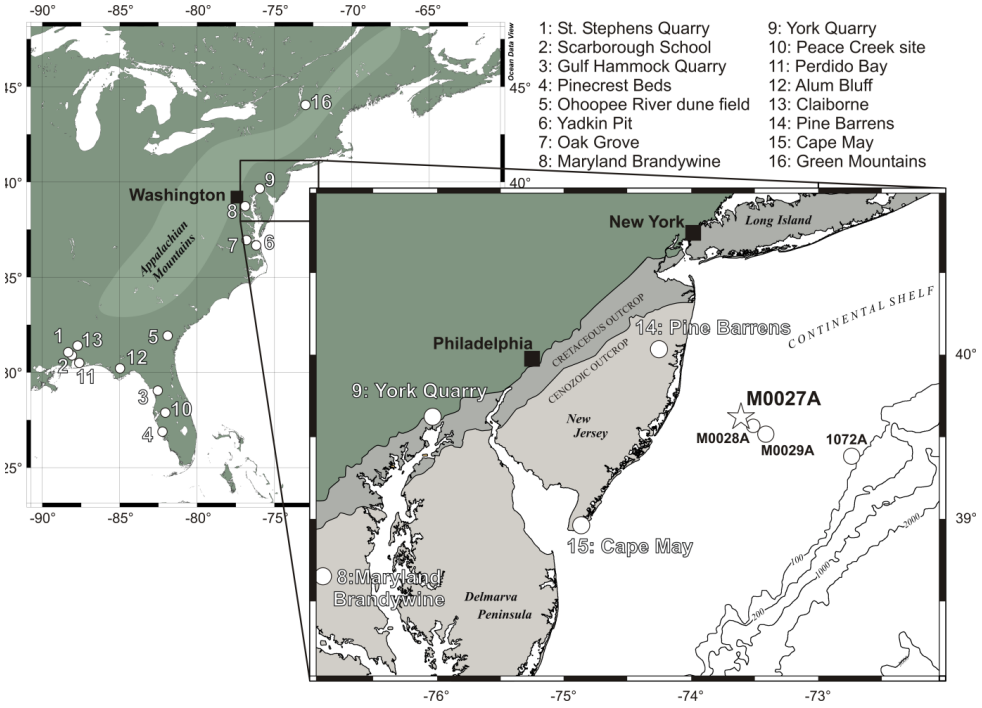

Figure 1.4 Map of eastern North America with a zoom into the area around New Jersey. White star indicates the position of Site M0027 (after Mountain et al., 2010; Schlitzer, 2011). Black squares mark the position of major cities.
White points indicate plant macrofossil outcrops, pollen profiles, and drilling sites referred to (1: Oboh et al., 1996; 2, 10, 11: e.g., Stults et al., 2010; 3, 8, 12: e.g., Jarzen et al. 2010; 4: Hansen et al., 2001; Jarzen and Dilcher, 2006; 5: Rich et al., 2002, 6: Groot, 1991; 7: Frederiksen, 1991a; 9: Pazzaglia et al., 1997; 13, 14, 15: e.g., Rachele 1976; 16: Traverse, 1994).

1.6 Aim and outline of the thesis

The overall aim of the this thesis is to shed light on the vegetation and climatic evolution in the hinterland of the middle Atlantic east coast of North America during the Oligocene and Miocene. In order to investigate the regional ecosystem evolution of eastern North America and to evaluate the relation to global climatic conditions, terrestrial palynomorphs of core sediments of Integrated Ocean Drilling Program (IODP) Expedition (Exp.) 313 to the New Jersey shallow shelf (NJSS) were studied. The excellent chronostratigraphic control and satisfactorily preserved microflora make the examination of IODP core sediments ideal for studying long-term ecosystem development in a research area, which is generally characterized by poor Palaeogene and Neogene continental records.

This thesis comprises relatively high temporal resolution (up to 65 samples per 300 000 yrs) pollen grain analyses of light (LM) and scanning electron microscopy (SEM) to gain a better understanding of regional floristic, vegetation and climatic evolution and their dynamic behaviour through geological time scales.

The second chapter gives an overview of the ecosystem development in the hinterland of the North American Atlantic coastal plain during the late Eocene to the middle Miocene and compares pollen-based palaeoclimatic estimates for the research region with globally occurring Cenozoic climatic events. It is based on a pilot study comprising 61 samples for the interval from 33 to 13 million years ago (Kotthoff et al., 2014). The subsequent chapters of this thesis (chapter 3, 4, and 5) are follow-up studies in much higher temporal resolution and focus on selected and characteristic climatic time intervals of the Cenozoic.

The third chapter focuses on the controversial pattern of regional terrestrial environmental conditions in terms of global palaeoclimatic reversal during the Miocene. The selected time interval comprises the Middle Miocene Climatic Optimum (MMCO) between ~17 and ~14.5 Ma (Flower and Kennet, 1994; Zachos et al., 2001a; 2008; Shevenell et al., 2004, 2008; Mudelsee et al., 2014), and the transition to global cooler conditions during the Mid-Miocene Climatic Transition (MMCT) between ~14.2 Ma and ~13.8 Ma (Flower and Kennet, 1994; Shevenell et al., 2008). It seems that the climatic conditions in the New Jersey hinterland are not in accordance with the drastic cooling observed in Europe (Mosbrugger et al., 2005; Donders et al., 2009). In Chapter 2 (Kotthoff et al., 2014) a diluted climatic impact of the global climatic turnover in the terrestrial ecosystem is suggested and several aspects which might have led to the indistinct pattern of global cooling in the New Jersey hinterland are discussed, however without clear conclusions. According to this, terrestrial palynomorphs of core sediments were reinvestigated in a considerable higher temporal resolution. Specifically, the following questions were assessed: (1) How did the vegetation and climate change in the hinterland of the NJSS during and after the MMCO? (2) Have regional factors such as topographic changes due to several uplift phases of the Appalachian mountain chain (Liu, 2014) weakened the global impact of climate change in the hinterland? (3) What kind of topographic and stratified forest composition is reflected in the palynological signature? (4) How different/similar was the hinterland of the NJSS in respect to other Miocene formations of the Northern Hemisphere?
The fourth chapter of the present thesis focuses on the terrestrial response to climatic

oscillations of the middle Oligocene to early Miocene. This time interval is marked by a series of unipolar glaciation periods (Pekar et al., 2002; Wade and Pälike, 2004; Pälike et al., 2006; Pekar et al, 2006). The climatic oscillations of that time contributed to a renewal of the North American (Graham, 1999) and other floras (e.g. Indonesia: Lelono and Morley, 2011). However, climate models suggest more constant climatic conditions for the Atlantic east coast during the Oligocene (von der Heydt and Dijkstra, 2006), implying a restricted vegetation renewal for the hinterland. In this context, the aim was (1) to infer possible long-term temporal and altitudinal spatial vegetation movement in the New Jersey hinterland. Furthermore, SEM was intensively used to gather higher specific pollen grain identification (2) to gain possible higher taxonomic information within the genus *Quercus*, as well as (3) to detect extinct lineages of the Fagaceae, which are reported from Europe (e.g. Denk et al., 2012). In addition, the chapter contrasts the spatiotemporal distribution of mesic taxa in the New Jersey hinterland during the Oligocene compared to the late Mid-Miocene.

The fifth chapter deals with the dynamic influence of orbital parameters on the biotic response to periodical environmental changes in the New Jersey hinterland during the middle early Burdigalian (18.0–17.7 Ma.). Changes in Earth's orbital parameters (eccentricity, obliquity and precession) lead to variation of the incoming solar budget, thus influencing regional and global climate conditions through the geological time scale (e.g. Kerr, 1978). Earth's orbital parameters during the early Miocene glacial phases corresponded to long-term (400 ka) and short-term (100 ka) eccentricity minima coupled to modulations of long-term (1.2 ka) obliquity maxima (Zachos et al, 2001b, Abels et al., 2005; Pälike et al., 2006; Holbourn et al., 2007; Liebrand et al., 2011; 2016; 2017). The investigated high-resolution pollen dataset allows the identification of vegetation changes coupled to orbital parameters. Research questions discussed in this chapter are: (1) Are there any palaeovegetation units corresponding to orbital parameters? (2) If so, what kind of ecological parameters are involved in the cyclic response of the vegetation?

Chapter 6 concludes the results of this thesis and highlights the most significant floristic, vegetative and climatic information for the New Jersey hinterland.

1.7 Outline of author contribution and assistant acknowledgements

We thank the entire IODP Expedition 313 Scientific Party and the IODP Core repository Bremen. We acknowledge the German Science Foundation (DFG), which supported the researches.

Chapter 2 based on:
Kotthoff, U., Greenwood, D.R., McCarthy, F.M.G., Müller-Navarra, K., Prader, S., Hesselbo, S.P., 2014. **Late Eocene to middle Miocene (33 to 13 million years ago) vegetation and climate development on the North American Atlantic Coastal Plain (IODP Expedition 313, Site M0027).** Climate of the Past 10, 1523–1539.

Author contribution: U.K. wrote the MS with substantial contributions of all authors. S.P. particularly contributed to sections concerning botanical aspects.
Acknowledgements: We thank M. Drljepan, R. Zanatta, V. Menke, K. Reichel, and S. Namyslo for their assistance with preparing and processing the samples, and during photographing. Discussions with C. Bjerrum, J. Browning, T. Donders, K. Dybkjær, L. Fang, M. Katz, K. Miller and P. Sugarman are gratefully acknowledged. Input from anonymous reviewers was very much appreciated and contributed to a significant condensing of the manuscript.

Chapter 3 based on:
Prader, S., Kotthoff, U., McCarthy, F.M.G., Schmiedl, G., Donders, T.H., Greenwood, D.R., 2017. **Vegetation and climate development of the New Jersey hinterland during the late middle Miocene (IODP Expedition 313 Site M0027).** Palaeogeography, Palaeoclimatology, Palaeoecology 485, 854–868.

Author contributions: S.P. wrote the MS with substantial contributions of U.K. and also of all other authors. S.P. counted and analysed data with support of T.D. (pollen identification), G.S. (statistical analyses) and D.R.G. (bioclimatic analyses).
Acknowledgements: We acknowledge A. Krueger, Palynology Lab at Brock University, and K.A. Harps, S. Angenendt and E. Czymoch, University of Hamburg, for sample processing and M. Theodor for support at the SEM. For pollen grain discussion we thank R. Zetter, M. Weber, and S. Ulrich, University of Vienna. SP thanks C. Schirarend of the Botanical Garden, University of Hamburg, for permission of collecting reference material, M. Head, Brock University, for advice dealing with dinoflagellate cysts, and U. Riller, University of Hamburg, for information on North American structural geology. We thank the anonymous reviewers for comments and suggestions, which improved the manuscript.

Chapter 4 based on:
Prader, S., Kotthoff, U., McCarthy, F.M.G., Schmiedl, G., Donders, T.H., Greenwood, D.R., 2018. **Plants in movement – Floristic and climatic characterization of the New Jersey hinterland during the Palaeogene-Neogene transition in relation to major glaciation events.** Biogeosciences Discussion. doi.org/10.5194/bg-2017-511.

Author contributions: S.P. wrote the MS with substantial contributions of U.K. and further contributions of all other authors. S.P. counted and analysed data with support of

T.D. (pollen identification), G.S. (statistical analyses) and D.R.G. (bioclimatic analyses).
Acknowledgements: We acknowledge A. Krueger, Palynology Lab at Brock University; E. Czymoch and K.A. Harps, University of Hamburg, for sample processing and Y. Milker, M. Theodor and R. Walter, for support at the SEM and J. Reolid for sea level oscillations discussion.

Chapter 5 based on:
Prader, S., Kotthoff, U., Bunzel, D., Milk, Y., McCarthy, F.M.G., Schmiedl, G., Donders, T.H., Greenwood, D.R., xxx. **Orbitally-driven palaeovegetation changes in the New Jersey hinterland during a short time interval (300.000 yrs) of the Burdigalian.** In preparation for submission.

Author contributions: S.P. is writing the MS with substantial contributions of all authors. S.P. counted and analysed data with support of T.D. (pollen identification), G.S. and Y.M. (statistical analyses) and D.R.G. (bioclimatic analyses). Spectral analyses were performed by D.B.
Acknowledgements: We acknowledge A. Krueger, Palynology Lab at Brock University; E. Czymoch and D. Kiesel, University of Hamburg, for sample processing and Y. Milker, M. Theodor and R. Walter for support at the SEM and J. Reolid for help with the interpretation of sedimentological processes.

Late Eocene to middle Miocene (33 to 13 million years ago) vegetation and climate development on the North American Atlantic Coastal Plain (IODP Expedition 313, Site M0027)

2.1 Introduction

The Eocene to Miocene witnessed the transition from warmer "greenhouse" to colder "icehouse" conditions (Zachos et al., 2001a, 2008) and a decreasing global sea level (e.g., Miller et al., 2005). These changes did not occur gradually or continuously, but with several reversals to warmer conditions, as well as short phases of rapid cooling (e.g., Zachos et al., 2001a; DeConto et al., 2008). These changes and their driving factors are mainly understood from marine climate records, while examinations integrating terrestrial proxies remain rare (e.g., Eldrett et al., 2009, 2014; Pross et al., 2012). This is particularly the case for eastern North America, whereas several integrated studies for Eurasia have been published during the last two decades (e.g., Mosbrugger et al., 2005; Jiménez-Moreno et al., 2005, 2007; Larsson et al., 2011; Quaijtaal et al., 2014).

The transition from the late Eocene to the Oligocene is characterized by a rapid global cooling (the "Oi-1 event") and the onset of large-scale Antarctic ice sheet growth, as indicated by $\delta^{18}O$ increases in marine sediments from different localities (e.g., Shackleton and Kennet, 1975, Miller et al., 1987; Liu et al., 2009). For the terrestrial realm, there are few and contradictory results: some terrestrial records show almost no climatic changes (Grimes et al., 2005) and only weak faunal reactions (Prothero and Heaton, 1996) during the transition, while others imply increased aridity, cooling (Zanazzi et al., 2007) and increased seasonality (Eldrett at al., 2009). The distribution of global vegetation changed significantly during the early Oligocene, with retreat of the tropical and paratropical biomes to the lower latitudes and an equatorward expansion of temperate vegetation (e.g., Wolfe, 1992, Leopold et al., 1992, Janis, 1993, Willis and McElwain, 2002). In the Northern Hemisphere, including North America, broad-leaved forests declined, and conifer forests migrated southwards (Janis, 1993). Several Oligocene short-term sea-level and climate fluctuations, sometimes called Oi events (e.g., Miller et al., 1991; Wade and Pälike, 2004) were probably tied to the orbital cycles, as shown by, e.g., Coxall et al. (2005), Wade and Pälike (2004), and Pälike et al. (2006). The late Oligocene was a time of global warming and retreat of ice sheets in Antarctica (Zachos et al., 2001a, 2008).

The transition to the Miocene was characterized by a strong cooling pulse, the Mi-1 event (Miller et al., 1987, 1991; Wright and Miller, 1992; Zachos et al., 2001b). Subsequently, starting at ~20 million years before present (Ma), global temperatures increased, culminating in the Mid-Miocene Climatic Optimum between ~17 and ~14 Ma (Zachos et al., 2001b). This overall warm interval was, however, interrupted and followed by several centennial-scale cooling events e.g., further Mi-events (Miller et al., 1987, 1991; Pagani et al., 1999) associated with growth of the Antarctic ice sheet, which also influenced the North Atlantic realm (e.g., Miller et al., 1991; Quaijtaal et al., 2014) and caused relative sea-level changes of e.g. ~60 m in the New Jersey shelf area (Miller et al., 2011). Furthermore, the early Miocene witnessed the spread of biomes dominated by grasses (Poaceae; Jacobs et al., 1999; Willis and McElwain, 2002; Strömberg, 2005). This spread and the loss of forest cover during the Miocene may have weakened the

biotic weathering feedback (Taylor et al., 2009) and thus contributed to the climate development from the Miocene until today (Pagani et al., 2009).
The Mid-Miocene Climatic Optimum was followed by a gradual cooling and ice sheet expansion during the late Miocene, while atmospheric CO_2 remained relatively stable compared to Eocene to early Miocene oscillations (Pagani et al., 2005). This cooling trend and increasing seasonality is generally reflected in pollen records from fluvial deposits from the middle Atlantic margin (Pazzaglia et al., 1997), but these records could only be correlated roughly with marine records. Pollen-based results for the same region presented by Groot (1991) are somewhat contradictory, indicating stable climate conditions at the close of the Miocene. However, the records described by Groot (1991) lack consistent age models and can thus not be compared directly with other climate archives.
In short, there remains a lack of studies that integrate changes in the marine realm (e.g., sea-surface water temperatures and sea-level changes) with vegetation and climate developments in the terrestrial realm during the Eocene, Oligocene and Miocene. The impact of cooling events like the Oi-1- and the Mi-1 events or of the Mid-Miocene-Climatic-Optimum on vegetation and regional climate in eastern North America has not yet been assessed.

An ideal approach for studies integrating marine and terrestrial ecosystem and climate changes is the examination of terrestrial and marine palynomorphs in long marine cores (e.g., Heusser and Shackleton, 1979; Eldrett et al., 2009, 2014; Pross et al., 2012, Contreras et al., 2013). Methods have been developed to calculate quantitative climate data (e.g., temperature, precipitation, and seasonality) from pollen assemblages. One of these methods is the "nearest-living-relative" ("NLR")/"co-existence" or "mutual climate range" method (e.g., Mosbrugger and Utescher, 1997; Pross et al., 2000; Thompson et al., 2012; Reichgelt et al., 2013; Eldrett et al., 2014): climatic limits of fossil plant taxa are assumed to be similar to those of their nearest living relatives. Therefore, the intervals of climate parameters for a given fossil flora, in which a maximal number of nearest relatives can coexist, can be considered the best possible description of the palaeoclimate under which the fossil flora lived (Thompson et al., 2012). The relative abundances of the analysed taxa are not considered in the NLR method – only their presence and absence. This makes the climate reconstructions less susceptible to transport-related and taphonomic bias. Taphonomic skewing of the palynological record can be used to interpret variations in terrigenous sediment influx into the marine realm, and can be used to reconstruct site-shoreline distances and sea-level fluctuations (e.g., McCarthy and Mudie, 1998; McCarthy et al., 2013), but differential preservation and transport characteristics of pollen taxa can hamper ecosystem- and climate reconstructions, altering the original pollen associations. These taphonomic problems can however be minimized/controlled by a) choosing research areas characterized by high sedimentation rates where oxidation of palynomorphs is less pronounced, either due to lower dissolved oxygen or rapid burial (e.g., Kotthoff et al., 2008a); b) sites sufficiently proximal to the coastline to minimize transportation bias (e.g., Mudie and McCarthy, 1994) and reduce the probability of resedimentation by choosing neritic sites (e.g., McCarthy and Mudie, 1998; Hopkins and McCarthy, 2002; McCarthy et al., 2004); and c) sedimentary settings that have remained tectonically stable.
These criteria have largely been met in the New Jersey shallow shelf area (NJSS; North American east coast, Fig. 1.4; Mountain et al., 2010b). The potential of this region for palaeoclimate research and for sea-level reconstruction has already been shown for records from the coastal

plain and the continental slope (Miller and Sugarman, 1995; Miller et al., 1996). Cores recovered from the NJSS in the framework of IODP Expedition 313 in 2009 (Fig. 1.4, Fig. 2.1) allow study of the palaeovegetation and palaeoclimate development in coastal eastern North America during certain intervals of the Oligocene and particularly the Miocene. In context of IODP Expedition 313 a robust age model was developed based on palaeontological, sedimentological, and geochemical data (Browning et al., 2013; Miller et al., 2013a).

Here, we present a new pollen record from Site M0027 from the New Jersey shelf which covers the interval from ~33 to ~13 Ma. While our record does not allow a continuous overview over this complete timespan, it offers several insights into shorter intervals, including the Oligocene-Miocene transition and the Mid-Miocene Climatic Optimum. With this record, we can reconstruct a longer history of the vegetation and climate development during the Oligocene and Miocene than obtained from previous palynomorph-based examinations for coastal eastern North America.

2.2 Geographical and geological setting

Hole M0027A was drilled into the New Jersey shallow shelf at 39°38.046'N and 73°37.301'W at 33.5 m water depth and a site-shoreline distance of 45 km (Fig. 1.4). Total penetration reached 631 mbsf, with a recovered interval of 547 m. The hole was aimed at sampling a thick early Miocene succession, but relatively thin and incomplete Pleistocene, middle to late Miocene and Oligocene sediments were also recovered (Mountain et al., 2010b). The Oligocene/Miocene sediment record from the New Jersey shallow shelf is characterized by several sedimentary sequences tied to transgression and regression phases (e.g., Mountain et al., 2010b, Browning et al., 2013, Miller et al., 2013a). Ages of these sequences are discussed in section 2.3.1. The succession below 420 mbsf was deposited mainly by mass wasting beyond the shelf break during glacioeustatic lowstands. The succession above 360 mbsf, however, has accumulated on the shelf during during highstands, and thus should not be prone to substantial resedimentation (McCarthy et al., 2013).

The palaeogeographic position of the research area has only slightly changed since the late Eocene. Reconstructions by Scotese et al. (1988) imply that during the Oligocene and Miocene, the region of New Jersey was situated ~2° further south than at present, and reached a position between 39 and 40°N during the Pliocene. Prevailing westerly winds thus transported pollen from the Atlantic Coastal Plain as they do today. These winds also currently push the Gulf Stream offshore, allowing polar surface currents to penetrate between the Gulf Stream and northeastern North America as far south as Cape Hatteras (Csanady and Hamilton, 1988). Although the modern Slope Water appears to have originated only ~1.4 Ma (McCarthy et al., 2000), a low salinity (but warmer) precursor to this water mass appears to have been created by abundant fluvial runoff since the Gulf Stream originated, separating northeastern North America from the warm, saline subtropical gyre, and thus resulting in greater seasonality than in the oceanic realm.

The time of the origin of the Gulf Stream remains hotly debated, but there is evidence of strong current activity on the Blake Plateau as early as the late Palaeocene-early Eocene (Pinet et al., 1981) and it was an intense western boundary current by the latest Miocene, when it experienced its greatest intensification based on deep erosion of the Blake Plateau (Kaneps, 1979). The palaeogeographic reconstructions of Scotese et al. (1988) for 20 Ma suggest that the North and

South Equatorial currents blown by the easterly trade winds would largely have recirculated northward in the Atlantic rather than continuing to the Pacific Ocean via the highly restricted seaway between the Americas, consistent with the sedimentary evidence from the Blake Plateau (Pinet et al., 1981).

The modern annual precipitation in the coastal regions of New Jersey is ~1100 mm, and average annual temperatures are ~12 °C (climate.rutgers.edu/stateclim/) with a warm, moist tropical airstream originating in the Gulf of Mexico producing a warm and humid climate east of the Pacific frontal zone that transports moisture-depleted air past the Rocky Mountains (Bryson and Hare, 1974). Grasslands occupy the semi-arid interior of North America west of this frontal zone, while the oak-pine-hickory forest of Davis and Webb (1975) is found where the Gulf Stream hugs the coastline and oak-pine forests (deciduous forest of Davis and Webb, 1975) are found north of Cape Hatteras, where seasonality is much greater. Tectonic uplift of the Appalachian Highlands during the middle Miocene (e.g., Poag et al., 1989; Pazzaglia and Brandon, 1996; Gallen et al., 2013) increased the altitudinal gradient, promoting the expansion of conifers at higher elevations, as characterises the region today (Delcourt et al., 1984).

2.3 Material and Methods

2.3.1 Age model

We used the age model of Browning et al. (2013) to assign ages to samples from Hole M0027A. The precision of the age model based on integrated microfossil biostratigraphy (dinoflagellate cysts, diatoms, calcareous nannofossils), strontium isotopes, and sequence stratigraphy (Browning et al., 2013; Miller et al., 2013a) varies: for the early Miocene, the potential error is below 0.5 Ma, while for the Oligocene, the potential error is between 0.5 and 1.0 Ma. The uncertainty is particularly high (1 to 1.5 Ma) for the upper sequences (m5 to m1; Fig. 2.1) deposited during the middle Miocene (between ~14 and ~11 Ma). However, Site M0027 yields sediments from the very early Rupelian/late Priabonian (~33.7 to ~32.2 Ma, sequence O1) and continuous records for the late Rupelian (~29.3 to ~28.2 Ma; sequences O3 to O5), the very late Chattian, including the transition to the Aquitanian (~23.5 to ~23 Ma; sequence O6), furthermore the early Burdigalian (~20.9 to ~19.2 Ma, sequences m6 and m5.8), and, with some shorter hiatuses, the late Burdigalian to Serravallian (~18 to ~11.6 Ma; subsequent sequences; Browning et al., 2013; Miller et al., 2013a). The sequences are also shown in Figures 2.1, 2.2, 2.3, and 2.4. Pronounced hiatuses occur during the early Rupelian (32.2 to 29.3 Ma), and most of the Chattian and Aquitanian (28.3 to 22.5 Ma).

Sediments of approximately ~5 cm^3 volume/~8 g dry weight were processed for palynological analysis at Brock University using standard techniques, including treatment with warm, dilute (0,02 %) sodium hexametaphosphate, weak (10 %) HCl and concentrated (40%) HF, and sieving through Nitex mesh to retain the > 15 µm fraction. *Lycopodium* spore tablets were added in order to calculate pollen concentrations (Stockmarr, 1971). Palynomorphs were identified at 400x/500x/1000x magnification using a Zeiss AxioScope.

Sixty-one samples from Site M0027 were analyzed for their palynomorph content. For most samples, between 200 and 300 nonsaccate pollen grains (NSPGs) and between 250 and 400 pteridophyte spores and pollen grains (total) have been counted. In case of three samples, the pollen sum was between 140 and 200 grains. In addition to pollen grains and pteridophyte spores,

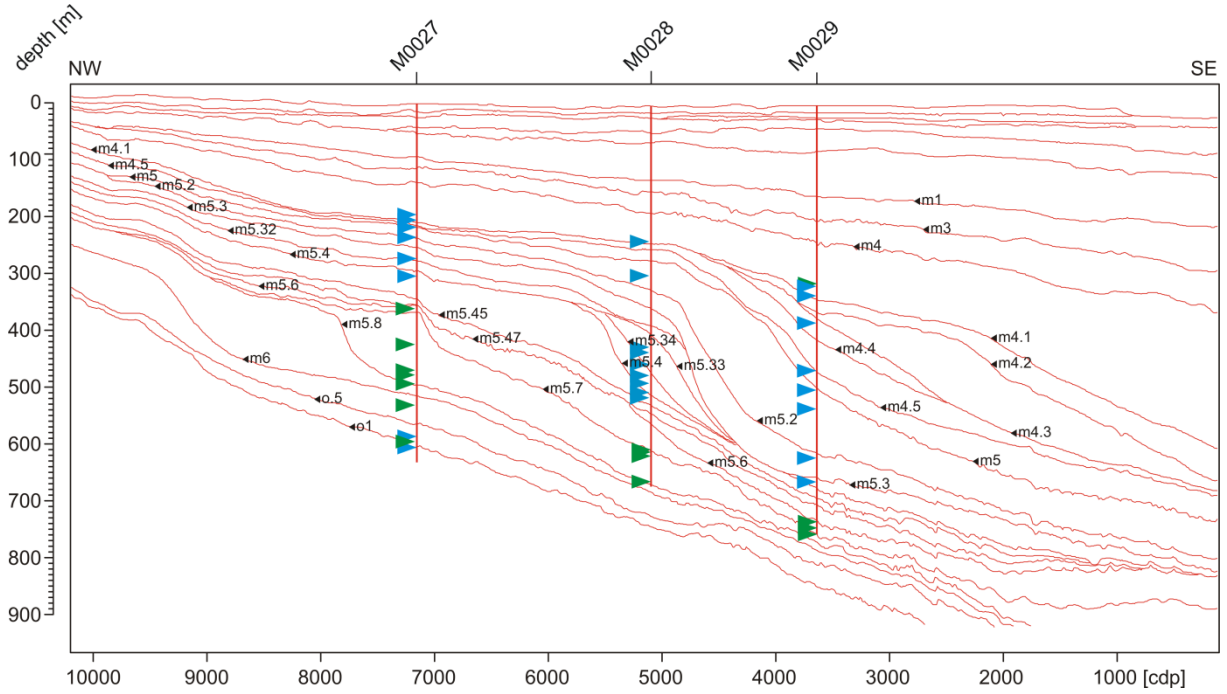

Figure 2.1 Depth-converted seismic stratigraphic framework for IODP expedition 313 boreholes (after Mountain et al., 2010b and Fang et al., 2013). Depths of samples with *Ulmus* pollen percentages >2,5 % are marked with blue triangles, samples with *Tsuga* percentages >1% are marked with green triangles (bisaccate pollen excluded from reference sum). Pollen data for Sites M0028 and M0029 were gathered in the framework of the IODP expedition 313 onshore science party (Mountain et al., 2010b), additional pollen data for Site M0029 derive from Fang et al. (2013).

fungal remains, foraminifer test linings (forams), and dinoflagellate cysts (dinocysts) were counted. We used the total number of NSPGs as reference sums for all percentage calculations (Figs. 2.2, 2.3). The data used for this study will be stored in the PANGEA database (www.pangea.de).

2.3.2 Assessment of palynomorph associations and pollen differentiation

A detailed review of the marine and terrestrial palynology at Sites M0027 and M0029, is given by McCarthy et al. (2013). This study showed that in sequences preceding sequence 5.8 (i.e. older than ~20.1 Ma; Fig. 2.1, 2.2), sediments primarily reached Site M0027 by mass wasting during glacioeustatic lowstands, influencing pollen assemblages, and thus hampering detailed palaeovegetation reconstructions based on relative occurrences. Considering these findings, we have excluded samples from intervals characterized by mass waste events and reworking at Site M0027 for which a strong bias due to transport effects was indicated (McCarthy et al., 2013). For the remaining samples analysed in the framework of our study, reworking of pollen and transport-related bias within nonsaccate pollen assemblages should be a minor issue.

Due to the particularly efficient airborne transport, longer floating time in the water column, and high resistance to oxidation, bisaccate pollen is generally over-represented in marine pollen assemblages and shows significant relative increase compared to other pollen types with increased distance from the coastline (e.g., Mudie, 1982; Hooghiemstra, 1988; Mudie and McCarthy, 1994; McCarthy et al., 2003). It has been shown that terrestrial modern pollen assemblages in eastern

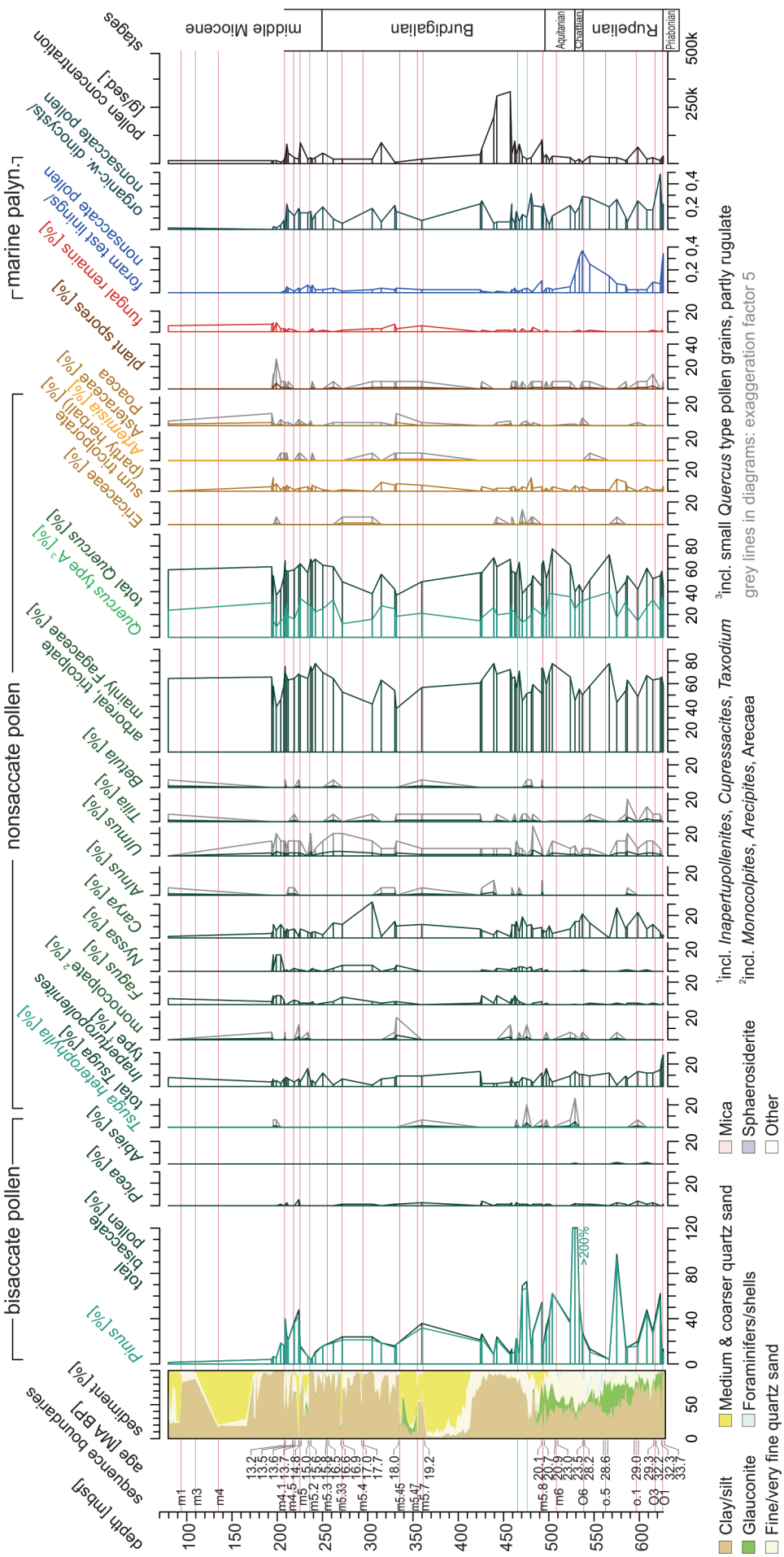

Figure 2.2 Sedimentological and palynological results for Site M0027. Shown versus depth: lithology; sequence boundaries; selected pollen types, pteridophyte spores and fungal remains (taxa <1 % excluded; percentages are based on the sum of nonsaccate pollen); marine palynomorphs (marine palynomorphs): foraminifer test lining/ nonsaccate pollen ratio, organic-walled dinoflagellate cyst/nonsaccate pollen ratio; pollen concentration (for some samples, the weight was estimated based on 3 the sample volume), stages. For taxa with low occurrences, exaggeration lines (x5) are shown in grey. Sequence ages are based on Browning et al. (2013).

North America, including coastal and continental shelf sediments, reflect the modern vegetation with exception of the genera *Pinus* (pine) and *Picea* (spruce), whose bisaccate pollen often originate from very distant regions (e.g. Davis and Webb, 1975; Mudie, 1982). In light of this, we have excluded bisaccate pollen from the reference sum on which pollen percentage calculations are based. However, high percentages of bisaccate pollen, e.g., *Pinus* pollen, are not necessarily tied to transport effects; they can still be related to climate-based changes in the catchment area and to extension of *Pinus* forests onto shelfal areas during sea-level lowstands (Lacourse et al., 2003, Kotthoff et al., 2008a). Herein, we use estimates of the site-shoreline distance based on the ratio of marine palynomorphs (dinocysts, forams) to NSPGs to validate the relevance of high bisaccate-pollen percentages, assuming that over-representation of bisaccate pollen is lower in samples with small relative abundances of dinocysts and foraminifer test linings.

For pollen identification, we used several works of Krutzsch (1963a, 1963b, 1967, 1970, 1971) and also descriptive publications and pollen keys of, e.g., McAndrews et al. (1973), Frederiksen (1979, 1980), Traverse (1994), Pazzaglia et al. (1997), Beug (2004), and Jarzen et al. (2010). Generally, we have assigned pollen grains to extant taxa (compare Table 2.2).

We have counted pollen of *Podocarpus* (i.e., *Podocarpidites*) separately; however, it should be noted that *Podocarpus* grains are very similar to *Pinus* grains and cannot be distinguished in all cases. Both genera contain several species that are very variable in pollen morphology, and the palynomorph *Podocarpidites* includes both "*Podocarpus*" as well as *Pinus* (Nichols and Brown, 1992), and may also represent related genera in the Podocarpaceae and not *Podocarpus* sensu strictu (Greenwood et al., 2013). *Arecipites*, other Arecaceae, and the "*Monocolpopollenites* type" were counted separately, but grouped together as "monocolpate" for the pollen diagram (Fig. 2.2). The differentiation of *Arecipites*-, *Monocolpopollenites*- and *Liliacidites*-related pollen grains is a matter of debate, e.g., there is uncertainty concerning the presence of *Arecipites* grains with reticulate structure (compare Krutzsch, 1970, Nichols et al., 1973). We have followed the approach of Krutzsch (1970) and in some cases assigned monocolpate grains with a fine reticulate structure (Plate 2.1) to *Arecipites*, but grains with a reticulum formed of clearly visible clavae and baculae were assigned to *Liliacidites* (e.g., Nichols et al., 1973). Generally, the morphology of Arecaceae pollen grains is highly diverse (e.g., Harley and Baker, 2001). Grains assigned to "other Arecaceae" were mainly monocolpate, in rare cases monoporate. Our conservative approach to identifying palm pollen in the New Jersey record may have yielded cooler temperature estimates for some samples due to palms being not identified as such, but as *Liliacidites.*

For the current study and the pollen diagram presented in Figure 2.2, we have assigned *Quercus*-type pollen grains to two groups, with *Quercus*-type A containing smaller and sometimes rugulate grains in contrast to bigger, never regulate grains. Pollen differentiation (*Tsuga*, inaperturate pollen, *Nyssa*/*Fagus*, *Ulmus*/*Zelkova*).

Several authors distinguish numerous *Tsuga* (*Zonapollenites*) species for the Miocene (e.g., Krutzsch, 1971), but we decided to assign *Tsuga* pollen grains to three types similar to present-day species. While *Tsuga mertensiana* pollen can be separated from other *Tsuga* species by its bisaccate morphology, present-day *T. canadensis* and *T. heterophylla* pollen (Plate 2-I) cannot easily be discriminated. Both are monosaccate, verrucate and characterized by an encircling frill-like structure. We used a more differentiated "frill" and the presence of microechinate processes on the muri to assign monosaccate *Tsuga* grains to the *T. heterophylla* type, following e.g. White and Ager (1994) and Barnett (1989).

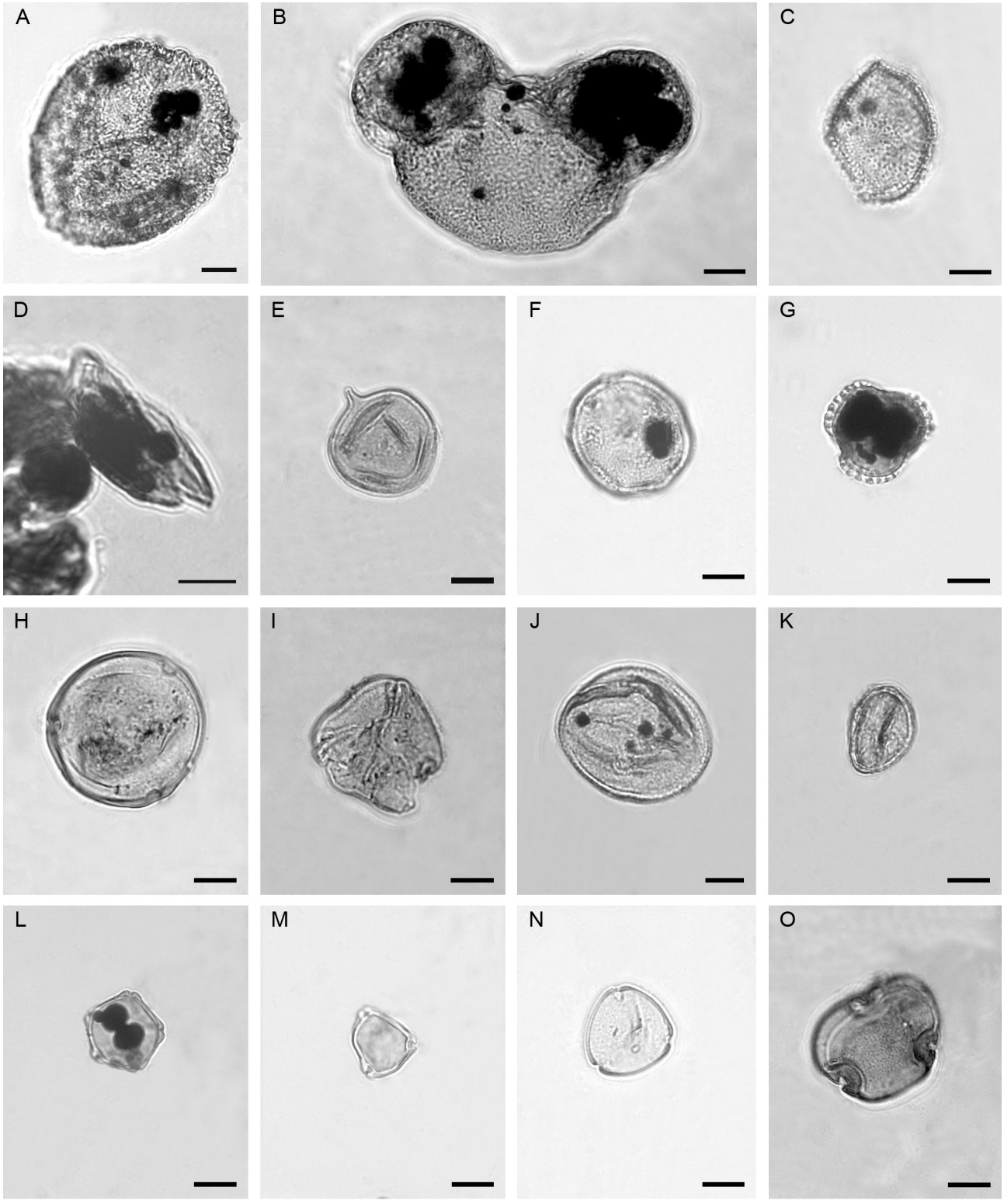

Plate 2-I Palynomorphs from Sites M0027, New Jersey shallow shelf. A: *Tsuga canadensis* type (core 116, ~335 mbsf), B: Pinus (core 95, ~272 mbsf) C: *Arecipites* type (core 115, ~332 mbsf), D: pyrite filled *Inaperturo-pollenites* type (pyrite-filled, core 101, ~290 mbsf), E: *Taxodium* (with well-preserved papilla, core 101, ~290 mbsf), F: *Liquidambar* (same sample as E), G: *Ilex* (core 109, ~315 mbsf), H: *Carya* (core 94, ~271 mbsf), I: *Nyssa* (core 209, ~586 mbsf), J: *Fagus* (same sample as E), K: *Quercus* (small type, same sample as B), L: *Alnus* (same sample as H), M: *Betula* (same sample as G); N: *Engelhardia* (same sample as E); O: *Tilia* (same sample as B). Scale bar: 10 µm.

Taxodium pollen was differentiated from other inaperturate pollen types, but particularly when pyrite grains were present inside the pollen grains (compare section 2.4 and Plate 2-I), the identification was hampered, so that in some samples, *Taxodium* pollen may have been assigned to the "other inaperturate pollen type". Therefore, in the pollen diagram (Fig. 2.2) pollen of the *Inaperturopollenites* type was grouped together with *Taxodium* and *Cupressacites* due to the morphological similarities of these pollen types (see also Larsson et al., 2011). Inaperturate grains were assigned to *Sequoia* when a long papilla was preserved (e.g., Krutzsch, 1971), in contrast to the shorter, often invisible papilla present in *Taxodium* and related taxa. The differentiation of *Sequoia* pollen is important since this taxon is not directly associated with swamps, unlike *Taxodium* and *Cupressacites*. Therefore *Sequoia* is associated with the conifer forest type, and not with the swamp/wet forest type (see Fig. 2.3).
While it is generally possible to distinguish *Nyssa* pollen grains from *Fagus* pollen grains (e.g., McAndrews et al, 1973; Traverse, 1994; Beug 2004), the differentiation was hampered in a few samples with slightly degraded pollen or pollen grains filled with pyrite (Plate 2-I). We have nevertheless decided to aim at a differentiation, since *Nyssa* is rather associated with swamp vegetation, while *Fagus* is characteristic of mid-latitude deciduous forests. *Zelkova* and *Ulmus* were not separated and all counted as *Ulmus*.

2.3.3 Vegetation types

To analyse changes in ecosystems in the hinterland of the New Jersey shelf, we have assigned the pollen and spores encountered in this study to groups based on the modern ecology of related genera (Fig. 2.3; Tab. 2.1), following similar approaches of, e.g., Jiménez-Moreno et al. (2005) and Larsson et al. (2011). While we have not assigned the same taxa to different vegetation types, several of the taxa mentioned in Table 2.1 can occur in different ecosystems. For example, the *Nyssa* (tupelo tree) is present within several vegetation types in recent south-eastern North America; however, *Nyssa* is particularly frequent in swamp associations due to its tolerance of wet soils and is therefore best placed into the swamp forest vegetation type. Similarly, Cupressaceae, including *Taxodium*, occur in a variety of environments, but the majority of North American species rather prefer wet conditions and include swamp taxa. Generally, the assignment to vegetation types allows a clearer interpretation of the pollen data and comparison with other palaeobotanical records.

2.3.4 Quantitative climate reconstructions

Climate was reconstructed by applying bioclimatic analysis (as modified by Greenwood et al., 2005; Reichgelt et al., 2013), a form of "nearest living relative" (NLR) analysis or mutual climate range technique (Thompson et al., 2012) to the spore-pollen record of land vegetation. Spore and pollen taxa with known NLR were identified from the fossil assemblages (Tab. 2.2). Climatic profiles were then assembled from both published and unpublished sources for each NLR with respect to various climate parameters such as mean annual temperature (MAT), coldest month mean temperature (CMMT), warmest month mean temperature (WMMT), and mean annual precipitation (MAP). Each profile contains the maximum and minimum values for a range of climate and related environmental variables with respect to an individual NLR taxon, based on their present-day distribution. For this study, the majority of climate profiles were obtained from Thompson et al. (1999, 2000b, 2012) and Fang et al. (2011) for trees and shrubs, and the

online database of Natural Resources Canada (2012) for non-trees, supplemented by data from sources outlined in Eldrett et al. (2014).

To determine the climate envelope that accommodated a majority of taxa from a given fossil assemblage with respect to a given climate parameter, the zone of overlap was calculated using the 10th percentile (as lower limit) and 90th percentile (as upper limit) of the total range for all NLRs represented in that sample (Greenwood et al., 2005; Reichgelt et al., 2013; Eldrett et al., 2014). This calculation removes or down-weights outliers; NLR taxa whose climate profile is at the extremes of the range of all taxa in the assemblage and is comparable to the weighted MCR method of Thompson et al. (2012). The estimate in bioclimatic analysis is presented as the midpoint between the lower and upper limits, with the error spanning from the lower to the upper limit (Greenwood et al. 2005; Pross et al., 2012; Thompson et al., 2012; Reichgelt et al., 2013). With this approach and by using mainly the climate profiles from Thompson et al. (1999, 2000b, 2012), we avoid problems discussed by Grimm and Denk (2012), who showed that MAT ranges provided for NLR in the widely-used PALEOFLORA database (www.palaeoflora.de) are partly inaccurate and that the precision reached with the coexistence approach based on this database is low. Thompson et al. (2012), however, demonstrated that for modern North American and Pleistocene vegetation assemblages; (1) there was a high degree of correlation between observed climatic values (including CMMT and MAT) and estimates from MCR approaches, (2) that estimates with sample NLR ≤ 10 were much less precise than for samples where $n \sim 20$ NLR, and (3) that presence-absence comparisons versus those based on taxon abundance avoid assumptions of fossil and modern vegetation being analogous. Their analysis also showed that MCR analysis of modern eastern North American coniferous forests and broadleaf forests (30 - 47 °N) yielded accurate and precise temperature estimates. All of our samples had at least 17 NLRs with climate profiles for our analysis, with the majority of the samples analysed with 20 or more NLRs with climate profiles. Whereas genera are typically used for NLRs in bioclimatic analysis (e.g., Reichgelt et al., 2013), in the present analysis *Tsuga* was differentiated by species. *Picea* and *Pinus* pollen was excluded from the reconstructions due to their over-representation in marine pollen records as also done by Eldrett et al. (2009, 2014), whereas *Podocarpus* was excluded due to concerns over the correct botanical affinity of these grains (Greenwood et al., 2013, compare section vegetation type 2.3.3).

Thompson et al. (2012) demonstrated that the extremes of the modern climate range (i.e., 0% and 100%) of NLRs yield wide climate estimates and so recommended assigning the 10th and 90th percentiles to the range of climatic tolerance of plant genera to increase precision. The weighting (i.e., exclusion of outliers) in bioclimatic analysis (sensu Greenwood et al. 2005) based on the 10th and 90th percentiles yields a warm estimate where a predominance of taxa with high minima are present, and a predominance of taxa with low minima yields a cool estimate. Particularly high temperature reconstructions in the bioclimatic analysis were therefore tied to the occurrence of thermophilic taxa such as palms (Arecaceae/*Arecipites*-pollen type; Arecaceae MAT 11.2 – 28.9°C, CMMT 2.1 – 27.2°C), together with mesothermic taxa with only moderate tolerance of cold winters (e.g., *Nyssa*, MAT 4.5 – 23.0°C, CMMT -10.4 – 18.9°C), whereas samples with notably cool estimates lacked these taxa (or contained only a few) and were rich in taxa with low winter tolerances (e.g., *Alnus* MAT -12.2 – 20.9°C, CMMT -30.9 – 14.1°C, *Fraxinus* MAT -2.3 – 24.4°C, CMMT -23.8 – 18.1°C).

2.4 Results

2.4.1 Quantitative palynology

~627 to ~540 mbsf, Eocene (Priabonian)?, Oligocene (Rupelian, ~33 to ~28 Ma)
The relative amount of marine palynomorphs (depicted in foram/NSPG ratio and dinocyst/NSPG ratio, Fig. 2.2) shows a decreasing trend from ~627 to ~580 mbsf and a subsequent increasing trend up to ~538 mbsf (sequence boundary O6). Bisaccate pollen generally shows a very similar trend of decreasing abundance. Notable exceptions are two samples at ~626 and ~624 mbsf with very low bisaccate pollen percentages (paired with relatively high percentages of swamp taxa pollen; Fig. 2.3) and one sample at ~576 mbsf with particularly high *Pinus* percentages. The sample at ~576 mbsf is furthermore characterized by very low pollen percentages of swamp taxa and increased herbaceous pollen percentages. Pollen of deciduous-evergreen forest taxa show percentages varying between 67 and 86 %. Dominant pollen taxa in this association are *Quercus* (oak) and *Carya* (hickory) and, to a lower degree, *Ulmus* (elm) and *Tilia* (linden). Increases in *Carya* pollen are often coupled with decreases in *Quercus*, *Ulmus*, and *Tilia* pollen and vice versa.
~540 to ~509 mbsf, Oligocene/early Miocene (late Chattian to early Aquitanian, ~28 to ~23 Ma)
The sediments between ~540 and ~509 mbsf probably represent the time interval from ~23.4 to ~23 Ma and thus the transition from the late Chattian to the Aquitanian. This interval is represented by four samples in our record. The third of these samples (from below) shows a high peak of bisaccate pollen (>200 %), while marine palynomorphs do not show such high values. The high percentages of bisaccate (namely *Pinus*) pollen are paired with occurrences of *Tsuga* (hemlock) pollen, relatively high *Carya* pollen percentages and a significant decrease in pollen of other arboreal taxa (particularly *Quercus*, *Tilia*, *Ulmus*). Furthermore, this interval contains the only Oligocene sample where steppic taxa reach relative occurrences of at least ~1 %, paired with relatively high abundances (around 2 %) of the "mesophytic understorey and non-steppic herbal taxa" group.

~509 to ~422 mbsf, Early Miocene (Aquitanian/early Burdigalian, ~21 to ~19 Ma)
This interval consists of two sequences (m6, m5.8) with sediments characterized by high content of pollen (Fig. 2.2). The foram/NSPG ratio is generally low, while the dinocyst/NSPG ratio varies and reaches up to ~0.3. There are occurrences of *Tsuga* pollen surpassing 2 % of the nonsaccate pollen assemblage at ~475 mbsf. This relative increase in *Tsuga* pollen is expressed to a higher degree at site M0029 (around ~733 mbsf/~20.1 Ma, with almost 10 % of nonsaccate pollen; Fig. 2.1). A similar peak is also revealed at Site M0028A at a depth of ~620 mbsf (Fig. 2.1; Mountain et al., 2010b). For all Sites, the hemlock peak is coeval with a strong increase in bisaccate pollen (mainly *Pinus*, at ~475 to ~470 mbsf at Site M0027), but a minor increase in the dinocyst/NSPG ratio (Fig. 2.2).
Generally, *Pinus* shows a decreasing trend for this interval. The *Pinus* pollen increase around 475 mbsf is coeval with an increase in *Carya* (over 18 %), Ericaceae, and *Nyssa* pollen, while members of the family Fagaceae, including *Quercus*, show a significant decrease from ~79 to ~45 %. Between ~467 and ~423 mbsf, there are still minor fluctuations in the pollen percentages of single taxa, but the percentages of combined deciduous-evergreen forest taxa remain relatively stable.

The pollen record also reveals occurrences of rare deciduous tree taxa such as *Juglans* and *Corylus*. Pollen concentration is particularly high around ~450 mbsf, while the number of marine palynomorphs is particularly low in the same interval. The interval from ~410 to ~365 mbsf at Site M0027, consisting of medium to coarse-grained sand, is barren of palynomorphs.
~360 to ~260 mbsf, early Miocene (late Burdigalian ~19 to ~16.5 Ma)
This interval is represented by seven samples in the pollen record from Site M0027. It is the first phase containing consistent occurrences of Poaceae (grass) pollen, but the percentages never exceed 2.5 % for all samples analyzed. During this interval, the percentages of different taxa (particularly Fagaceae, *Carya*, *Nyssa*) within the deciduous-evergreen-mixed-forest group vary significantly, while the combined percentages show a weak increasing trend of ~10 %. The second half of the interval is characterized by a significant increase in *Quercus* and a decrease in *Carya* pollen percentages.

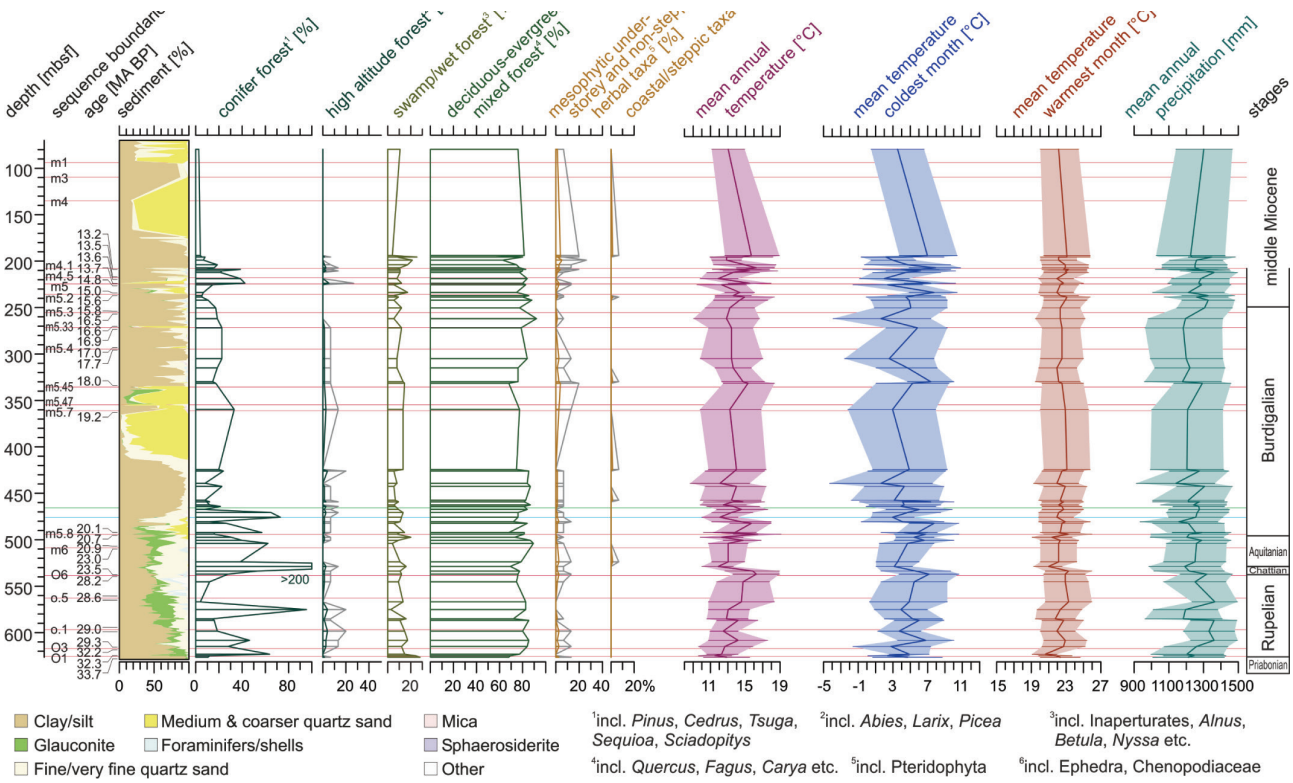

Figure 2.3 Lithology, palynological results, and pollen-based climate results for Site M0027. Shown versus depth: lithology, sequence boundaries, pollen percentages integrated into vegetation types (percentages are based on the sum of nonsaccate pollen), pollen-based quantitative climate data, stages. Sequence ages are based on Browning et al. (2013).

~250 to ~79 mbsf, Middle Miocene (Langhian/Serravallian, Tortonian? ~16 to ~11.6 Ma)

Nineteen samples from Site M0027 represent the interval between ~16 to ~11.6 Ma (~250 to ~80 mbsf) in our pollen record. Between ~250 and ~199 mbsf (~16 to ~13 Ma), *Quercus*/ Fagaceae pollen and combined pollen percentages of deciduous-evergreen mixed forest taxa decrease. Samples from ~199 mbsf to ~190 mbsf show strong variation in pollen percentages of deciduous-evergreen forest taxa (Fig. 2.4). In addition to relatively frequent *Ulmus* (elm) pollen, the sediments between ~250 and ~79 mbsf also contain small amounts of *Tilia*, *Alnus*, *Carpinus*, and *Ostrya* pollen grains. The samples between ~210 and ~190 mbsf reveal a decrease of conifer (mainly *Pinus*) pollen and strong increase in fungal remains.

The uppermost sample (from sequence m1; ~79.6 mbsf) probably has an age of ~11.6 Ma (Browning, pers. comm.). This sample is not particularly different from older Miocene samples and characterized by low percentages of bisaccate pollen and marine palynomorphs, and also high percentages of fungal remains.

2.4.2 Pollen-based climate reconstructions

Pollen-based temperature values are generally well constrained for the record from Site M0027, with uncertainties varying between 2 to 4 °C for mean annual temperatures (Fig. 2.3). Mean temperatures of the warmest month generally show less variation between samples than those of the coldest month. The mean annual precipitation curve for Site M0027 is less variable than the reconstructed temperatures. The values vary between ~1140 and ~1370 mm/a, which is within the range of the values encountered today in New Jersey.

Relatively warm temperatures are indicated for the lowermost, probably Priabonian-aged sample

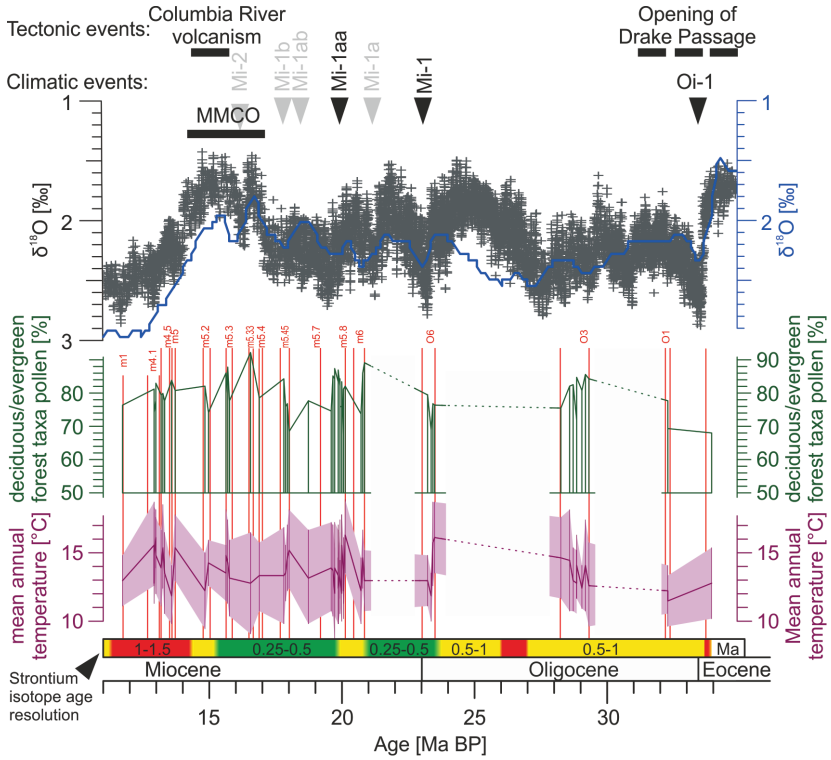

Figure 2.4 Pollen-based mean annual temperature reconstruction and deciduous/evergreen forest taxa pollen percentages for Site M0027 vs. age compared to a stacked and smoothed oxygen isotope record from the Pacific (after Cramer et al., 2009), global oxygen isotopes after Zachos et al. (2001a, 2008), and global events (position of Mi events after Miller et al., 1991; Pekar and DeConto, 2006). Age model for Eocene to Miocene samples after Browning et al. (2013) and Miller et al. (2013a). Strontium isotope age resolution after Browning et al. (2013); green: 0.25 to 0.5 Ma, yellow: 0.5 to 1.0 Ma, red: >1.0 Ma.

Table 2.1 Assignment of pollen types at Site M0027 to vegetation types.

Vegetation type	Conifer-forest	High-altitude conifer forest	Swamp/wet forest	Deciduous-evergreen mixed forest	Mesophytic understorey and non-steppic herbal taxa	Coastal or steppic taxa
associated pollen	*Cedripites/ Cedrus* *Pinus* *Sciadopitys* *Sequoia* type *Tsuga* *Podocarpus*	*Abies* *Picea* *Larix*	*Alnus* *Acorus* *Betula* *Cupressacites* Cyrillaceae *Inaperturo-pollenites* *Myrica* *Nyssa* *Nympha* type *Salix* *Sapotaceae* *Symplocos* type *Taxodium* type	*Acer* *Arecaceae* v. *Arecipites* *Carpinus* *Carya* *Castanea* *Celtis* *Cornus* *Corylus* *Cycadopites* type *Engelhardia* Ericaceae *Eucommia* Fagaceae v. *Fagus* *Fraxinus* *Ginkgo* *Ilex* *Iuglans* *Liquidambar* *Liriodendron* type *Magnolia* *Monocolpopol-lenites* *Platanus* *Platycarya* *Pterocarya* *Quercus* *Quercoidites* *Rhus* *Taxus* *Tilia* *Tricolporopol-lenites cingulum* type *Ulmus* type.	Pteridophyta *Sphagnum* *Osmunda* Asteraceae (excl. *Artemisia*) Poaceae *Sparganium* Apiaceae Menyanthaceae	Chenopo-diaceae *Ephedra* *Artemisia*

v. = varia

Table 2.2 List of fossil palynomorphs, next living relatives, sources of climatic range data

Taxon identified in the record	NLR used	Climate range source
Osmunda	North American species of *Osmunda* s.l.	5
Cycadopites	Cycads: N American species; Chinese species; Australian species	1,2,3
Ginkgo	*G. biloba*	2
Abies	N American species of *Abies*	1
Cedrus/Cedripites	*Cedrus atlantica, C. brevifolia, C. deodara, C. libani*	4
Inaperturapollenites hiatus	*Metasequoia glyptostroboides*	2
Sciadopitys	*Sciadopitys verticillata*	4
Sequoiapollenites	*Sequoia sempervirens*	1
Taxus	N American species of *Taxus*	1
Tsuga canadensis	*Tsuga canadensis*	1
Tsuga heterophylla/diversifolia type	*Tsuga heterophylla* + *T. diversifolia*	1
Tsuga mertensiana	*T. mertensiana*	1
Arecipites (Arecaceae)	All Australian genera, all Chinese genera, plus these genera from these areas: New Zealand, *Rhopalostylis*; North, Central & South America, *Sabal, Serenoa, Brahea, Washingtonia, Trithrinax;* N Africa, *Phoenix* (also from China)	1, 2, 3, 4, 6
Arecaceae varia	As above	1, 2, 3, 4, 6
Acer	N American species of *Acer*	1
Acorus	*Acorus americanus*	5
Alnus	N American species of *Alnus*	1
Betula	N American species	1
Carpinus	N American species of *Carpinus* + *Ostrya*	1
Carya	N American species of *Carya*	1
Castanea/*Tricolporites cingulum*	N American species of *Castanea*	1
Celtis	N American species of *Celtis*	1
Cornus	N American species of *Cornus* (woody only)	1

Corylus	N American species of *Corylus*	1
Engelhardia (*Momipites punctatus*?)	Chinese species of *Engelhardia*	2
Eucommia type	*Eucommia ulmoides*	2
Fagus	N American species of *Fagus*	1
Fraxinus	N American species of *Fraxinus*	1
Ilex	N American species of *Ilex*	1
Juglans	N American species of *Juglans*	1
Liriodendropollis	*Liriodendron tulipifera*	1
Liquidambar	*Liquidambar styraciflua*	1
Magnolia	N American species of *Magnolia*	1
Menyanthes type	*Menyanthes trifoliate*	5
Myrica/*Triatriopollenites*	N American species of *Myrica*	1
Nuphar	N American species of *Nuphar*	5
Nymphaea	N American species of *Nymphaea*	5
Nyssa	N American spp of *Nyssa*	1
Ostrya	N American species of *Carpinus* + *Ostrya*	1
Planera	*Planera aquatic*	1
Platycarya	*Platycarya strobilacea*	2
Prunus	N American species of *Prunus*	1
Pterocarya	Chinese species of *Pterocarya*	2
Quercus (partly rugulate, small)	N American species of *Quercus*	1
Quercus (big)	N American species of *Quercus*	1
Rhus type (Anacardiaceae)	N American species of *Rhus*	1
Salix	N American species of *Salix*	1
Symplocos and *Porocolpopollenites*	*Symplocos tinctoria*	1
T. villensis (*Castanopsis*, Fagaceae)	*Castanopsis chrysophylla*	1
Tilia	N American species of *Tilia*	1
Tricolpites retiformis (*Platanus*)	N American species of *Platanus*	1
Ulmus	N American species of *Ulmus*	1

Data sources: 1 Thompson et al. (1999, 2000, 2012); 2 Fang et al. (2011); 3 Australian National Herbarium online + ANUCLIM 6.1; 4 GBIF + WorldCLIM; 5 NRC Canada; 6 Reichgelt et al. (2013).

(MAT: ~13 °C, CMMT: ~5 °C). MAT values for the subsequent sample from the early Oligocene are lower by 1.2 °C, CCMT values are 2.3 °C lower.
During the Oligocene, MAT values show a generally increasing trend, culminating in particularly high values of ~16 °C for two samples around ~535 mbsf (~23.4 MA).
MAP reconstructions indicate generally more humid conditions during the Rupelian than during the following intervals with exception of two samples at depth of ~585 and ~576 mbsf. The high temperature values during the late Oligocene are followed by a rapid decline to ~12 °C at the transition to the early Miocene (~530 mbsf; Fig. 2.4).

For the time interval reflected in sequence m6 and the lower part of m5.8 (~503 to ~439 mbsf; reflected in 18 samples), average MATs of ~14 °C have been reconstructed, showing a slight decreasing trend. Samples reflecting particularly cool conditions around ~12 °C are revealed at ~475 mbsf (~20 Ma), ~462 mbsf (19.9 Ma), and at ~439 mbsf (~19.7 Ma).
Reconstructions for the interval from ~18 Ma to ~16.6 Ma (~335 to ~250 mbsf) reveal a cooling trend to MATs of ~13 °C with a minimum at ~262 mbsf. At the end of this interval, MAP reconstructions indicate more humid conditions, which prevail until ~11 Ma. Between ~16 to 14.5 Ma (~255 to ~225 mbsf), MAT values vary significantly between ~12 °C to ~15 °C.
The subsequent time interval (~14.5 to ~12 MA; ~225 to ~80 mbsf) shows slightly higher average MAT (~14.5 °C), with peak values (> 16 °C) at ~13 MA (around ~208 mbsf). Samples indicating relatively low temperatures during this interval are positioned at depths of ~218 mbsf (13.6 Ma) and of ~199/196 mbsf (~12.9 Ma).

2.5 Discussion and comparison with other vegetation records

In the following, we present an interpretation of the vegetation and climate development in the hinterland of the New Jersey shelf, integrating the relative abundances of terrestrial and marine palynomorphs and the pollen-based quantitative climate analyses with further results from IODP Expedition 313. The results and interpretations are compared with other records from the North Atlantic, eastern/central North America, and Europe, and with global climate records, particularly oxygen isotope records.

2.5.1 Eocene(?), Oligocene (Rupelian, ~33 to ~28 Ma)

For the lowermost two samples analysed (~627 and ~624 mbsf), high relative abundances of marine palynomorphs, particularly foraminifer test linings, compared to nonsaccate pollen, imply a particular long site-shoreline distance. Under such circumstances, bisaccate pollen should be particularly over-represented. The very low percentages of bisaccate pollen in these samples thus imply that conifer forests were rare in the catchment area of the Site M0027 during the very late Eocene/very early Oligocene. It cannot be unambiguously determined whether the lowermost sediments from Site M0027 are from the Priabonian or the early Oligocene (Browning et al., 2013). But if the lowermost sample analyzed herein is of Priabonian age, then the temperature changes over the Eocene-Oligocene boundary in hinterland of the New Jersey shelf (with a decrease in MAT of 1.2 °C and 2.3 °C in CMMT) are weaker than changes found by Eldrett et al. (2009), who calculated a decrease of annual temperature of ~3 °C (from ~13 to ~10 °C) at the transition from the Eocene to the Oligocene in the high latitudes, based on

the NRL method applied to sediments from the Norwegian-Greenland Sea. Similarly to the findings of Eldrett et al. (2009), Liu et al. (2009) showed that sea-surface temperatures decreased by ~5 °C in the high latitudes at the Eocene-Oligocene transition.

The relatively minor changes in pollen associations (excluding a strong decrease in swamp/wet forest taxa, Fig. 2.3) between the samples at ~627 and ~624 mbsf indicates that air temperature may have been a less important control factor for vegetation development at that time and only influenced particular thermophilous species. This is consistent with results of Oboh et al. (1996), who also could not find significant palaeobotanical changes at the Eocene-Oligocene boundary in records from south-eastern North America (including St. Stephens Quarry, Fig. 1.4, No. 1), while marine proxies at St. Stephens Quarry indicate significant changes in marine ecosystems at the Eocene-Oligocene Boundary.
The decreasing trend in marine palynomorphs from ~627 to ~580 mbsf (~33 to ~28.8 Ma; Fig. 2.2) indicates a shortening site-shoreline distance, with a subsequent lengthening of the distance up to ~538 mbsf, which is coeval with increasing MATs. A relatively dry phase during a generally humid interval with MAP below 1200 mm is indicated for ~28.8 Ma by two samples, of which the second also indicates a spread of conifers and a decrease of swamp forest vegetation.
Generally, the vegetation in the catchment area was dominated by oak-hickory (*Quercus*-*Carya*) forests (with changing frequency of elms and lindens). While *Alnus* (alder) is common in western and northern North-American records from the Eocene/Oligocene, its presence in Oligocene sediments from southeastern North America has to our knowledge not yet been confirmed, and evidence from the Eocene is rare. *Alnus* pollen was identified by Gray (1960) in Eocene sediments from Alabama (Fig. 1.4, No. 13), but Frederiksen (1979) found *Alnus* pollen in Palaeocene, but not Eocene samples in Virginia (Oak Grove, Fig. 1.4, No. 7), and studies from the Eocene of Florida (Jarzen and Dilcher, 2006; Fig. 1.4, No. 3) did not reveal the presence of this genus. Swamp vegetation was widespread during the late Eocene and the early Oligocene, whilst the following intervals witnessed only slight variations until the middle Miocene.

2.5.2 Oligocene/Miocene transition (late Chattian/early Aquitanian, ~23 Ma)

The findings described in sections: 2.4.1 (~540 to ~509 mbsf, Oligocene/early Miocene [late Chattian to early Aquitanian, ~28 to ~23 Ma]) and 2.4.2 indicate that the time interval from ~23.4 to ~23 Ma (~535 to ~523 mbsf) was characterized by warm temperatures and a long site-shoreline distance, but that a sudden cooling (Fig. 2.4) by ~ 4 °C (MAT) led to an expansion of conifer forests, including a spread of *Tsuga*. The *Tsuga* pollen grains found within this interval probably belong to different species (*T. canadensis*, *T. heterophylla*, and *T. mertensiana*). These findings are consistent with phylogenetic results by Havill et al. (2008), implying that the split of these species occurred during the Eocene/Oligocene. The increase in *Tsuga* pollen is of particular interest since this genus, particularly *Tsuga heterophylla*, can tolerate cool climates, but needs humidity and cannot tolerate persistent drought (e.g., Havill et al. 2008). As temperatures dropped at ~23.4 Ma, the site-shoreline distance shortened, as indicated by the decrease in marine palynomorph/NSPG ratios, particularly in the foram/NSPG ratio (Fig. 2.2). This temperature drop and shortening of the site-shoreline distance is probably linked to the Mi-1 event (see section 2.5.6).

2.5.3 Early Miocene (Aquitanian/early Burdigalian, ~21 to ~19 Ma)

The frequent occurrences of *Tsuga* pollen at all three Sites around ~20 Ma (~492 and ~475 mbsf at Site M0027, Fig. 2.1 and Fig. 2.3), paired with very high percentages of *Pinus* pollen (at Site M0029 at around ~733 mbsf and at Site M0028A at a depth of ~620 mbsf) may be partly caused by over-representation due to the good transport properties of these pollen types – particularly given the location beyond the clinoform rollover at all three sites. Nonetheless, considering the coeval decrease in deciduous-evergreen forest, we infer that around ~20 Ma cooler, but humid conditions prevailed in the hinterland of the New Jersey shelf, causing a spread of conifer taxa in the catchment area. MAT values of ~1240 mm around this interval compared to lower averaged values of ~1200 mm (Fig. 2.4) during the middle and lower Burdigalian support this scenario. The cool conditions indicated for ~20 Ma, ~19.9 Ma, and ~19.7 Ma may be related to Mi-events (see below). The presence of *Fagus* and *Juglans* in the area is confirmed by findings of respective pollen grains in the early Miocene Brandon lignite from Vermont, an area north of New Jersey (Fig. 1.4, No. 16) (Traverse, 1994).

The site-shoreline distance probably continued to shorten during the related interval as implied by decreasing abundances of marine palynomorphs. Using also foraminifer-based water-depth calculations, McCarthy et al. (2013) infer a generally falling sea level for this interval. The pollen record may thus represent a particularly local signal here that may have been altered by changes in river systems. The sediment record indeed indicates a significant change in the environment to decreasing river influence between ~480 and ~470 mbsf (Miller et al., 2013a).

2.5.4 Early Miocene (late Burdigalian ~19 to ~16.5 Ma).

The relatively weak changes the ratios between marine palynomorphs and NSPGs over this interval point to only minor changes in the site-shoreline distance, while at almost the same time, starting at ~18 Ma, the hinterland of the NJSS witnessed a decrease of MATs by ~2.5 °C. Due to slight uncertainties in the age model (0.25 to 0.5 Ma, Browning et al., 2013; Fig. 2.4), it is unclear if the particularly low MAT values at ~262 mbsf are the regional reflectance of the Mi-2 event (e.g., Miller et al., 1991). The weak increase in combined deciduous-evergreen mixed forest taxa with a relative decrease of *Carya* (hickory) presence during the second half of this interval (starting at ~17.9 Ma) may indicate increasingly humid conditions, which is also partly reflected in the quantitative climate data. These indicate a significant increase of MAP starting with the onset of the MMCO (at ~16.6 Ma/~262mbsf).
The occurrences of Poaceae pollen indicate that grasses were present within the vegetation in the Atlantic Coastal Plain during the early Miocene, but our pollen record implies that they never became an important factor during the time interval examined in the framework of this study. There are only a few intervals during the subsequent middle Miocene during which Poaceae showed slightly higher abundances. The generally rare occurrences of true grasses in the Atlantic coastal plain can be explained with the consistent humid conditions in the catchment area, presumably tied to the presence of the proto-Gulf Stream since at least the early Eocene (Pinet et al., 1981).

2.5.5 Middle Miocene (Langhian/Serravallian, ~16 to ~11.6 Ma)

Generally, the pollen assemblages found in the middle Miocene sediments from Site M0027 are very similar to those found in the neighbouring pollen record from the York Quarry (Fig. 1.4, No. 9) with *Quercus*, *Carya*, and *Pinus* being dominant taxa, and the consistent presence of Taxodiaceae, Cupressaceae, *Ulmus*, *Ilex*, *Liquidambar*, *Pterocarya*, and *Castanea*-like pollen (Pazzaglia et al., 1997). The Langhian/Serravallian pollen percentages and pollen-based climate reconstructions from Site M0027 imply several changes in ecosystems, particularly spreads in swamp forests and understorey plants. Similarly, climate conditions varied significantly.

The similarity of the sample at ~79.6 mbsf to the Miocene samples below indicates that it is also of Miocene age. The relatively high MATs (~13.2 °C) for this sample fit well with palaeoflora-based estimations from New Jersey (Pine Barrens; Fig. 1.4, No. 14). The palaeoflora suggests warm and temperate conditions for this region at ~11 Ma (Greller and Rachele, 1984). Based on the palynoflora, Rachele (1976) estimated the annual precipitation to 1270 mm, average January temperature to 6 °C and average July temperature to 24 °C. These results cannot directly be tied to the record from Site M0027, but match relatively well with our results for the sample at ~79.6 mbsf (MAP: ~1305 mm, CMMT: ~3.0 °C, WMMT: ~22.2 °C). Our results are furthermore consistent with findings by McCartan et al. (1990) who analyzed a palaeoflora from upland deposits of the southern Maryland Coastal Plain (Fig.1.4, No. 8). The climate was probably warmer in southeastern North America. Palaeobotanical records from the middle Miocene Alum Bluff Flora (Fig. 1.4, No. 12) indicate warm-temperate conditions (e.g., Jarzen et al., 2010).

The plant associations found in early/middle Miocene sediments (reflecting the MMCO and the subsequent interval) from the NJSS are very similar to those encountered in similar-aged marine/marginal marine sediments from Atlantic Western Europe (e.g., Larsson et al., 2011). However, the MATs reconstructed for the Miocene of the Atlantic Coastal Plain (averaged MAT to ~13.7 °C for the interval from ~16.5 to ~14 Ma and ~14.3 °C thereafter) are colder by ~1 to almost 4 °C compared to records from Denmark (~17.5 °C, Larsson et al., 2011), Serbia (~15.5 °C, Utescher et al., 2007), or Bulgaria (~ 15 °C, Utescher et al., 2009), with European records from higher altitudes showing lower temperatures. Considering that the present-day MATs in the European regions mentioned above are significantly lower (e.g., ~9 °C in Denmark; ~11 °C in Serbia) than in New Jersey (~12 °C, section 2.2), this seems to be a discrepancy, even considering that the palaeolatitudes of the European records were ~ 5° lower during the MMCO (e.g., Scotese et al., 1988).

2.5.6 Further comparison with global signals and outlook

The pollen-based quantitative climate record presented here for Site M0027 must remain fragmentary due to several hiatuses and the insufficient pollen preservation in coarse-grained sediments, even if the sample resolution will probably be increased during subsequent studies. The age model established by Mountain et al. (2010b) and Browning et al. (2013) still allows a comparison with supra-regional climate records (Fig. 2.4).
If directly compared to global climate changes as indicated in oxygen-isotope values (Zachos et al., 2001a, 2008; Cramer et al. 2009), the averaged mean annual temperature record shows

similar signals during the Palaeogene. The transition from the Priabonian to the early Oligocene is reflected in a temperature decrease (Fig. 2.4), but this decrease is weaker than records from the high latitudes (Eldrett et al., 2009; Liu et al., 2009). Furthermore, a shift to less humid conditions is indicated by the decrease in swamp/wet forest taxa (Fig. 2.3), though the pollen-based precipitation reconstructions for the transition interval are not precise enough to reveal such a shift. Around ~29 Ma, an increase in MATs is congruent with a slight decrease in the oxygen-isotope values. Unfortunately, the interval from 28 to 26 Ma is not yet recovered from the NJSS, but the Mi-1 cooling event Mi-1 (Miller et al. 1987, 1991; Wright and Miller 1992) is reflected by shifts in palaeovegetation (Fig. 2.2, Fig. 2.3) and a rapid fall in MATs (Fig. 2.3, Fig. 2.4; compare section 2.5.2).

For the early Miocene, there are still congruencies between the results from the NJSS and the global marine signals (Fig. 2.4). We suggest that the several decreases in mean annual and winter temperatures (Figs. 2.3 and 2.4) for the interval between ~21 and ~19 Ma can be local expressions of the Mi-1a and Mi-1aa events (Pekar and DeConto, 2006). The MAT peak at ~18 Ma and the subsequent rapid decrease is also congruent with the oxygen isotope data (Fig. 2.4). However, for the interval between ~17 to 14.5 Ma (~272 to ~225 mbsf at Site M0027), which should reflect the MMCO, the regional temperature signals from the NJSS and the global signal reflected in the benthic oxygen-isotope record seem to be decoupled (Fig. 2.4). The MAP values show a significant increase after at the onset of the MMCO (at ~16.5 Ma), but the MAP remain continuously high from there on, even after the end of the MMCO. The deciduous-evergreen forest taxa pollen curve seems to some degree to resemble the isotope curve, but the averaged MATs over the MMCO imply a temperature of only ~14 °C, (less than in preceding and subsequent intervals). The obviously only minor impact on the North Atlantic Coastal Plain of North America is surprising, since the MMCO had a strong impact on the terrestrial realm on the eastern side of the North Atlantic (e.g., Mosbrugger et al., 2005. Quijtaal et al., 2014; see also section: 2.5.5).
One possible explanation for the discrepancy between indications for warm climate during the MMCO in other records and hints to relatively cool temperatures in our record could be a problem in the age model. The strontium-isotope- and microfossil-based age control could be erroneous by 1 to 1.5 Ma for the samples between ~225 and ~190 mbsf (sequences m5, m4.5, and 4.1; compare section 2.3.1). If shifted by 1.5 Ma to the past, the samples from these depths could reflect the second part of the MMCO at ~15 Ma. But even if this were correct, there would still be a discrepancy with the first part of the MMCO at ~16.5 Ma. For this time, the age control is particularly good (Fig. 2.4; Browning et al., 2013).

Another possible explanation would be that the hinterland of the NJSS was not very susceptible to global climate changes during the middle Miocene due to the moderating effect of the North Atlantic in that region. Climate model results assessing differences between the MMCO interval and present-day conditions (e.g. Herold et al., 2011, 2012) show only minor differences between MMCO and present-day conditions for the eastern US coast (including the region around New Jersey), while the northern North American (Canadian) coast and the regions around the Gulf of Mexico reveal strong differences. However, the climate models used in the studies of Herold et al. (2011, 2012) also indicate minor changes for western Europe, which is not congruent with results from European pollen records showing very warm conditions during the middle Miocene

(e.g., Mosbrugger et al., 2005; Utescher et al., 2007; Larsson et al., 2011; compare section: 2.5.5). A further option to explain the surprisingly low temperatures reconstructed for the hinterland of the NJSS would be topographical changes resulting in regional vegetation and climate changes. Climate model results by Herold et al. (2009) imply for the Miocene that topographical lowering of high mountain ranges such as the Andes and the Tibetian plateau can significantly increase regional temperatures. Vice versa, an uplift of mountain ranges could cause a shift in vegetation and a temperature decrease. Poag and Sevon (1989), Pazzaglia and Brandon (1996), and Gallen et al. (2013) discuss an uplift phase of the Appalachian Highlands (Fig. 1.4) during the middle Miocene based on sedimentation rates at the U.S. Atlantic continental margin and on analyses from the Cullasaja River basin (Southern Appalachian Highlands). Since the Appalachians are close to the NJSS, a tectonic uplift – even if not resulting in a significant spread of high altitude forests in the catchment area – could cause a decrease and even emigration of thermophilous taxa. This could be a possible explanation for the surprisingly low temperatures reflected in our pollen.

The current research state probably does not allow a final interpretation. During future research, the Oligocene and Miocene palynomorph assemblages of Site M0027 will be analysed in a higher resolution. Particularly the interval covering the MMCO will be the focus of further studies.

Vegetation and climate development of the New Jersey hinterland during the late middle Miocene (IODP Expedition 313 Site M0027)

3.1 Introduction

Several long-term climatic reorganisations occurred within the Cenozoic Era, which led to the retreat of vegetation units and the reestablishment of plant and climax communities. The biogeographic history of taxa and their individual ecophysiological behaviour generate plant communities with a specific temporal and spatial restricted resolution (Huntley and Webb, 1989). The Mid-Miocene Climatic Optimum (MMCO) from ~17 to ~14.5 Ma represents the last warm time interval during the Miocene in Earth history with limited ice on East Antarctic and no substantial perennial ice caps on the Northern Hemisphere (Flower and Kennet, 1994; Zachos et al., 2001a; 2008; Shevenell et al., 2004, 2008; Mudelsee et al., 2014). The establishment of the Antarctic cryosphere at ~15 Ma (Wright et al., 1992; Shevenell et al., 2004; Mudelsee et al., 2014) and a subsequent growth of Antarctic ice volume led to global deep water cooling and the Mid-Miocene Climatic Transition (MMCT) between ~14.2 Ma and ~13.8 Ma (Flower and Kennet, 1994; Shevenell et al., 2008). The MMCT marks the end of the MMCO and the onset of a long-term global cooling (Wright et al., 1992; Flower and Kennett, 1994; Zachos et al., 2001a; 2008). Around the transition period from the global warmer conditions of the MMCO to stepwise cooler conditions, the vegetation cover of the North American continent underwent transformations. Wolfe (1994) and White et al. (1997) reported a significant temperature drop during the MMCT in northwesternmost North America, which caused the disappearance of warmth-loving plants, especially of thermophilous members of Cupressaceae at ~15.5 Ma (White et al., 1997). Plant macrofossils in lake sediments from Nevada indicate that genera like *Diospyros*, *Nyssa*, *Fagus* or *Carya* went extinct regionally after ~15.6 Ma due to reduction in summer rainfall (Axelrod, 1995). In the Great Plains in central North America, extending sagebrush steppes became the dominant vegetation type at ~12 Ma, as reported from the Snake River Plain (Davis and Ellis, 2010). Phytolith analyses from Montana, Nebraska and Wyoming imply a spread of grass-dominated habits for the same time interval, but were equivocal as to whether this shift was climatically driven or due to other ecological factors (Strömberg, 2005; Chen et al., 2015). There are several studies with focus on Miocene sediments from the middle eastern Atlantic coastal plain of North America and from farther inland that investigate palaeoclimatic and palaeoenvironmental development based on terrestrial palynomorphs (Rachele, 1976; Greller and Rachele, 1984; Frederiksen, 1984; Owens et al., 1988; Groot, 1991, 1992; Traverse, 1994; Pazzaglia et al., 1997) and macrofossils (McCartan et al., 1990; Tiffney, 1994). All these studies suffer from poorly constrained age models and are often based on terrestrial palynomorphs only (e.g. Rachele, 1976; Traverse, 1994). In terms of palaeoclimatic reversal to global cooler conditions, Groot (1991) and Pazzaglia et al. (1997) have interpreted palynomorph assemblages on a longer geological timescale. Pazzaglia et al. (1997) suggest a progressive deterioration to terrestrial cooler conditions, with a weaker cooling intensification during the Miocene than during the Pliocene and Pleistocene. In contrast Groot (1991) mentions that palaeoclimatic conditions remained fairly stable during the Miocene and Pliocene and states that a shift to

terrestrial cooler conditions took place not earlier than at the beginning of the Pleistocene. Generally, conditions seem to contrast the sharp cooling observed in continental Europe (Mosbrugger et al., 2005; Donders et al., 2009).
However, the current investigations can only roughly be compared at a global scale due to their poorly constrained age models. Therefore, a better understanding of climate and vegetation development during the middle and late Miocene at the eastern coast of North America is needed.
The terrestrial palynomorph assemblage in marine sediments is the result of the interplay between pollen production, transport mechanism, shoreline distance and ocean circulation pattern (Heusser, 1988; van der Kaars, 2001) Several studies (e.g. Heusser, 1983, 1988; Hooghiemstra and Agwu, 1986; van der Kaars, 2001) have shown that the microfloristic composition in neritic marine sediments correlates well with contemporary onshore vegetation and the major vegetation types. Terrestrial palynomorphs in marine sediments are therefore well suited for palaeovegetation and palaeoclimatic reconstructions of intervals with a poor continental record. Palaeoclimate can be reconstructed via pollen records based on the assumption that climatic requirements of fossil plant taxa are presumably similar to those of their nearest living relatives (Chaloner and Creber, 1990) or potential modern analogues (Denk et al., 2013).
This approach was already successfully applied to macrofossil and or microfossil assemblages from the terrestrial and the marine realms (Greenwood et al., 2005; Pross et al., 2012; Denk et al., 2013; Prebble et al., 2017). However, for accurate results a careful selection of the relevant modern analogue and accompanying bioclimatology is required (Grimm et al., 2015).

In this context, Integrated Ocean Drilling Program (IODP) Expedition (Exp.) 313 to the New Jersey shallow shelf (NJSS) offers prospects to investigate terrestrial ecosystem development in eastern North America. The NJSS is characterized by high sedimentation rates, and, being situated at a passive continental margin, this region is generally tectonically stable, though a rejuvenation of the Appalachian Mountains during the Miocene is discussed by several authors (e.g. Gallen et al., 2013; Liu, 2014: see below).
The sediment cores of IODP Exp. 313 have a robust age model (Browning et al., 2013; Miller et al., 2013a) and contain well-preserved microfossil assemblages.
Previous studies on IODP Exp. 313 sediment cores concerning terrestrial ecosystem development were carried out using terrestrial organic matter (Fang et al., 2013) and terrestrial palynomorphs (Kotthoff et al., 2014). The investigation of Kotthoff et al. (2014) focused on the regional terrestrial environmental conditions of the New Jersey hinterland during the Oligocene and Miocene, but only at low resolution. According to Kotthoff et al. (2014) no clear impact of the MMCT on the terrestrial ecosystems in the hinterland of the NJSS was indicated. Among other factors, the authors suggested that a Miocene uplift of the Appalachian Mountains might explain the minor influence of the MMCO on the region. For a better understanding of the regional vegetation composition and climatic pattern, and to examine if an Appalachian uplift is in accordance with palynological results, we have reinvestigated palynomorphs of sediment cores of Site M0027, in significantly higher temporal resolution, with a focus on the second half of the MMCO and the MMCT.

3.2 Material and methods

3.2.1 Geological setting and age model of Site M0027

The sediments analysed in this study derive from Site M0027 at the landward edge of the IODP Expedition 313 transect. At this site, one hole (M0027A) was drilled into the New Jersey shallow shelf at 39°38.046'N and 73°37.301'W at 33.5 m water depth and a site-shoreline distance of 45 km (Fig. 1.4). An interval of 547 m of sediment was recovered, with a relatively thick (~300 m) Miocene section characterized by several sedimentary sequences tied to transgression and regression phases (Browning et al., 2013, Miller et al., 2013a). The succession below 420 mbsf was deposited during glacioeustatic low stands, with mass wasting beyond the shelf break being an important factor. The sequences above 360 mbsf, on which our research is focusing, were mainly accumulated on the shelf during sea-level high stands, implying only minor re-sedimentation, while the uppermost sequences discussed in this study were again deposited during intervals of lower sea level (McCarthy et al., 2013).

The age model of site M0027 is based on calcareous nannofossils, dinoflagellate cysts, planktic diatoms, Sr isotopes, and sequence stratigraphy (Browning et al. 2013). Accordingly, the sediments analysed in the framework of our study have been deposited between ~15.8 and ~12.7 Ma and belong to five sequences. Sequence m5.3 (256.19 to 236.15 mbsf) covers an age interval from ~15.8 to ~15.6 Ma (Langhian) and shows, compared with the other analysed sequences, the best agreement of the used age model proxies, with an uncertainty of 0.25 to 0.5 Ma. The estimated age of Sequence m5.2 (236.15 to 225.45 mbsf) is ~15.0 to ~14.8 Ma (Langhian) with a potential error of 0.5 to 1 Ma. For all other sequences, the age resolution has a potential error between 1 and 1.5 Ma. Their ages are best approximated as ~13.7 to ~13.6 Ma (Serravallian) for Sequence m5 (225.45 to 218.39 mbsf), ~13.5 to ~13.2 Ma (Serravallian) for Sequence m4.5 (218, 39 to 209 mbsf), and ~13.0 to ~12.7 Ma (Serravallian) for Sequence m4.1 (209 to 135 mbsf). The analysed sequences are within Lithological Unit II and III at Site M0027, which comprises clay and silt with a low amount of sand and granules (Expedition 313 Scientists, 2010b). The upper part of Sequence m5.3 and Sequences m5.2 and m5 were deposited during transgressive phases representing warmer intervals, cooler intervals are reflected by Sequences m.4.5 and m4.1 (Katz et al., 2013, McCarthy et al., 2013).

Reconstructions by Scotese et al. (1988) imply that the research region was situated ~2° further south during the Miocene than at present, and reached a position between 39 and 40°N during the Pliocene.

3.2.2 Site selection and origin of terrestrial palynomorphs

Of the three sites drilled during IODP Exp. 313, Site M0027 is closest to the coast and was therefore selected for environmental reconstruction because the taphonomic effects of selective transport of pollen grains increase offshore, (Heusser, 1983; Mudie and McCarthy, 1994). The increasing amount of bisaccate pollen grains in marine sediments is related to the physical properties of the pollen grain shape (Grega et al., 2013). The palaeo-water depth at Site M0027 fluctuated between inner and outer shelf during the middle Miocene (Katz et al., 2013; McCarthy et al., 2013).

The terrestrial palynomorphs at Site M0027 reflect a broad catchment area of different vegetation types of the hinterland of NJSS. The major transport mechanism of terrestrial palynomorphs

into the western North Atlantic were probably westerlies which were already developed during the Miocene and blew pollen grains into the study area as they do today (Mudie and McCarthy, 1994). The transport of palynomorphs by fluvial systems is a further fundamental factor of terrigenous influx into the NJSS, which would have increased as a function of wetter climates and/or uplift of the Appalachian Mountains. To evaluate the fluvial influence into the NJSS, Shannon-Wiener-Index and Fisher´s alpha diversity index were performed. The relative pollen grain diversity in the counted assemblages reflects the fluvial influence in marine sediments.

3.2.3 Sample processing and counting

Sample processing was done at Brock University (St. Catharines, Canada) following a modified protocol by Bates et al. (1978). Samples of ~5 cm^3 sediment were disaggregated in 0.02 % sodium hexamethaphosphate, treated with 25 % hydrochloridic acid and subsequently with 48 % hydrofluoric acid. All samples where sieved through a 10 µm Nixon mesh. The first part of the processed material was mounted in glycerine jelly. The remainder was subsequently acetolyzed following Zetter and Ferguson (2001). The processed samples were mixed with glycerine and stored in test tubes.
Pollen and spores were counted and identified using the acetolyzed material. In general, 300-400 terrestrial palynomorphs were counted for percentage calculations. Since bisaccate pollen grains tend to be overrepresented in marine pollen records (Mudie and McCarthy, 1994; Kotthoff et al., 2008c), they are excluded from the pollen reference sum used for percentage calculations. Additional taxa were searched afterwards and recorded to improve the palaeoclimate reconstructions, which are based on the presence/absence of taxa (compare section 3.2.4).

In order to achieve a reliable ratio between pollen and dinoflagellate cysts (P:D), considering the sensitiveness of some organic-walled dinoflagellate cyst to acetolysis (Marret, 1993; Mudie and McCarthy, 2006), we furthermore counted 300 marine and terrestrial palynomorphs using non-acetolyzed material. The P:D is an indicator for transport mechanism and sea-level fluctuations (Mudie and McCarthy, 1994; McCarthy and Mudie, 1998; McCarthy et al., 2013).
In total, 84 samples from five late Mid-Miocene sequences (m5.3: 20 samples; m5.2: 11; m5: 10; m4.5: 27; m4.1: 16) were analysed with a Zeiss Axioscope A1 at 630x magnification.

3.2.4 Palaeoclimate reconstructions

The palaeoclimatic reconstructions are based upon the microfloristic findings of Site M0027 and follow the bioclimatic analysis method of Greenwood et al. (2005). Fundamental background for this and similar approaches (Mosbrugger and Utescher, 1997; Fauquette et al, 1998; Denk et al., 2013; Utescher et al., 2014) is the nearest living relative concept (NLR: Chaloner and Creber, 1990), which implies that a given fossil taxon lived under similar climatic conditions as its living representative. The sum of all climatic signatures of the identified taxa generates a climatic overlapping zone in which the fossil flora could coexist (Mosbrugger and Utescher, 1997; Greenwood et al., 2005; Utescher et al., 2014). The border of the overlapping zone is given by the 10th percentile (lower) and the 90th (upper) percentile (Greenwood et al., 2005). Taxa only identified at family level (e.g. Sapotaceae, Cyperaceae, Anacardiaceae) were generally excluded from the palaeoclimatic reconstruction, as well as taxa, which occur in a variety of ecosystems/habitats (e.g. *Vitis*). *Myrica* and *Morella* (Myricaceae) overlap in their pollen

morphology (Grímsson et al., 2016a). The generated climatic profile is based on *Morella* spp. with exclusion of the boreal taxon *Myrica gale* (compare Thomson et al., 2000a, 2000b, 2006). Genera like *Betula*, *Salix* or *Alnus* flourish under various macroclimate and are unfavourable climate indicators. These taxa increased the error ranges of the estimated values and were thus excluded. The identification of Cupressaceae pollen grains at genus level is a matter of debate (e.g. Larsson et al., 2010). Recently Grimm et al. (2015) and Grimm and Potts (2016) stated that the identification of these pollen grains is impossible using light as well as scanning electron microscopy, while other authors (Hofmann and Zetter, 2005; Grímsson and Zetter, 2011) differentiate between different Cupressaceae genera. In order to contribute this debate we have differentiated between non-papillate (Plate 3-I, M) and papillate pollen grains of Cupressaceae (Plate 3-I, N and O). The Cupresssaceae pollen grains with a papilla were again subdivided in cf. *Sequoia* (Plate 3-I, N) and cf. *Taxodium*/*Glyptostrobus* (Plate 3-I, O). Furthermore, we differentiated a third category of Cupressaceae with grains which presumably have a papilla (Plate 3-I, P). This group was not part of the performed climate reconstruction, but it was included in percentage values for the papillate pollen grain morphotype (Fig. 3.2). To show the sensitivity of some members of the Cupressaceae (e.g. *Sequoia*) in terms of climate reconstruction, herein, we have generated two variations of climatic estimates. Variation 1 includes *Sequoia* and *Taxodium*/*Glyptostrobus*, whereas they are excluded in variation 2. For both variations, four climatic estimates were calculated: mean annual temperature (MAT), mean annual precipitation (MAP), and mean annual temperature of the coldest month (CMMT) and warmest month (WMMT). All obtained estimates are based on climatic profiles from modern North American species (Thomson et al.,1999, 2000a; 2000b, 2006) and Chinese species (Fang et al., 2011). Estimates are furthermore based on data from the Natural Resources Canada (NRC) and Global Biodiversity Information Facility (GBIF) using WorldClim. A summary of all used NLRs together with the climate source is given in Table 3.1. The highest number of NLRs used in variation 2 is 27 at 252.16 mbsf (Sequence m5.3), and the lowest number is 6 at 209.03 mbsf (m4.1), respectively.

3.2.5 Assignment to palaeovegetation units

Pollen grains where assigned to different vegetation units. The criteria of positioning pollen grains and spores to different phytocoenoses are based on modern analogues. Due to overlap of vegetation belts and taxa thriving in several vegetation communities (growing preferences of generalist versus specialist taxa) this approach is artificial. However, it allows us to obtain an understanding of the existing vegetation in a specific area during a certain time and thereby of related possible environmental shifts (e.g. Pross et al., 2012).

The arrangement includes altitudinal zonation beside soil conditions and uses the following phytocoenoses or vegetation units: Unit 1: high-altitude conifer forest; Unit 2: mid-high altitude conifer forest; Unit 3: Cupressaceae; Unit 4: mesophytic forest growing on well-drained soils; Unit 5: mesophytic forest growing on moist/wet soils; Unit 6: mesophytic understorey; Unit 7: plant community associated to coastal environments, growing on sun-exposed sandbanks (Tab. 3.1).

a: Fang et al. (2011), b Thomson et al. (1999, 2000a, 2000b), c NRC, d GBIF+WorldCLIM
1 high-altitude conifer forest; 2 mid-high-altitude conifer forest. 3 Cupressaceae 4 mesophytic forest growing on well-drained soils; 5 mesophytic forest growing on moist/wet soils; 6 mesophytic understorey; 7 plant community associated to coastal environments, growing on sun-exposed sandbanks.

Table 3.1 Summary of identified taxa of Site M0027 together with source of climatic range and arrangement to a vegetation unit, alphabetically ordered.

Taxon	Climate source	NLR used	Vegetation Unit
Gymnosperms			
Abies	-		1
Cathaya	a	*C. argyrophylla*	2
Cedrus	b		2
Sequoia	b	*S. sempervirens*	3
Taxodium/Glyptostrobus	b/a	*T. distichum G. pensilis*	3
Ephedra	-		7
Larix	-		1
Picea	-		1
Pinus subg. *Pinus*	-		2
Pinus subg. *Strobus*	-		2
Sciadopitys	d	*S. verticillata*	2
Tsuga aff. *heterophylla*	b	*T. heterophylla*	2
Tsuga canadensis	b	*T. canadensis*	4
Tsuga caroliniana	b	*T. caroliniana*	4
Angiosperms			
Acer	b	*Acer* spp. (NA)	4
Alangium	-		4
Alnus	-		5
Anacardiaceae	-		4
Apiaceae	-		6
Arceuthobium	-		4
Artemisia	-		6
Asteraceae tubuliflorae type	-		6
Betula	-		5
Carpinus/Ostrya	b	*Carpinus* and *Ostrya* spp. (NA)	4
Carya	b	*Carya* spp. (NA)	5
Caryophyllaceae	-		6
Castaneoideae	b		4
Celtis	b	*Celtis* spp. (NA)	4
Chenopodiaceae/Amaranthaceae	-		7
Cornus	b	*Cornus* spp. (woody, NA)	4
Corylus	b	*Corylus* spp. (NA)	4
Cyperaceae	-		6
Diospyros	b	*Diospyros* spp. (NA)	4
Engelhardioideae	-		4
Ericaceae	-		4
Eucommia	a	*E. ulmoides*	4
Euonymus	-		4
Fabaceae	-		6
Fagus	b	*F. grandifolia*	4
Fraxinus	b	*Fraxinus* spp. (NA)	5
Ilex	a	*Ilex* spp. (NA)	5

Table 3.1 Continued

Juglans	b	*Juglans* spp. (NA)	4
Lamiaceae	-		6
Liliaceae	-		5
Liquidambar	b	*L. styraciflua*	5
Liriodendron	b	*L. tulipifera*	4
Lonicera	-		4
Loranthus	-		4
Magnolia	b	*Magnolia* spp. (NA)	4
Morella/Myrica	a	*Morella* spp. (NA)	5
Nuphar	c	*Nuphar* spp. (NA)	6
Nymphaea	c	*Nymphaea* spp. (NA)	6
Nyssa	b	*Nyssa* spp. (NA)	5
Onagraceae	-		6
Pachysandra	-		6
Parthenocissus	c	*Parthenocissus* spp. (NA)	4
Persicaria	-		6
Platycarya	b	*P. strobilacea*	4
Poaceae	-		6
Polygala	-		6
Polygonum	-		6
Pterocarya	a	*Pterocarya* spp. (China)	4
Quercus	b	*Quercus* spp. (NA)	4
Reevesia	a	*Reevesia* spp. (China)	4
Rhamnaceae	-		5
Rosaceae	-		4
Salix	-		5
Sapotaceae	-		5
Sparganium /Potamogeton	-		5
Symplocos	b	*S. tinctoria*	5
Thypha	-		5
Tilia	b	*Tilia spp.* (NA)	4
Ulmus/Zelkova	b	*Ulmus spp.* (NA)	5
Viburnum	b	*Viburnum spp.* (NA)	4
Viscum	-		4
Vitis	-		5
Pteridophytes			
Lycopodium	-		5
Osmunda	c	*Osmunda* s.l. (NA)	5
Polypodiaceae	-		5

3.3 Results

3.3.1 Palynomorph assemblages

The analysed fossil microflora from the hinterland of the NJSS is moderately diverse; all identified taxa are summarized in Table 3.1. In total 79 taxa (13 gymnosperms, 63 angiosperms and 3 pteridophytes) were identified. Most taxa belong to groups which nowadays comprise trees and shrubs. Sporomorphs deriving from herbs, lianas and epiphytes were generally rare. Plates 3-I and 3-II represent selected palynomorphs of different vegetation belts. *Cathaya* (Pinaceae) Plate 3-I, A and B; *Diospyros* (Ebenaceae), Plate 3-I , R; *Persicaria* (Polygonaceae) Plate 3-II, A; *Pachysandra* (Buxaceae) Plate 3-II, B; *Viscum* (Santalaceae) Plate, 3-II, B; *Reevesia* (Malvaceae) Plate 3-II, G; *Lonicera* (Caprifoliaceae) Plate 3-II, H; *Polygala* (Polygalaceae) Plate 3-II, L; *Polygonum* (Polygonaceae) Plate 3-II, Q, represent new identified pollen grains for the middle eastern North American Atlantic coastal plain.

The pollen diagram in Figure 3.2 shows relative percentages of frequent taxa. The most abundant taxon in all analysed samples is *Quercus* (min: 29 % max: 83 %, in average 60 %), followed by *Carya* (min. 1 %, max: 22 %, average 6.4 %), *Fagus* (min: 1 %, max. 21 %, average 5.3 %), *Pinus* subg. *Strobus* (min: 0 %, max. 9 %, average 2.3 %), *Cathaya* with 2.1 % in average (min: 0 %, max: 11 %) and the Cupressaceae (min: 0 %, max: 38 %, average 6 %). Cupressaceae pollen grains with a papilla were in average (4.4 %) more abundant than the non-papillate morphotype (2.0 %). However, within the Cupressaceae pollen grains with a papilla, the pollen grains for which the papilla could unequivocally be identified represented only 2.1 %, while for the remainder of this type, the papilla was not clearly visible (compare section 3.2.4). Other taxa were found in significantly lower quantities (e.g. Cyperaceae, Poaceae, Ericaceae, Sapotaceae) or are only represented by single pollen grains (e.g. *Alangium*, Apiaceae, Lamiaceae, *Lonicera*). The assignments of taxa to vegetation units are listed in Table 3.1 and are numbered as listed in section 3.2.5. The percentage contributions of all phytocoenoses/vegetation units are shown in Figure 3.3. The mixed mesophytic forest growing on dry soils is the main vegetation type in all analysed sequences (Fig. 3.3) and shows fairly constant pollen percentages over the intervals analysed. The floristic composition of the mixed mesophytic forest is characterised by a considerable *Quercus* and *Fagus* input. Other taxa like *Tilia*, *Juglans*, *Diospyros*, Castanoideae, *Acer* or *Liriodendron* represent minor elements and are often completely absent. The high-altitude conifer forest, the mid-altitude conifer forest and the Cupressaceae show significant fluctuations along the analysed time interval.

In Sequence m5.3 (256.19 to 236.15 mbsf), reflecting the time interval from ~15.8 to ~15.6 Ma (Langhian), the percentages of Vegetation Units 1 (high-altitude conifer forest) and 2 (mid-altitude conifer forest) expand and reach several peaks, but towards the end, they decline (Figs. 3.2 and 3.3). Within this sequence, the increase in bisaccate pollen does not correlate with the P:D ratio, which remains constant throughout. The entire Sequence m5.2 (14.8 to 15.0 Ma) is characterized by a strong increase of Cupressaceae pollen grains (20 % in average) which does not correspond with the P:D ratio (Fig. 3.3). The Shannon-Wiener-Index (Fig. 3.3) is constantly lower than in all other analysed time intervals for this sequence. The Fisher´s alpha diversity index shows the same trend. Rare components in this sequence are pollen grains associated to the high-altitude vegetation belt. The mid-altitude vegetation unit recuperates and reaches peak occurrences at 221.03 mbsf. Afterwards, the mid-altitude vegetation unit strongly

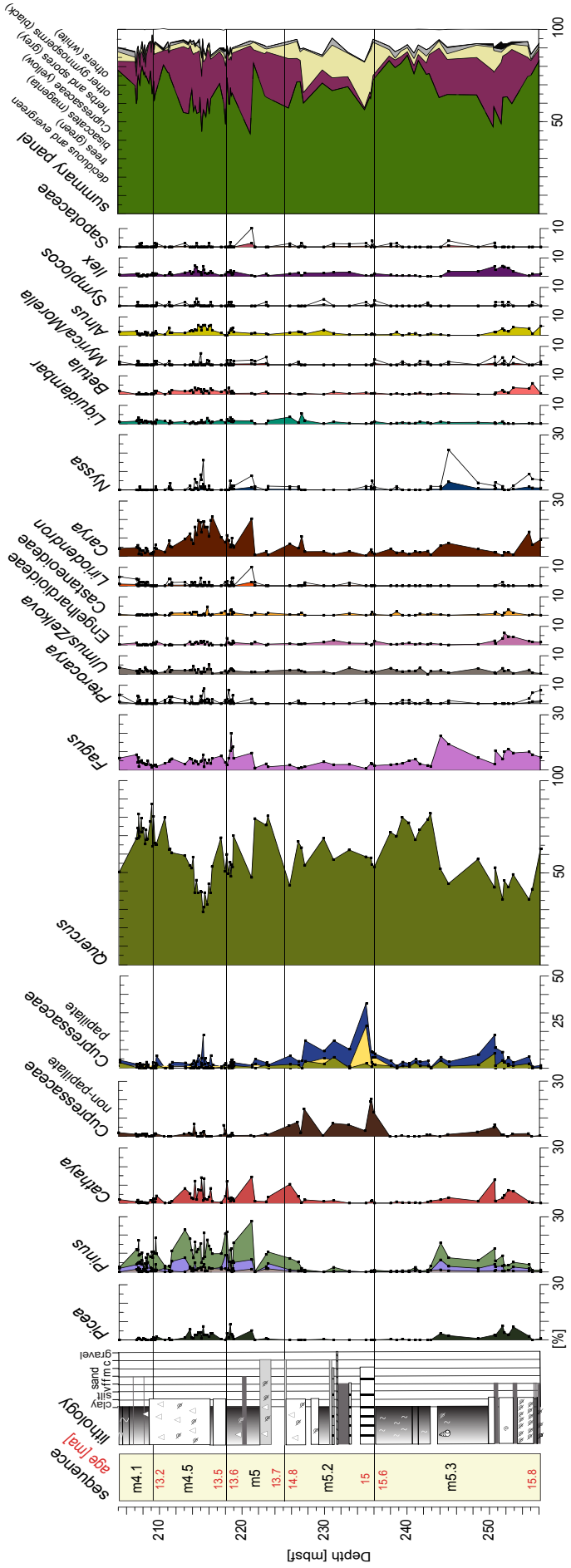

Figure 3.2 Relative pollen percentages of selected taxa of Site M0027 (pollen sum excluding bisaccates) plotted against depth (white areas: 5x exaggeration) *Pinus*: black: *Pinus* subg. *Pinus*: light grey: *Pinus* subg. *Strobus*, grey: sum of *Pinus* unidentified included. Papillate Cupressaceae: black: cf. *Sequoia*; light grey: cf. *Taxodium*/*Glyptostrobus*; grey: sum of papillate and presumably papillate Cupressaceae. Summary panel showing changes of the major groups (pollen sum including bisaccates): deciduous and evergreen trees (green), bisaccates (magenta), Cupressaceae (yellow), herbs and spores (grey), other gymnosperms (black), others (white). Sequence boundaries and ages after Browning et al. (2013). Lithology after Mountain et al. (2010b): bioturbation (S), shell fragments (slashed shells), shell debris (triangle), gastropods.

Plate. 3-I LM images of selected pollen grains of different vegetation units. A. *Cathaya* (213.55 mbsf), B. presumably aberrant pollen grain of *Cathaya* (244.91 mbsf), C. *Picea* (213.55 mbsf), D. aff. *Cedrus* (215.06 mbsf), E. *Pinus* subg. *Strobus* (212.93 mbsf), F. *Pinus* subg. *Pinus* (235.62 mbsf), G. *Abies* (218.03 mbsf), H. *Larix* (244.91 mbsf), I. *Tsuga* aff. *heterophylla* (252.47 mbsf), J. *Tsuga caroliniana* (214.86 mbsf), K. *Tsuga canadensis* (212.93 mbsf), L. *Ephedra* (234.88 mbsf), M. non-papillate Cupressaceae (243.92 mbsf), N. papillate Cupressaceae cf. *Sequoia* (208.23 mbsf), O. papillate Cupressaceae cf. *Taxodium*/*Glyptostrobus* (248.47 mbsf), P. Cupressaceae presumably with papilla (235.92 mbsf), Q. *Sciadopitys* (214.15 mbsf), R. *Diospyros* (243.92 mbsf), S. *Alangium* (211.15 mbsf), T. Sapotaceae (221.03 mbsf), U. *Liriodendron* (207.23 mbsf), V. *Magnolia* (212.93 mbsf), W. *Parthenocissus* (234.88 mbsf), X. *Fagus* (217.32 mbsf), Y. *Nyssa* (227.48 mbsf), Z. *Celtis* (207.73 mbsf), Aa. *Juglans* (214.15 mbsf), Bb. *Pterocarya* (205.01 mbsf). Scale bar = 10µm.

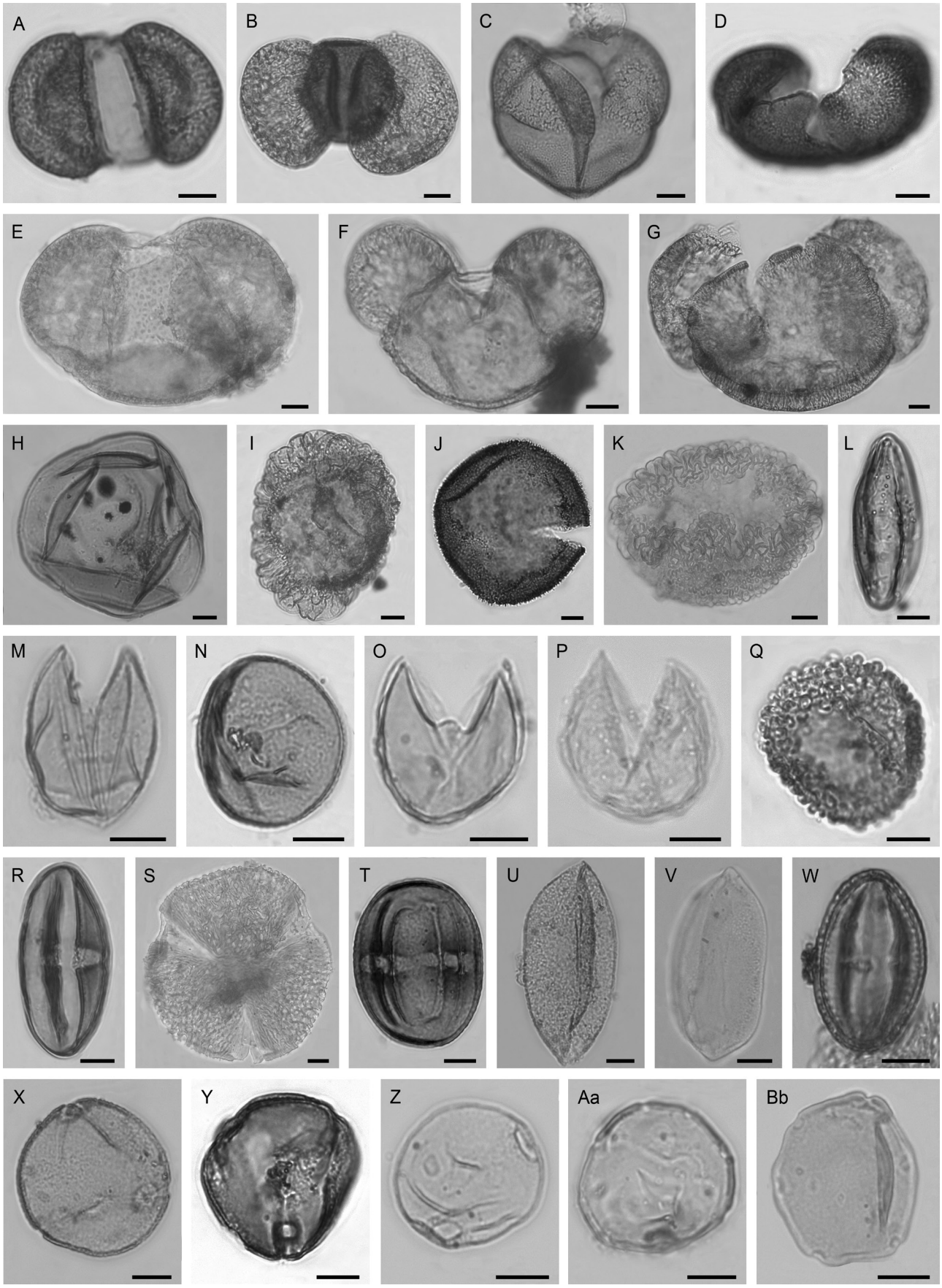

Plate. 3-I

fluctuates throughout Sequences m5. to m4.1. Vegetation Unit 1 (high-altitudes conifer forest) reveals a similarly fluctuating picture. In the second half of Sequence m5, bisaccate pollen grains assigned to the mid-altitude conifer forest show a stronger increase than the P:D ratio. However, Vegetation Units 1 and 2 correspond with the pollen/dinoflagellate cyst ratio.

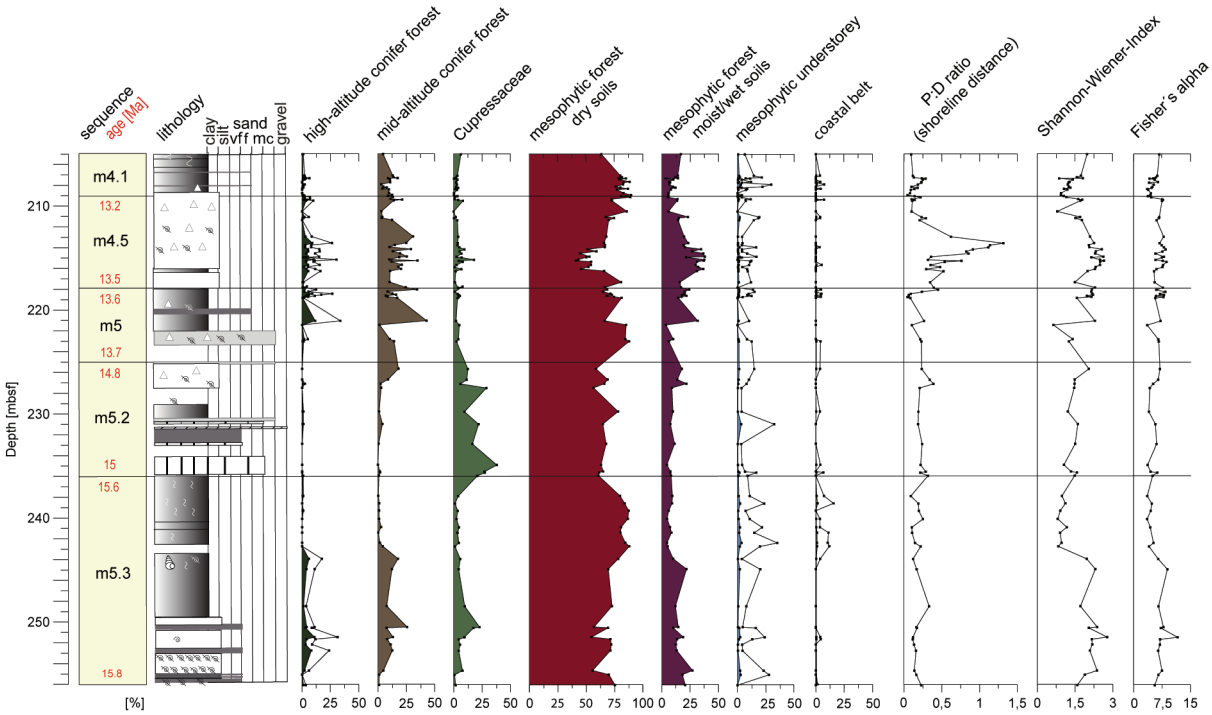

Figure 3.3 Different vegetation units in the hinterland of NJSS during the late middle Miocene (high-altitude forest 5x exaggerated; mesophytic understorey and coastal belt 10x), pollen/dinoflagellate cyst ratio indicating shoreline distance, Shannon-Wiener-Index and Fisher´s alpha diversity Index. Assignment of identified taxa to vegetation units is shown in Table 3.1. Sequence boundaries and ages after Browning et al. (2013). Lithology after Mountain et al. (2010b): bioturbation (S), shell fragments (slashed shells), shell debris (triangle), gastropods.

Table 3.2 Summary of average climatic values and average error of estimated value of each sequences of both applied approaches with and without thermophilous Cupressaceae.

Variation 1 (Cupressaceae incl.)					
Sequence	m4.1	m4.5	m5	m5.2	m5.3
MAT [°C]	13.0 (± 4)	13.4 (± 4)	13.2 (± 4)	13.5 (± 4)	13.3 (± 5)
WMMT [°C]	22.1 (± 5)	21.9 (± 4)	21.9 (± 4)	21.6 (± 5)	21.9 (± 5)
CMMT [°C]	4.3 (± 5)	3.5 (± 6)	4.7 (± 5)	4.4 (± 5)	4.8 (± 4)
MAP [mm]	1259.3 (± 365)	1272.5 (± 332)	1274.7 (± 333)	1258.7 (± 364)	1276.5 (± 337)

Variation 2 (Cupressaceae excl.)					
Sequence	m4.1	m4.5	m5	m5.2	m5.3
MAT [°C]	13.0 (± 5)	12.7 (± 5)	13.3 (± 5)	13.1 (± 5)	13.2 (± 5)
WMMT [°C]	22.4 (± 5)	22.0 (± 4)	22.1 (± 4)	21.9 (± 5)	22.2 (± 5)
CMMT [°C]	2.4 (± 8)	2.4 (± 6)	3.1 (± 7)	2.9 (± 7)	3.0 (± 7)
MAP [mm]	1266.6 (± 355)	1277.6 (± 321)	1282.2 (± 320)	1264.4 (± 348)	1284.3 (± 326)

3.3.2 Palaeoclimate

The bioclimatic analysis of the analysed microflora results in a warm humid climate during the late Mid-Miocene in both applied variations (Fig. 3.4). In variation 1 (Cupressaceae included) estimated mean annual temperature (MAT) oscillate during the late Mid-Miocene between 10.9 °C ± 6.1 °C (207.34 mbsf) and 14.8 ± 6.4 °C (218.63 mbsf). Estimated winter temperatures (CMMT) were with one exception (-1.9 °C ± 10.6 °C at 210.51 mbsf) always situated above the freezing point ranging from 1.5 °C ± 7.5°C to 6.5 °C ± 5.3 °C (235.52 mbsf; 248.47 mbsf). Palaeoclimatic estimates of summer temperatures (WMMT) indicate moderate warmth. Estimated WMMT fluctuate between 20.2 °C ± 4.6 °C (235.92 mbsf) and 23.1 °C ± 4 °C (208.94 mbsf). Precipitation data demonstrate high annual rainfall for the study area > 1000 mm (Fig. 3.4). Generated palaeoclimatic profiles for variation 2 (without Cupressaceae) are as follows: smallest estimated MAT 10.9 °C ± 6.2 °C (210.51 mbsf), highest at 235.52 mbsf with 15.0 °C ± 5.5 °C. CMMT: -2 °C ± 10.5 °C (210.51 mbsf), 6.3 °C ± 7 °C (248.47 mbsf). Most of the generated CMMTs are located near the freezing point but with large uncertainties (Fig. 3.4). WMMT: 20.7 °C ± 4.6 °C (234.88 mbsf) and 24 °C ± 3.9 °C at 209.03 mbsf. Annual precipitation data are, as in variation 1, always > 1000 mm. Both reconstructions show considerable uncertainty in the estimation range, but the range is significantly smaller for variation 1. Average values of generated climatic profiles of both variations of each sequence are summarized in Table 3.2. The greatest difference between both variations is visible in the generated CMMTs (Fig. 3.4, Tab. 3.2). For variation 1, the use of Cupressaceae taxa increases the generated CMMTs in average by 1-2 °C and markedly diminishes the range of the estimated values, i.e. this approach reduces uncertainty in the estimates. There are almost no differences, though, between both applied variations regarding the error of estimated values and mean annual precipitation and WMMT (Fig. 3.4, Tab. 3.2). The generated MAT of both applied variations show similar fluctuations along the analysed timescale but differ in the range of values (Fig. 3.4).

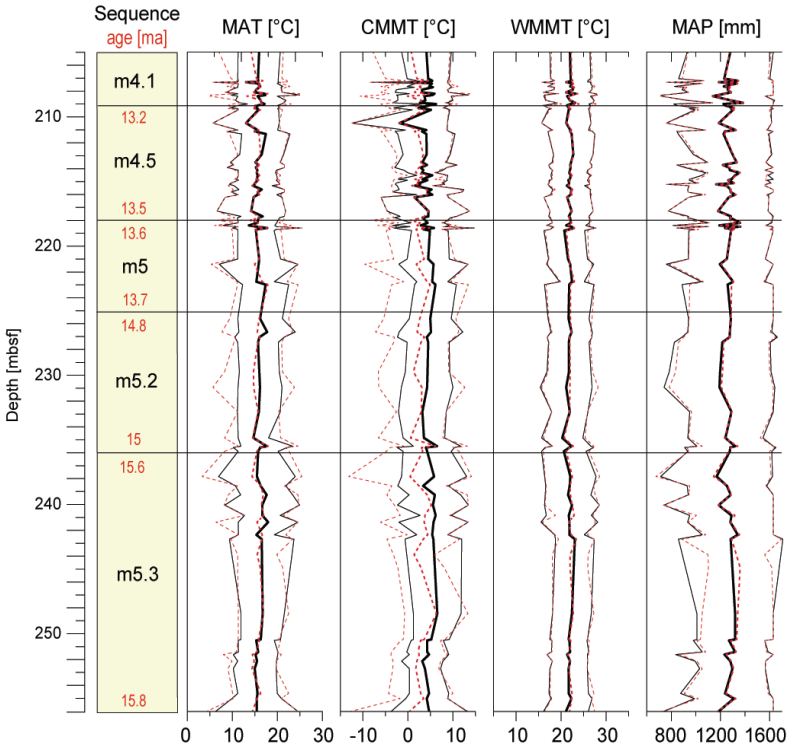

Figure 3.4 Pollen-based palaeoclimate reconstructions (after Greenwood et al., 2005) in two variations (variation 2 excluding Cupressaceae) plotted against depth for Site M0027. MAT: mean annual temperature, CMMT and WMMT mean annual temperature of the coldest and warmest month, MAP: mean annual precipitation. Outer lines: error of estimated value; dashed orange: variation 2, black: variation 1. Sequence boundaries and ages after Browning et al. (2013).

3.4 Discussion

3.4.1 Vegetation composition

Considering the ecological present-day preferences of hardwood genera like *Quercus*, *Fagus*, *Acer*, *Tilia*, *Liriodendron*, *Alangium*, extended mixed mesophytic forest in well-drained lowland is indicated as dominant vegetation type in the hinterland of the NJSS. It is probable that several species of Castaneoideae flourished in the catchment area; but with respect to the low resolution of the light microscope, these species are not distinguishable (Bouchal et al., 2014). Sporadically appearing taxa (e.g. *Juglans*, *Acer*, and *Tilia*) and well-represented canopy trees of the mesophytic forest formed the climax community throughout all analysed sequences.
The occurrence of shrubs (e.g. *Viburnum*, *Lonicera*), subshrubs (e.g. *Pachysandra*) and epiphytes (e.g. *Viscum*), together with the hardwood taxa mentioned above, implies a multi-layered forest, even though pollen grains of these three groups are very rare. The identified herbs like Poaceae, Cyperaceae, Asteraceae, *Persicaria* and Apiaceae probably inhabited the forest margins. Azonal backswamps and riparian forests flourished most likely in the close vicinity of rivers and streams. Such humid environments are indicated by species of *Carya*, *Liquidambar*, *Betula*, Sapotaceae, *Alnus*, *Myrica*/*Morella*, *Nyssa*, *Symplocos*, the fern *Osmunda*, various other fern species of Polypodiaceae, and various monocotyledons with sulcate reticulate ornamentation (Plate, 3-II, E and F). The abundances of the Vegetation Unit 5 (mesophytic forest on moist/wet soils; visualized in Fig. 3.3) indicate a minor vegetation belt. This fits as well for the Vegetation Unit 6 (representing sun-exposed sandbanks in coastal environments; Fig. 3.3). On edaphically drier slopes on mid and high elevation (Peet, 1988; Price and Harden, 2013), the mixed mesophytic forest is replaced by conifers, since they have advantages over angiosperms on drier and nutrient-limited slopes (Sperry et al., 2006). The relative amount of bisaccate pollen grains in the sediments from Site M0027 depicts a distant source area (Fig. 3.3). It is evident that *Pinus* and *Picea* have grown in lower altitudes of the western Canadian Arctic during the middle Miocene (Williams et al., 2008) and the recent single living species *Cathaya argyrophylla* does not reflect the once widespread ecological range of the genus (Liu and Basinger, 2000). The lack of *Cathaya* in other Miocene North American formations, with exception of the Clarkia formation of Idaho (Kvaček and Rember, 2000), is probably rather related to an assignment of this pollen grain to other Pinaceae, probably to the genus *Pinus* (as in Kotthoff et al., 2014) than to an absence of the taxon (for pollen morphological description see: Liu and Basinger, 2000; Grímsson and Zetter, 2011). Between 15.8 and 15.6 Ma (Sequence m5.3) the spreading of the Vegetation Units 1 and 2 correlate negatively with the marine vs. terrigenous flux and reflect a shorter site-shoreline distance. It is highly unlikely that the spreading of these phytocoenoses is related to the Mi-2 event, which took place at ~16.3 Ma (Wright et al., 1992, Browning et al., 2013). Sequence m5.3 was deposited during the MMCO. The spreading of the mid- and high-vegetation units is perhaps an indirect signal of the uplift of the Appalachian mountain chain, which probably occurred during deposition of Sequence m5.3 (Gallen et al., 2013; Liu, 2014). An increased sedimentation occurred around ~15 Ma along the eastern Atlantic margin, indicating that the eastern flank of the Appalachians reached a maximum elevation around this time (Liu, 2014). Increased physical weathering is typical for tectonically active regions (Lyons et al., 2005) and limits the formation of depth of the soil horizon (Carey et al., 2005). Conifers predominantly occur on such shallow nutrient-poor soils (Farjon, 2010). The probably enlarged

area with infertile soils led to an increase of the conifer forests. This probably would have made it easier for the comparatively heavy *Larix* pollen grains to reach the marine realm, and thus explain why such grains are frequently occurring in the sediments of Sequence m5.3.
The relative increase and diminution of bisaccate pollen grains in Sequence m4.5 (~13.5 to ~13.2 Ma) and m4.1 (~13.0 to ~12.7 Ma) is probably predominantly a taphonomic transport signal. These changes correspond well with the fluctuating P:D ratio (reflecting sea-level changes; Fig. 3.3) and the estimated palaeo-water depth (Katz et al., 2013) and do almost certainly not signalize a floristic reversal triggered by climatic shifts.

3.4.2 The Cupressaceae

The Cupressaceae family contains genera with wide ecological requirements (Farjon, 2010) and impedes an unambiguous assignment of Cupressaceae pollen grains to vegetation units. The Cupressaceae with papillate pollen grains contain genera like *Taxodium*, *Metasequoia*, *Sequoia* or *Cryptomeria*, whereas genera like *Juniperus*, *Cupressus* or *Thuja* are assigned to the non-papillate pollen morphotype. During the Miocene, taxa like *Taxodium*, *Sequoia*, or *Glyptostrobus*, have been widespread (Manchester, 1999) and show a strong affinity to habitats in azonal riparian forests or in backswamps, because they prefer moist environments (Farjon, 2010). Plant macrofossils of *Taxodium* sp. are reported from the Miocene Brandywine flora (McCartan et al., 1990), which is situated in close proximity to the NJSS. It is thus most likely that *Taxodium* also existed in the hinterland of the NJSS.
If extended estuarine *Taxodium* swamp forests had existed in the hinterland, pollen grains of this genus would dominate the dataset. Such a pattern is reported from other studies (e.g. Hofmann and Zetter, 2005; Larson et al., 2011). The abrupt shift in Sequence m5.2 (15–14,8 MA), shown in Figure 3.2 and 3.3, were Cupressaceae pollen grains with a papilla encountered in the sediments from Site M0027 co-dominate the pollen assemblage, could mirror a short-term local change and would probably be linked to edaphic changes. *Taxodium*, for example, can form forests of nearly pure stands (Conner and Brody, 1989; Dicke and Toliver, 1990; Farjon, 2010) in permanently inundated areas (Conner and Brody, 1989; Dicke and Toliver, 1990) or in areas with longer flooding durations (Townsend and Walsh, 2001; Donders et al., 2005). Increased soil moisture content could have fostered the development of a swamp forest dominated by Cupressaceae. *Nyssa*, a co-dominant tree species in wetlands (Dicke and Toliver, 1990) was not as widespread in the hinterland of the NJSS during deposition. The bottomland forest (mixed mesophytic forest on moist/wet soils) does not show a coeval increase. It rather reflects a reversed correlation with the Cupressaceae of the papillate type (Fig. 3.2 and 3.3). This is probably connected to the lower tolerance of bottom hardwood tree species like *Liquidambar* or *Symplocos* to longer hydroperiods (Townsend and Walsh, 2001; Donders et al., 2005).
The relative high amount of pollen grains assigned to the non-papillate morphotype encountered in the same time interval could belong to the genus *Juniperus*. This genus is usually assigned to seasonal arid environments because the majority of species with an affinity to such habitats. However, several recent species of *Juniperus* are adapted to river mouths in vicinity to the ocean (e.g. *Juniperus virginiana* var. *silicicola*) or grow on sand dunes in wet coastal areas (Farjon and Filer, 2013). Thus, we cannot rule out that an amount of pollen grains assigned to the Cupressaceae of the non-papillate morphotype derived from Cupressaceae members, which were adapted to suchlike habits. Some of the pollen grains assigned to the non-papillate morphotype

could also derive from several genera of the Taxaceae family as well. The recent living species *Taxus canadensis* for example can flourish in bogs (Farjon and Filer, 2013). Additionally it is assumed that *Torreya taxifolia* and *Taxus floridana* once had a wider distribution area than today; both grow in the shelter of humid broadleaved forests, but on the other hand they are not adapted to longer hydroperiods (Farjon and Filder, 2013). We can also not rule out that a small amount of Cupressaceae pollen grains assigned to the non-papillate type encountered in Sequence m5.2 could belong to the papillate morphotype of the Cupressaceae pollen grains. Pollen grains were often strongly misshapen, which probably covered the papilla.
According to the relatively low diversity within Sequence m5.2 (Shannon-Wiener Index and Fisher´s alpha diversity index, Fig. 3.3), higher fluvial influence, which probably could have increased the Cupressaceae pollen grain transport into the marine realm, can be excluded as a further explanation. The lithology of this sequence reflects a close vicinity to the coast (Miller et al., 2013a) and the reconstructed high sea level is consistent with coastal flooding (McCarthy et al., 2013) that might have favoured an elevated input of Cupressaceae pollen grains, which probably derived from a swamp forest.

3.4.3 Floristic implication and comparison of contemporaneous mesic forest types and other Miocene formations

The present-day New Jersey vegetation reveals floristic relationships between eastern Asia and North America by the occurrence of today disjunct plant genera such as *Liquidambar*, *Nyssa*, *Pachysandra*, *Symplocos*, and *Magnolia*. The abundances of *Quercus*, *Carya*, and *Pinus* pollen grains in the New Jersey Site M0027 record are comparable to a modern oak hickory forest in eastern North America (Dyer, 2006; Williams et al., 2006). This is consistent with the findings of abundant taxa in previous studies on eastern North American Miocene formations (Rachele, 1976; Owens et al., 1988; Groot, 1991; Pazzaglia et al., 1997). The late-Mid-Miocene vegetation of the NJSS hinterland is similar to the mesophytic forest of the Sino-Japanese Floristic Region (Manchester et al., 2009), which is characterized by contemporaneously endemic growing plant genera like *Cathaya*, *Sciadopitys*, Engelhardioideae (*Engelhardia*), *Pterocarya*, *Alangium*, and *Eucommia*. Additionally, several rare plant genera like *Lonicera*, *Reevesia*, *Alangium*, or *Diospyros* are shared with distantly deposited formations like the Shangwang Formation in China (Liu and Leopold, 1992) or the Usibelli Group of Alaska (Leopold and Liu, 1994). The microfloristic assemblage of Site M0027 shows a typical composition of the once widespread mixed mesophytic forest of the Northern Hemisphere (Tiffney and Manchester, 2001; Milne and Abbott, 2002). In addition, the microfloristic composition shows affinities to present-day eastern Mexico, which also reflects a Cenozoic relict area of the mesophytic forest (Manos and Meireles, 2015).

3.4.4 Evaluation of the bioclimatic analysis

The palaeoclimate data reconstructed here for the NJSS using bioclimatic analysis (Greenwood et al., 2005; Prebble et al., 2017) indicates humid warm-temperate conditions during the late middle Miocene. Some generated CMMTs are below or near the freezing point, but with large uncertainties (Fig. 3.4). Low mean annual winter temperatures are a major stress factor for plant distribution (Woodward and Williams, 1987; Prentice et al., 1992). The microfloristic spectrum is dominated by pollen grains derived from temperate plants. These taxa have the

ability to tolerate occasional frosts due to their physiological and morphological perception. Representatives of Symplocaceae and Ebenaceae are minor components in the sediments from Site M0027A. Today, these families are mainly distributed in the tropics and subtropics, but also contain deciduous, temperate outliers like *Diospyros* and *Symplocos* (eFloras, 2008). Representatives of both genera at the NJSS during the analysed time interval were most likely temperate and deciduous and would have tolerated the prevailing CMMT conditions. The Sapotaceae and *Alangium* (Alangiaceae) do not solely thrive in pantropical regions (Pennington, 2004; eFloras, 2008; Feng et al., 2009). *Alangium chinese* for example, extends into temperate regions (Feng et al., 2009). The Engelhardioideae probably had a greater ecological range during the Cenozoic (Kvaček, 2007), and modern species of *Reevesia* (Malvaceae) flourish in seasonally drier pantropical regions (Fang et al., 2011) of Asia and Mexico (eFloras, 2008). In modern subtropical areas and tropical semi-deciduous forests, episodic frosts frequently occur (Larcher, 2005). This implies that all taxa could have persisted the calculated CMMTs.

The estimated CMMTs of variation 2 (*Taxodium/Glyptostrobus* and *Sequoia* excluded) have the largest estimated range of temperatures (> 5°C; Fig. 3.4). In areas which are occupied by *Quercus*-dominated forest formations, winter temperatures around the freezing point occur, though without persistent snow cover (Box, 2015). The broad climatic CMMTs values estimated in the framework of this study (reconstruction variation 2, Fig. 3.4) are partly tied to the removing of climate-sensitive taxa like *Taxodium*/*Glyptostrobus* or *Sequoia*. Reconstructions excluding these taxa are discussed here considering the ongoing discussion whether Cupressaceae are distinguishable or not. If *Taxodium*/*Glyptostrobus* and *Sequoia* were included, the error ranges of the estimated values (Fig. 3.4) would be reduced and especially the generated CMMTs would be in average 2°C higher. An additional parameter, which often leads to a broad range of estimated climate values in allochthonously deposited taphocoenoses, is the mixture of plants of different climatic origins (Fauquette et al., 2006; Jiménez-Moreno et al., 2010). However, in this investigation the broad range of estimated climate values is mainly based upon the fact that most of the identified plant genera have broad climatic tolerances. Nevertheless, the zonal vegetation reflects a humid warm-temperate climate. Pollen grains probably originating from high altitudes (e.g. *Picea*, *Larix*) were excluded from the estimates. However, the presence of mid- and high-altitude taxa implies in all analysed sequences a topographical temperature gradient. The best estimated values, reflected by the smallest ranges, are generated for annual precipitation indicating humid conditions during time of deposition. Taking all parameters together, a typical humid warm-temperate climate or Cfa climate sensu Köppen-Geiger (Kottek et al., 2006) prevailed and enabled the mixed mesophytic forest to dominate the hinterland during the analysed time interval. The climatic concept is emphasised by the overwhelming amount of *Quercus* pollen grains, even considering that *Quercus* is a copious pollen grain producer.

3.4.5 Regional and global floristic and climatic implications

Comparing climatic conditions among other Miocene deposits and the New Jersey hinterland, a roughly similar climatic pattern is observed from the Shangwang Formation in China (deposited during the first part of the MMCO; Liu and Leopold, 1994; Sun et al., 2002; Yang et al., 2007). This is probably induced by a similar main composition of the floristic elements of the mesophytic forest (Fagaceae, Juglandaceae) and the occurrence of several rare taxa like

Lonicera, *Reevesia*, *Alangium* or *Diospyros* (Liu and Leopold, 1992) in both our Site M0027 record and the Shangwang Formation. The comparability of both records may be delimited though: Sediments of the Shangwang Formation have been deposited in a hilly landscape representing an early MMCO local climate (Sun et al., 2002). Nevertheless, the hinterland of the NJSS and the Shangwang Formation have similar palaeoclimatic conditions during the MMCO, but differ in their present-day respective climate conditions (Lieth et al., 1999; Kottek et al., 2006). Liu and Leopold (1992) state that the present-day montane floristic compositions along the Yangtze River are similar to those encountered in the Mid-Miocene Shangwang Formation. Today, the humid warm temperate climate regime, or Cfa climate (Kottek et al., 2006), still controls the Atlantic coast of southeast North America and southeast Asia (e.g. area along the Yangtze River, Honshu Island) and corresponds well with the modern relict distribution of the mesophytic forest (Milne and Abbott, 2002).

The selected climate interval covers the time span of the second half of the MMCO and the transition to global cooler conditions. During the time intervals of the late Mid-Miocene represented in our Site-M0027 record, a humid warm temperate climate regime prevailed in the New Jersey hinterland. While dinoflagellate cyst assemblages from the NJSS (McCarthy et al. 2013) seem to represent the subsequent gradual cooling phase after the MMCO (e.g., Flower and Kennet, 1994; Shevenell et al., 2008) it is not reflected in the pollen-based bioclimatic analyses presented here. The global cooling events Mi3-a and Mi3-b, which occurred around ~14.2 Ma and ~13.8 Ma (Miller et al., 1996; Abels et al., 2005; Donders et al., 2009), are not reflected in our record because the respective time interval lies between Sequences m5.2 and m5.

In the second half of Sequence m5, bisaccate pollen grains of the mid-altitude conifer forest increased, but the P:D ratio does not show a coeval strong increase. Thus, this signal may not be caused by transport-related bias, but instead reflect a real cooling event, which resulted in pushing conifer taxa adapted to cool conditions to lower elevations. The subsequent increase of bisaccate pollen grains in Sequences m4.5 and m4.1 could be related to cooler conditions after the MMCT, but this signal is dubious because it could be caused by transport effects (see section 3.4.2). In any case, our record implies that humid warm temperate climate conditions predominated also after the MMCT in the hinterland of the NJSS. This is particularly noteworthy since the results of McCarthy et al. (2013) and Katz et al. (2013) imply that Sequences m4.5 and m4.1 have been deposited during intervals of lower sea level and cooler conditions in the marine realm.

Climate models run by Herold et al. (2011, 2012) indicated that the North American Atlantic coastal region was in general not as climate sensitive in the Miocene as it was in other regions, for example Europe. In particular, the buffering effect of the proto-Gulf Current loop (Pinet et al., 1981) influenced the climate and vegetation cover of this region (see below). Additionally, the rejuvenation of the Appalachian mountain chain (Gallen et al., 2013; Liu, 2014) probably took place during time of the deposition of the analysed sediments at Site M0027 (Kotthoff et al., 2014). However, the impact of the Appalachian uplift on the regional climate was probably not as pronounced on the eastern as on the western side of the Appalachian Mountains, due to the proximity of the NJSS hinterland to the Atlantic Ocean. To the west of the Appalachians in Montana, Nebraska and Wyoming, open habitat grass-dominated vegetation was expanding, although the cause of this shift is equivocal (Strömberg, 2005; Chen et al., 2015).

Kotthoff et al. (2014) assumed that the uplift of the Appalachian Mountains influenced their bioclimatic analyses for the investigated geological time, resulting in a blurring of the impact of

the MMCO. The mountain uplift could have reduced the suitable areas for thermophilous taxa and thus also the probability that the respective pollen grains are found in the palynological samples. Consequently, the bioclimatic reconstructions would then yield lower temperatures during the uplift phase. However, considering the high counting sums achieved in our new study, and considering that areas suitable for thermophilous taxa would probably still be present in the coastal lowlands, this mechanism appears questionable for our record. The comparability with investigations of climate development in Europe during the Miocene (e.g. Böhme et al., 2007) is difficult because of the reliability of the method used (Grimm and Denk, 2012). However, compared with a south hemispheric pollen based climate reconstruction (Prebble et al., 2017), the NJSS shows much cooler climatic conditions. In both investigations, the same bioclimatic analysis was applied. A terrestrial membrane lipids-based climate record of north Europe shows 5-7 °C warmer temperatures as well throughout this interval (Donders et al., 2009), compared to our record from the hinterland of the NJSS.

The regional climate conditions of the NJSS hinterland probably was balanced by the thermal influence of the Gulf Stream, even though the timing of the onset and intensification of the Gulf Stream is still controversial (e.g. Kaneps, 1979; Mullins and Neumann, 1979; Pinet et al., 1981; Mullins et al., 1987). It is assumed that it is most likely connected to the closure of the Isthmus of Panama (Potter and Szatmari, 2009) during the late Miocene and early Pliocene (Coates and Obando, 1996).

Similar stable terrestrial ecosystem conditions over the MMCO and MMCT are reported from Iceland (Denk et al., 2013) and from Hungary (Erdei et al., 2007). The terrestrial environment in these regions was either also influenced by the Gulf Stream (Denk et al., 2013) or was stabilized by volcanic activity (Erdei et al., 2007). Similarly, climatic estimates from New Zealand show also a muted MMCT signal (Prebble et al., 2017).

In all these studies the shift to cooler conditions is delayed by several million years. In case of the hinterland of the Atlantic Coastal Plain, the floristic depletion related to climatic turnover is probably likewise delayed and most likely linked to decreasing winter temperatures during the late Pliocene or early Pleistocene, as also suggested by Wing (1998). In New Zealand for example, distinct decreasing winter temperatures were responsible for the climatic turnover during the latest Miocene and Pliocene (Prebble at al., 2017).

Plate. 3-II LM images of selected pollen grains and spores of different vegetation units. A. *Persicaria* (212.93 mbsf), B. *Pachysandra* (215.06 mbsf), C. Lamiaceae (218.23 mbsf), D. *Viscum* (217.83 mbsf), E. aff. Liliaceae: middle view (213.95 mbsf), F. aff. Liliaceae: same pollen grain as 5: upper view (213.95 mbsf), G. *Reevesia* (255.88 mbsf), H. Castaneoideae (222.79 mbsf), I. *Vitis* (208.75 mbsf), J. *Lonicera* (214.67 mbsf), K. *Morella*/*Myrica* (252.16 mbsf), L. *Polygala* (257.55 mbsf); M. Onagaceae (214.93 mbsf), N. *Viburnum* (209.39 mbsf), O. Anacardiaceae (207.07 mbsf), P. Cyperaceae (214.15 mbsf), Q. *Polygonum* (211.35 mbsf), R. Apiaceae (217.83 mbsf), S. *Artemisia* (257.56 mbsf), T. Fabaceae (252.16 mbsf), U. Engelhardioideae (235.92 mbsf), V. *Ulmus* (217.83 mbsf), W. *Eucommia* (235.92 mbsf), X. Polypodiaceae (218.83 mbsf), Y. *Osmunda* (237.87 mbsf), Z. Trilete spore indet. (215.35 mbsf), Aa. Pteridaceae indet. (214.15 mbsf). Scale bar = 10µm.

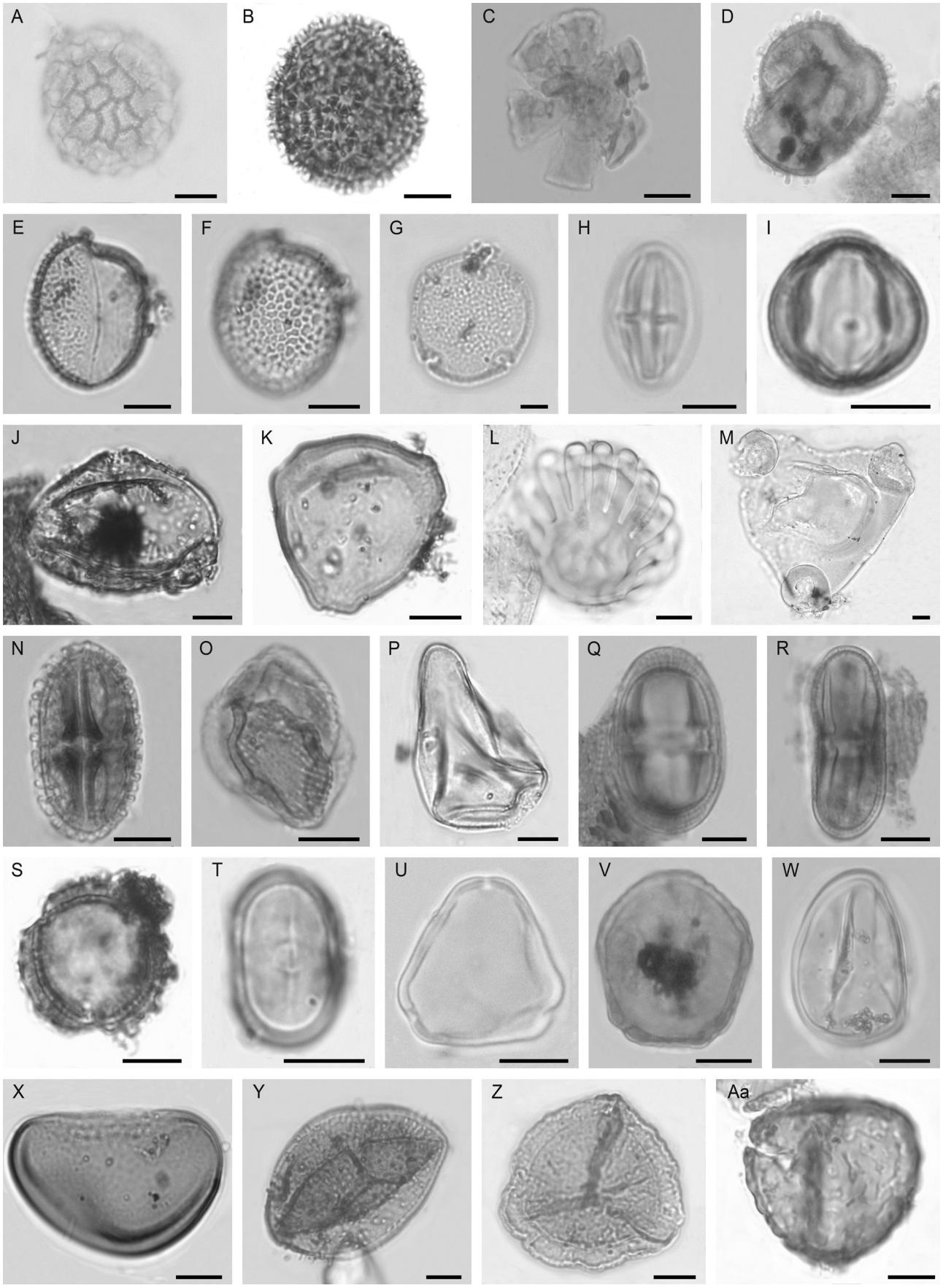

Plate. 3-II

Plants in movement – Floristic and climatic characterization of the New Jersey hinterland during the Palaeogene-Neogene transition in relation to major glaciation events

4.1 Introduction

At the Eocene-Oligocene boundary (EOB) at ~33.7 Ma global climate began to transform from a greenhouse to an icehouse state (Zachos, et al., 2001b; Pagani et al., 2005; Eldrett et al., 2009). Various mechanisms are under debate as to what caused the large-scale glaciation of Antarctica around the first Oligocene isotopic event (Oi-1 event), including the opening of the Drake Passage (Scher and Martin, 2006), the decline of atmospheric carbon dioxide concentrations (Pagani et al., 2005), and orbital forcing (Coxall et al, 2005). The Oligocene is marked by a series of eight unipolar glaciation periods (Pekar et al., 2002), during which Antarctica experienced ice sheet growth, resulting in large glacioeustatic sea level fluctuations (Pekar et al., 2002; Wade and Pälike, 2004; Pälike et al., 2006; Pekar et al, 2006). Waxings and wanings of Eastern Antarctic ice sheets (EAIS; Zachos et al., 2001) during the Oligocene were not all of the same magnitude. The strongest glacial episode during this epoch is represented by the Oi-2b event (27.0 Ma – 26.6 Ma; Pekar et al., 2006) (Pälike et al., 2006), which resulted in a glacioeustatic lowering of ~45 m (Pekar et al., 2002). These climate oscillations are attributed to insolation changes associated with orbital forcing (Wade and Pälike 2004; Pälike et al., 2006).

The inception of the Miocene isotopic event 1 (Mi-1 event), the second largest climatic aberration since the Oi-1 event (Lear et al., 2004), coincides with the Oligocene-Miocene boundary (OMB) at 20.03 Ma (Liebrand et al., 2011). It represents the first and largest cooling episode during the Miocene with a sea-surface temperature decline of ~ 2 °C occurring prior the event (Lear et al., 2004). Mechanisms behind this global cooling event are probably related to late Oligocene atmospheric carbon dioxide levels being near to those of modern times (Pagani et al., 2005; Roth-Nebelsick et al., 2014) and orbital forcing (Zachos et al., 2001; Pälike et al., 2006).
From a terrestrial perspective, the equator to pole climatic gradient became more pronounced since the Oi-1 global event, resulting in a predominantly temperate climate in the mid latitudes of the Northern Hemisphere (Hably et al., 2000). This time interval was important for a renewal of the North American (Graham, 1999) and other floras (e.g. Eldrett et al., 2009). Most records of early Oligocene age from the mid latitudes of Europe indicate a prevailing deciduous vegetation character with intermixed Eocene floristic elements like *Eotrigonobalanus* (e.g. Velitzelos et al., 2014). Only a few early Oligocene records imply highly diverse broad-leaved macrofloristic assemblages in the mid latitudes (Kovar-Eder, 2016). Terrestrial records of the Southern Hemisphere indicate an increase of temperate tree taxa in the fossil record too, with *Nothofagus* being the dominant taxon (e.g. Prebble et al., 2017).

Most information about the floristic and climatic history of the Oligocene of North America is derived from western (e.g. Meyer and Manchester, 1997; Grímsson et al., 2016b) and interior deposits (e.g. Wolfe and Schorn, 1989; 1990) of the continent. For the early Oligocene, records

from the western part of North America document a dominance of temperate climates, promoting the growth of deciduous forests with a small portion of broadleaf evergreens in the understorey (Meyer and Manchester, 1997) and persistent single warmth-loving elements of the Eocene (Grímsson et al., 2016b). At the same time, intensifying seasonality triggered the development of open landscapes and dry conifer woodlands in the interior of the country (Wolfe and Schorn, 1989; 1990). By the end of the Oligocene, the prevailing climate determined the formation of open grasslands in the western interior of North America (Retallack, 2004; Strömberg, 2005).

The palaeofloristic and terrestrial environment of eastern North America is not well understood due to a scarcity of fossil Oligocene floras (e.g. Frederiksen, 1991b). Generally, terrestrial palynomorphs deposited in marine and continental sediments are well suited for the reconstruction of palaeoclimate (e.g. Eldrett et al., 2009), palaeovegetation (e.g. Kmenta and Zetter 2013) and biogeographic history (e.g. Grímsson et al., 2016b). Sediment cores drilled in the framework of the Integrated Ocean Drilling Program (IODP) Expedition (Exp.) 313 to the New Jersey Shallow Shelf (NJSS) allowed for the reconstruction of Oligocene and Miocene terrestrial ecosystem development in eastern North America. The recovered deposits contain generally well preserved marine and terrestrial palynomorphs. Furthermore, a robust age model (Browning et al., 2013) was developed for these cores. Kotthoff et al. (2014) gave an overview of the OMB, including the related Mi-1 cooling event indicated by temperature decline and conifer expansion. However, only a few records world-wide (e.g. Prebble et al., 2017) deal with the response of plant cover to Oligocene global climatic oscillations. Because global climate changes do not affect all regions at the same scale, biotic responses may differ from one environment to another (Utescher et al, 2015). Climate models indicate more constant conditions for the Atlantic east coast during the Oligocene than for other regions (von der Heydt and Dijkstra, 2006), implying a restricted vegetation turnover for the hinterland.

In these contexts, we have evaluated the regional floristic behaviour of the NJSS hinterland to provide a more detailed insight into a mid-latitude terrestrial system during the middle Oligocene and the early Miocene and thus to contribute to a better understanding of patterns of plant persistence/migration.

4.2 Material and methods

4.2.1 Geological setting: Site M0027

Selection, age model and core sediment description

Our study focuses on sediments from Site M0027 recovered during IODP Expedition 313 to the New Jersey Shallow Shelf (NJSS). The drilling position of Hole M0027A is at 39°38.046'N and 73°37.301'W at 33.5 m water depth and at a site-shoreline distance of 40 km (Fig. 1.4). Site M0027 is the only of three recovered sites containing Oligocene sequences (Browning et al., 2013; Miller et al., 2013a, 2013b).

The age model is based on calcareous nannofossils, dinoflagellate cysts, planktic diatoms, Sr isotopes, and sequence stratigraphy (Browning et al., 2013; Miller et al., 2013a). The sampled part of the Oligocene is not well resolved in the seismic profile (Browning et al., 2013; Miller et al., 2013a, 2013b), either because of the minimal lithological expression or the increasing burial

depth; however, Oligocene sequences were identified via core and log inspections (Browning et al., 2013; Miller et al., 2013a, 2013b).

The analysed core sediments comprise four sequences, which correlate with sea level high stands, while no sediments were deposited during sea-level lowstands (likely connected to glacial phases). Sequence O3 (617 to 538.68 mbsf), the oldest analysed sequence, was deposited between ~29.3 to ~28.2 Ma (late Rupelian/Chattian; Fig. 4.2). This sequence contains two intra-sequences, which are tied to facies changes: Sequence o.1 at 596.3 mbsf (~29.0 Ma) and Sequence o.5 at 563.0 mbsf (~28.6 Ma; Miller et al., 2013a).

Sequence O6 (538.68 to 509 or 515 mbsf) reflects the uppermost part of the Oligocene and the transition to the early Miocene (Chattian/Aquitanian) and is not visible seismically (Browning et al., 2013 Miller et al., 2013a, 2013b). A coring gap between 509 and 515 mbsf impedes giving a precise upper sequence boundary of O3 and the basal sequence boundary of the early Miocene Sequence m6 respectively (Miller et al., 2013a). Miller et al. (2013a) set a synthetic sequence boundary at 510 mbsf.

The estimated age of sequence O6 is best dated to ~23.5 to ~23.0 Ma and has a potential age error of ~0.25 and ~0.5 Ma. The early Miocene Sequence m6 (509 or 515 to 494.87 mbsf) covers an age interval of ~20.9 to ~20.7 Ma (Aquitanian). Sequence m5.8 (494.87 to 361.28) is dated to ~20.1 to ~19.2 Ma (late Aquitanian/early Burdigalian). Ages of the analysed Miocene sequences m6 and m5.8 have a potential error of ~0.5 to ~1 Ma.

All analysed sequences lie within Lithological Unit VII, comprising coarse-grained to fine-grained sands interbedded with silty clay laminae (Expedition 313 Scientists, 2010b).

Reconstructions by Scotese et al., (1988) imply that the NJSS study area was situated ~2° further south during the Oligocene and Miocene, and reached its modern position between 39° and 40°N during the Pliocene. The onset of significant topography change and significant increase in relief variation of the Appalachian Mountains started at ~20 Ma; prior to this time the Appalachians showed low modifications in relief and elevation (Liu, 2014).

4.2.2 Palynology

Sample processing and analyses

The first part of the sample processing was performed at Brock University (St. Catharines, Canada) following a modified protocol after Bates et al. (1978). For all samples ~5cm³ sediment were disaggregated in 0.02 % sodium hexamethaphosphate, treated with 25 % hydrochloridic acid and subsequently with 48 % hydrofluoric acid (HF) and sieved through a 10 µm Nixon mesh. The processed material was mounted in glycerine jelly. The second part of the sample processing was done at the laboratory of the University of Hamburg using the remainder of the first processing step following a modified protocol from Zetter and Ferguson (2001). Due to the moderate preservation, acetolyzation was performed without chlorination. In several samples, palynomorph preservation was limited so that further chemical treatment (acetolyzation) was completely omitted. In these cases, counting and identification of terrestrial palynomorphs were done using the material solely treated with HF.

Around 300-400 terrestrial palynomorphs were identified using mostly the acetolyzed treated material. For percentage calculations, bisaccate pollen grains were excluded from the reference sum as these grains tend to be overrepresented in marine records (Mudie and McCarthy, 1994; Eldrett et al., 2009).

Additionally, 300 marine/terrestrial palynomorphs were counted separately using the non-acetolyzed material due to sensitivity of gonyaulacoid (autotrophic) dinoflagellate cyst (dinocysts) and most of the thin-walled protoperidinoid dinocysts (heterotroph) are sensitive to acetolysis (Mudie and McCarthy 2006).
The P:D ratio (pollen versus dinoflagellate cyst) is an indicator for transport mechanisms and sea-level fluctuations (McCarthy et al., 2003), where high P:D indicates low sea level and/or enhanced run off. In sum, 56 samples were analysed spanning the time interval of the middle late Oligocene (Sequence O3 and Sequence O6) to the early Miocene (Sequence O6, Sequence m6 and Sequence m5.8). Sequence O3 includes 26 samples, 19 samples were counted for Sequence O6, 10 for Sequence m6 and Sequence m5.8 includes only 1 sample Pollen grain identification and counting were done using a Zeiss Axioscope A1 at 630x magnification.

Additionally, some pollen grains were analyzed via SEM. The diagnosis of pollen grain ornamentation of different infrageneric groups of *Quercus* follows the description of Grímsson et al. (2015) and Bouchal et al. (2014). We applied the Shannon-Wiener-Index (H*(s)*) in order to assess changes in diversity.

a: Fang et al. (2011), b Thomson et al. (2000a, 2000b), c NRC, d GBIF+WorldCLIM
1 high-altitude conifer forest; 2 mid-high-altitude conifer forest. 3 Cupressaceae 4 mesophytic forest growing on well-drained soils; 5 mesophytic forest growing on moist/wet soils; 6 mesophytic understorey; 7 plant community associated to coastal environments, growing on sun-exposed sandbanks.

Table 4.1 Summary of identified taxa for Site M0027 together with sources of climatic range and assignments to vegetation units, alphabetically ordered.

Taxon	Climate source	NLR used	Vegetation unit
Gymnosperms			
Abies	-		1
Cathaya	a	*C. argyrophylla*	2
Cedrus	b		2
Cupressaceae	-		3
Ephedra	-		7
Larix	-		1
Picea	-		1
Pinus subg. *Pinus*	-		2
Pinus subg. *Strobus*	-		2
Sciadopitys	d	*S. verticillata*	2
Tsuga canadensis	b	*T. canadensis*	4
Tsuga caroliniana	b	*T. caroliniana*	4
Angiosperms			
Acer	b	*Acer* spp. (NA)	4
Alnus	-		5
Anacardiaceae	-		4
Apiaceae	-		6
Artemisia	-		6
Betula	-		5
Carpinus/*Ostrya*	b	*Carpinus* and *Ostrya* spp. (NA)	4
Carya	b	*Carya* spp. (NA)	5
Castaneoideae	b	*Castanea* spp./ *Castanopsis chrysophylla*/ *Lithocarpus densiflorus*	4
Cedrelospermum ?	-		extinct 4
Chenopodiaceae/ Amaranthaceae	-		7
Clethra	-		4
Cornus	b	*Cornus* spp. (woody, NA)	4
Corylus	b	*Corylus* spp. (NA)	4
Cyperaceae	-		6
Diospyros	b	*Diospyros* spp. (NA)	4
Elaeagnus	-		4
Engelhardioideae	-		4
Eotrigonobalanus	-		extinct
Ericaceae	-		4
Eucommia	a	*E. ulmoides*	4
Fabaceae	-		6
Fagus	b	*F. grandifolia*	4
Fraxinus	b	*Fraxinus* spp. (NA)	5

Table 4.1 Continued

Gordonia	b	*G. lasianthus*	4
Hamamelidaceae	-		4
Humulus	-		5
Ilex	a	*Ilex* spp. (NA)	5
Itea	b	*I. virginica*	5
Juglans	b	*Juglans* spp. (NA)	5
Juglandaceae	-		4
Liliaceae	-		5
Liquidambar	b	*L. styraciflua*	5
Lonicera	-		4
Magnolia	b	*Magnolia* spp. (NA)	4
Myrica/*Morella*	a	*Morella* spp. (NA)	5
Nyssa	b	*Nyssa* spp. (NA)	5
Oleaceae	-		4
Ostrya	b	*Ostrya* spp. (NA)	4
Parthenocissus	c	*Parthenocissus* spp. (NA)	4
Platanus	b	*Platanus* spp. (NA)	4
Poaceae	-		6
Prunus	b	*Prunus* spp. (NA)	4
Pterocarya	a	*Pterocarya* spp. (China)	4
Quercus	b	*Quercus* spp. (NA)	4
Reevesia	a	*Reevesia* spp. (China)	4
Rhamnaceae	-		5
Rosaceae	-		4
Salix	-		5
Sapotaceae	-		5
Symplocos	b	*S. tinctoria*	5
Tilia	b	*Tilia spp.* (NA)	4
Ulmus	b	*Ulmus spp.* (NA)	5
Ulmus/*Zelkova*	b	*Ulmus* spp. (NA)	5
Vitaceae	-		5
Vitis	-		5
Zelkova	a	*Zelkova* spp. (China)	5
Pteridophytes			
Equisetum	-		5
Lycopodium	-		5
Osmunda	c	*Osmunda* s.l. (NA)	5
Polypodiaceae	-		5

Reconstruction of palaeovegetation and palaeoclimate

Terrestrial palynomorphs were grouped into six artificial palaeovegetation units: 1: high-altitude conifer forest; 2: mid-altitude conifer forest; 3: Cupressaceae; 4: mesophytic forest growing on well-drained soils; 5: mesophytic forest growing on moist/wet soils; 6: mesophytic understorey; 7: plant community associated to coastal environments, growing on sun-exposed sandbanks. Grouping was done according to growing preferences of modern analogues, including soil condition and altitudinal zonation (Tab. 4.1). This superordinate artificial grouping is congruent with the vegetation units of the late Mid-Miocene of the same area (Prader et al., 2017). The generalisation allows inference of shifts within the terrestrial vegetation.

Reconstructions of palaeoclimatic conditions used the bioclimatic analysis after Greenwood et al. (2005) and Prebble et al. (2017), which is based on the nearest living relative concept (NLR). Differences to the likewise NLR-based Coexistence Approach (Utescher et al., 2014) are described in detail in Prebble et al. (2017).

Four different climatic parameters were generated as a standard to characterize the palaeomacroclimatic conditions: mean annual temperature (MAT), coldest month mean temperature (CMMT), warmest month mean temperature (WMMT), and mean annual precipitation (MAP). The generated palaeoclimatic estimates were based on climatic profiles of North American and Chinese species. Climatic profiles were taken from Thomson et al. (2000a; 2000b; 2006) for North American species and from Fang et al. (2011) for Chinese species. Further estimates are based on data from Natural Resources Canada (NRC) and Global Biodiversity Information Facility (GBIF) using WorldClim.

In this study, pollen grains identified at family level only were generally excluded from the palaeoclimate reconstruction. Different representatives of a family can have totally different growing preferences and would generate climatic overlaps of huge range. The Juglandaceae subfamily Engelhardioideae, whose members have a very similar pollen grain ornamentation were as well excluded. Similarly, several genera such as *Alnus* or *Betula* were excluded in a second step since they flourish under heterogenous macroclimatic conditions nowadays.

In the case of the Castanoideae (Fagaceae subfamily), which often are distinguishable via scanning electron microscope (Bouchal et al., 2014), we have generated a climatic envelop of the entire subfamily. The pollen ornamentation of the genera *Morella* and *Myrica* (Myricaceae) are identical (Grímsson et al., 2016a) and several former *Myrica* spp. are now included into the genus *Morella* (Herbert, 2005). The climatic profile used for our study is based on *Morella* spp. with exclusion of the boreal genus *Myrica gale* (compare Thomson et al., 2000a, 2000b, 2006). The genus *Craigia* (Tiloideae, Malvaceae), which was widespread during the Cenozoic in the Northern Hemisphere (Bůzek, et al., 1989) but is today restricted to China and Vietnam (eFloras, 2008), has *Tilia*-like pollen grains (Kvaček et al., 2002). However, we used the climatic profile for *Tilia* in this case because the shape of the apertures and the tectum of the analysed pollen grains of Site M0027 referred more to *Tilia* (Plate 4-III, O-P; Plate 4-II, I).

4.3 Results

4.3.1 Terrestrial palynomorphs

Fair preservation of pollen grains allowed for identification of 72 taxa. Table 4.1 gives a summary of all identified terrestrial palynomorphs. Light Micrograph (LM) images of several well-preserved plant microfossils are shown on Plates 4-I and 4-II and Plate 4-III illustrates SEM images of selected pollen grains. Within the 56 analysed samples, *Quercus* is the most abundant taxon, represented by three infrageneric groups: Group Quercus (Plate 4-III C-D), Group Quercus/ Lobatae (Plate 4-III: E-H) and aff. Group Protobalanus (Plate 4-III: I-J). The number of *Quercus* pollen grains reaches > 50 % in most samples, except those at 572.15 mbsf and 570.02 mbsf (Fig. 4.2). In addition, *Eotrigonobalanus* is also part of the microfloristic assemblage (Plate 4-III, K-L). Pollen of the subfamily Engelhardioideae (Juglandaceae) is also abundant (min: 0.4 %, max: 21.7 %) and shows a decreasing trend towards Sequence m6 (20.9 – 20.7 Ma) (Fig. 4.2). Genera such as *Liquidambar*, *Elaeagnus*, *Acer*, *Fagus*, *Nyssa* or *Artemisia* are sporadically present as are spores of pteridophytes. The most abundant palynomorphs are the gymnosperms *Pinus* (0.4 % to 32.7 %) and *Cathaya* (0 % to 27.1 %). Pollen grains of *Pinus* subg. *Strobus* outnumbered *Pinus* subg. *Pinus* in all samples (Fig. 4.2). The subdivision of *Pinus* at subgeneric level and of bisaccate pollen in general was often hindered by limited preservation. The sum of bisaccate representatives fluctuated through the entire analysed time interval and reached the highest relative abundance of 120.8 % at 533.45 mbsf (Fig. 4.3). The Shannon-Wiener Index (H*(s)*), generally varied between 1 and 2 indicating relative low diversity, but shows distinct peaks >2 between 560.01-572.15 mbsf, 529.97-533.54 mbsf and 495.72-495.91 mbsf (Fig. 4.3).

Table 4.2 Summary of average climatic values and average errors of estimated values for each analysed sequence from the middle and late Oligocene and early Miocene (Sequence m5.8 compromise only one analysed sample).

Sequence	MAT [°C]	CMMT [°C]	WMMT [°C]	MAP [mm]
O3	14.0 (±4.1)	4.1 (±5.1)	23.9 (±3.0)	1312.2 (±293.9)
O6	15.0 (±3.6)	5.5 (±5.2)	24.5 (±2.4)	1332.6 (±278.8)
m6	13.8 (±4.8)	4.4. (±6.0)	23.5 (±3.6)	1297.4(±324.2)
m5.8	15.4 (±2.5)	6.1 (±4.0)	24.8 (±1.9)	1359.9 (±270.1)

Plate 4-I LM images of selected pollen grains of identified taxa of Site M0027. A. *Cathaya* (535.46 mbsf), B. *Cathaya* (537.38mbsf), *Cedrus* (518.03 mbsf), D. *Picea* (562 mbsf), E. *Picea* (495.91 mbsf), F. *Larix* (495.91 mbsf), G. *Tsuga canadensis* (570.02 mbsf), H. *Tsuga caroliniana* (574.05 mbsf), I. *Ephedra* (582.02 mbsf), J. *Abies* (579.85 mbsf), K. *Pinus* subg. *Pinus* (560.01), L. *Pinus* subg. *Strobus* (584.92), N. *Sciadopitys* (495.91 mbsf), O. Cupressaceae non-papillate (541.5 mbsf), P. Cupressaceae papillate (495.32 mbsf), Q. Cupressaceae presumably with papilla (541.5 mbsf), R. *Ulmus* (498.54 mbsf), S. *Zelkova* (560.01 mbsf), T. *Liquidambar* (574.05), U. *Acer* (601.88 mbsf), V. *Ilex* (601.88), W. *Juglans* (495.91 mbsf), X. *Pterocarya* (495.72 mbsf), Y. *Carya* (540.3 mbsf), Z. Engelhardioideae (540.3 mbsf), Aa. Engelhardioideae (533.54 mbsf). Scale bar = 10µm.

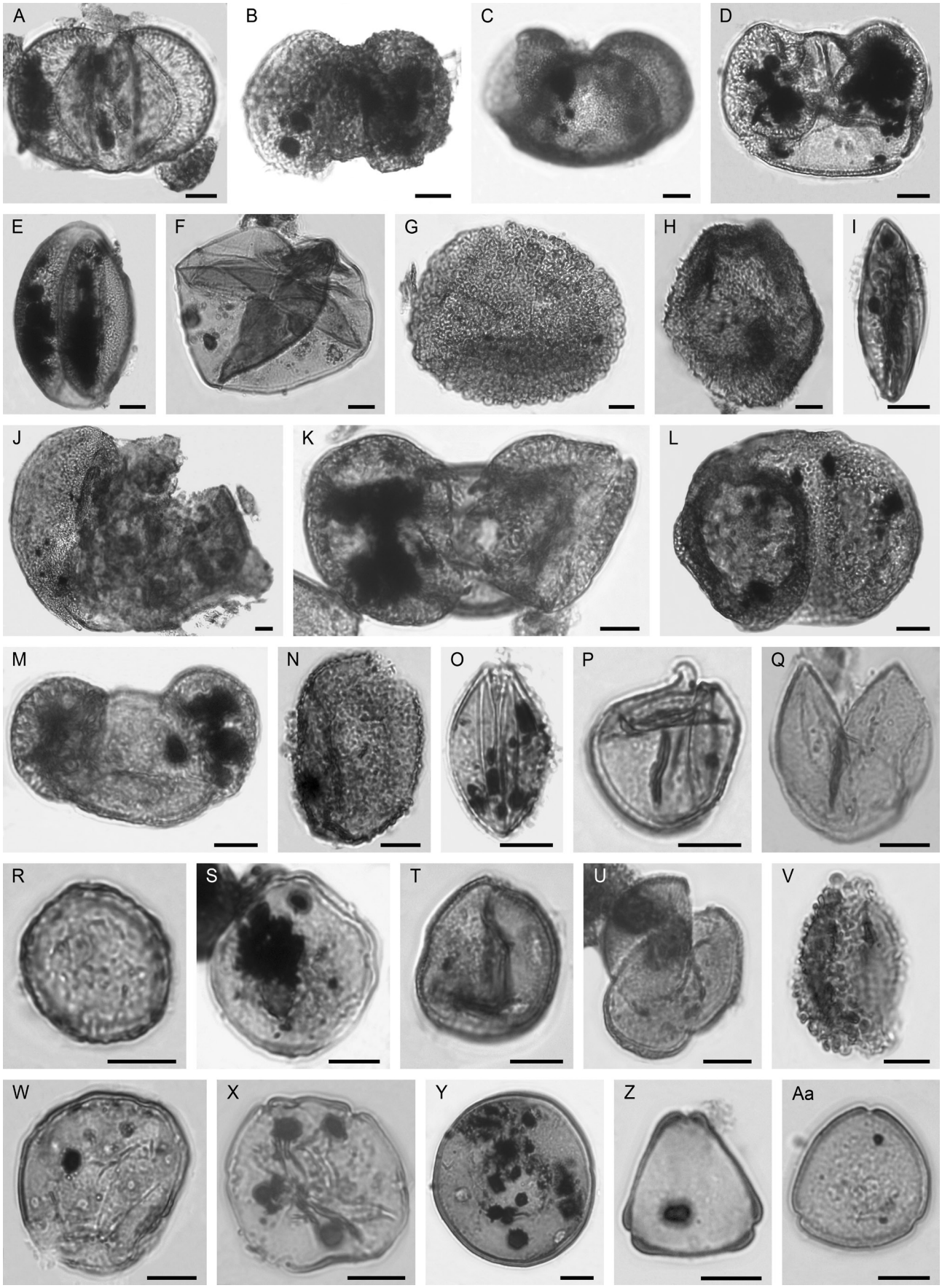

Plate 4-I

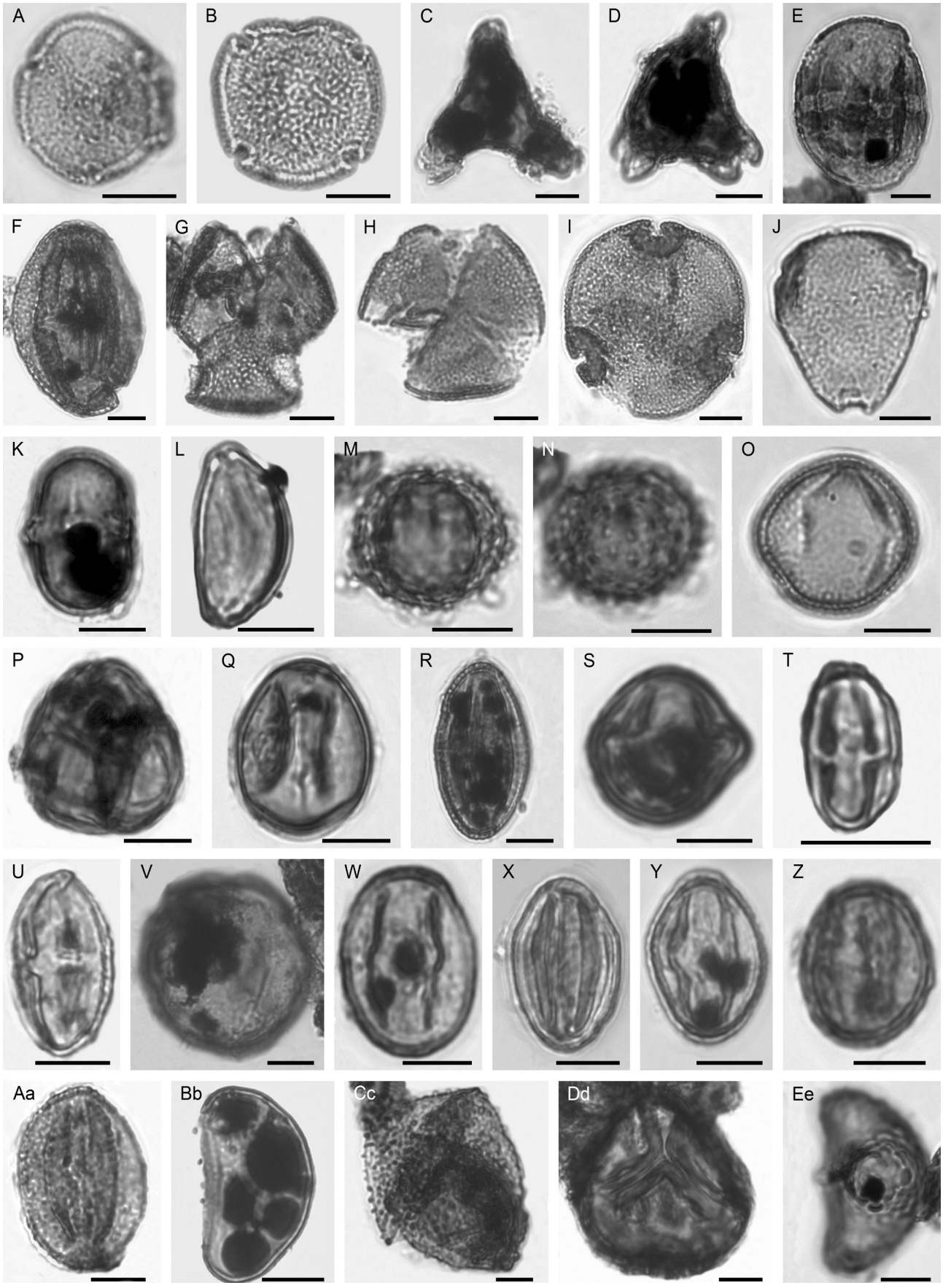

Plate 4-II

Plate 4-II LM images of selected pollen grains of identified taxa of Site M0027A. A. *Reevesia* (591.98 mbsf), B. *Reevesia* (603.58 mbsf), C. *Elaeagnus* (601.88 mbsf), D. *Elaeagnus* (597.94 mbsf), E. Sapotaceae (597.94 mbsf), F. *Gordonia* (600.16 mbsf), G. *Gordonia* (509 mbsf), H. *Gordonia* same pollen grain as in Plate 4-III (574.05 mbsf), I. *Tilia* (597.94 mbsf), J. *Symplocos* (570.02 mbsf), K. Fabaceae (579.85 mbsf), L. *Itea* (584.92 mbsf), M. *Artemisia*: middle view (521.62 mbsf), N. *Artemisia*: upper view (521.62 mbsf), O. *Fraxinus* (611.76 mbsf), P. Ericaceae (520.9 mbsf), Q. *Eucommia* (521.62 mbsf), R. *Parthenocissus* (495.91 mbsf), S. *Clethra* (574.05 mbsf), T. Castaneoideae (494.91 mbsf), U. *Eotrigonobalanus*; same pollen grain as in Plate 4-III (574.05 mbsf), V. *Fagus*; same pollen grain as in Plate 4-III (574.05 mbsf), W. *Quercus* Group Quercus/ Lobatae; same pollen grain as in Plate 4-III, E-F (574.05 mbsf), X. *Quercus* Group aff. Protobalanus; same pollen grain as in Plate 4-III, I-J (574.05 mbsf), Y. *Quercus* Group Quercus same pollen grain as in Plate 4-III C-D (574.05 mbsf), Z. *Quercus* (574.05 mbsf), Aa. *Quercus* (585.7 mbsf), Bb. Polypodiaceae (584.73 mbsf), Cc. *Osmunda* (574.05 mbsf), Dd. Trilete spore indet (509 mbsf), Ee. Spore indet (532.62 mbsf). Scale bar = 10µm.

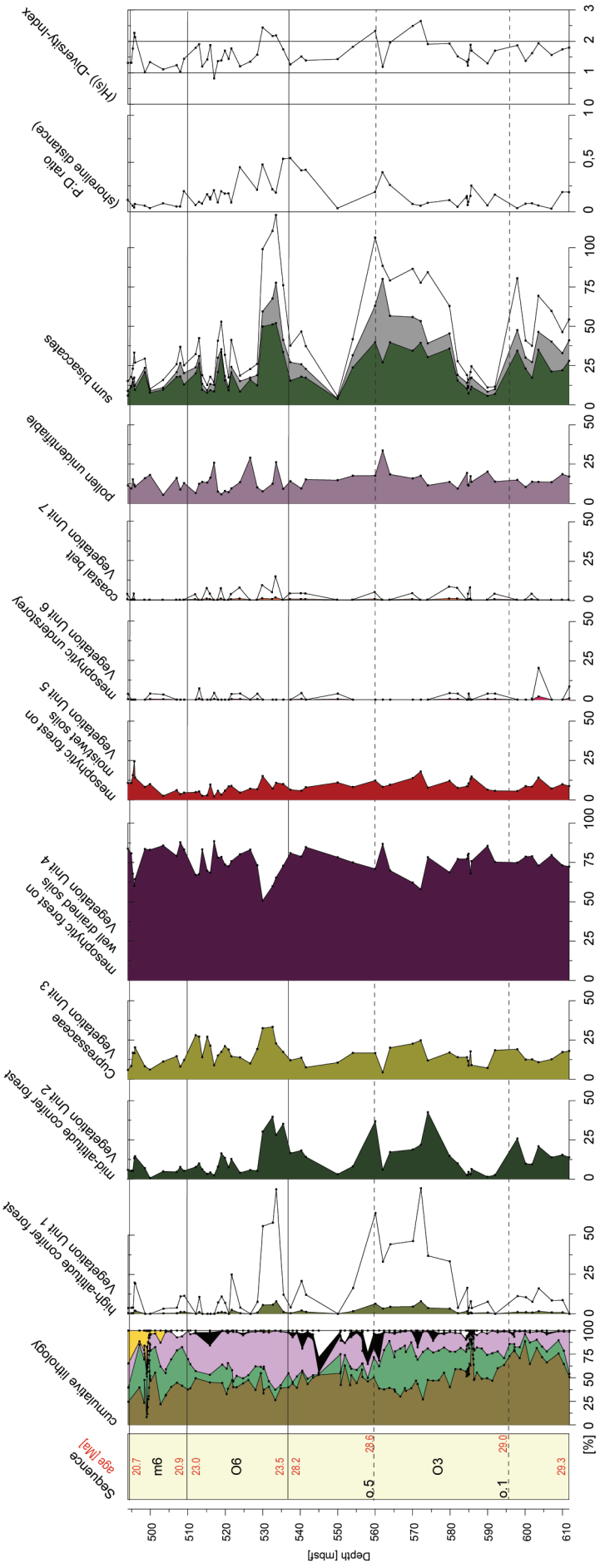

Figure 4.3 Vegetation units of the NJSS hinterland during the middle Oligocene to early Miocene plotted against depth. Taxa are assigned as listed in Table 4.1 (transparent: 10x exaggerated: Vegetation Unit 1, Vegetation Unit 6, Vegetation Unit 7; sum of bisaccates: grey: unassigned bisaccate pollen grains; green: percentages of destroyed parts of bisaccate pollen grains (H*(s)*)-Diversity-Index. Pollen-dinoflagellate ratio (P:D) indicating site-shoreline distance. Sequence boundaries and age model after Browning et al. (2013) and Miller et al. (2013a, 2013b): dashed lines: intrasequences. Cumulative lithology after Miller at al. (2013a): brown: clay and silt; green: glauconite; violet: quartz sand; yellow: medium and coarser quartz sand; black: carbonate; white: mica and other.

4.3.3 Estimated palaeoclimate of NJSS

The bioclimatic analysis indicates humid warm-temperate climatic conditions for the entire dataset (Fig. 4.4). Average estimated MAT for the entire record was 14.6 °C ± 4.0 °C. Palaeoclimatic estimates of CMMT are 5.2°C ± 5.3 °C and of WMMT 24.1°C ± 2.9 °C in average. All average palaeoclimatic estimations of each individual sequence are summarized in Table 4.2. The palaeoclimatic conditions of the New Jersey hinterland remained relatively constant over the preserved interval. Considering each investigated sequence individually, an average weak cooling and warming is reflected within the humid warm-temperate climate. Around the OMB (Fig. 4.4) between ~ 533 mbsf and ~ 529 mbsf a stepwise decline to lower temperatures is reflected (MAT and WMMT ~ -3°C; CMMT ~ -5°C). The only estimated palaeoclimatic parameter which remained fairly constant over the analysed time is MAP (Fig. 4.4), reflecting humid conditions (always >1000mm).

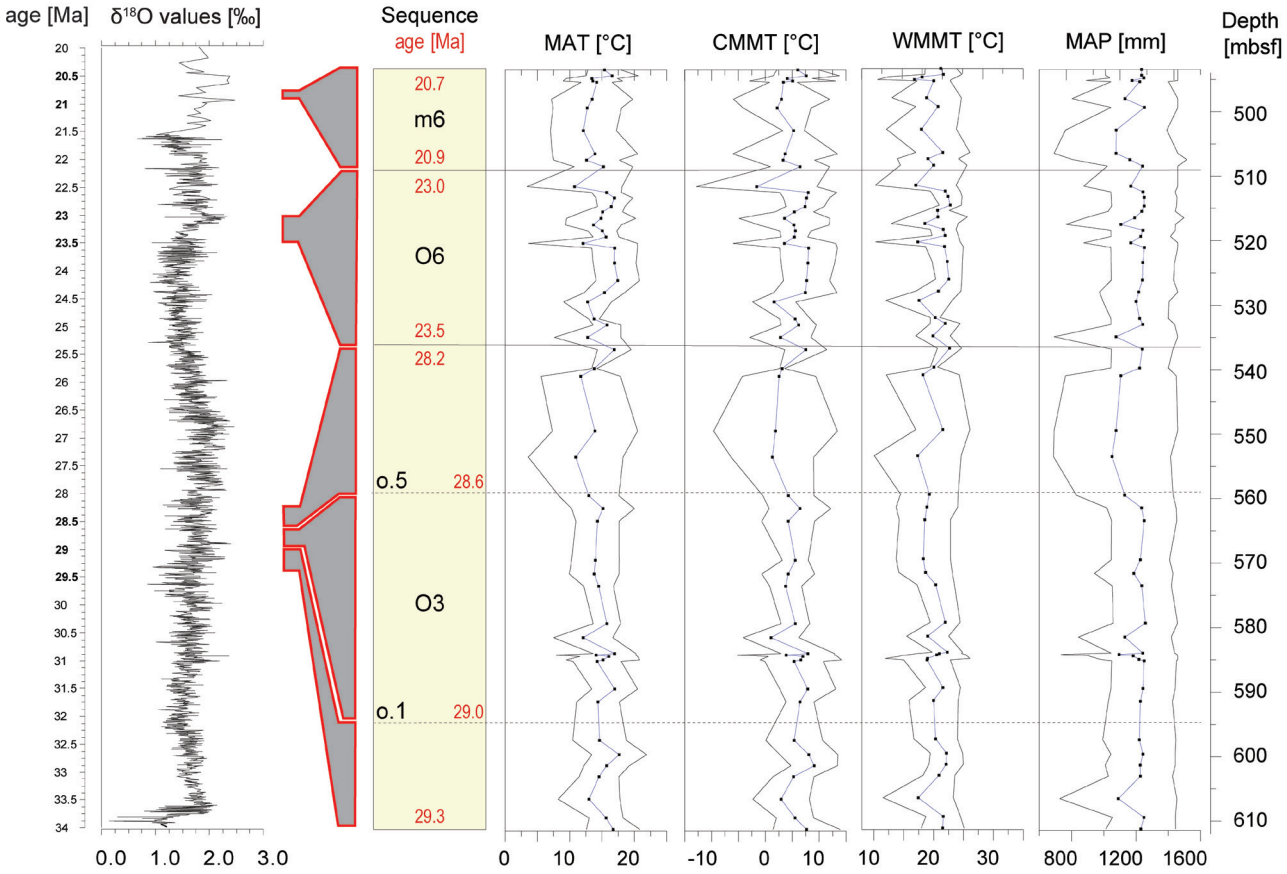

Figure 4.4 Calculated palaeoclimate during the middle Oligocene and early Miocene for the hinterland of the NJSS based on identified pollen grains from Site M0027 following the bioclimatic analysis after Greenwood et al. (2005) and Prebble et al. (2017) plotted against depth. Compared with $\delta^{18}O$ values of ODP Site 1218 (equatorial Pacific) after Wade and Pälike (2004) plotted against age. Please consider the different age models.
MAT: mean annual temperature; CMMT: coldest moth mean temperature; WMMT: warmest month mean temperature and MAP: mean annual precipitation; outer lines: error of estimated values (present day climate parameters of Toms River (New Jersey): MAT 11.7 °C; CMMT: 5.7 °C; WMMT: 17.7 °C; MAP: 1239 mm, after US Climate Data, 2017)

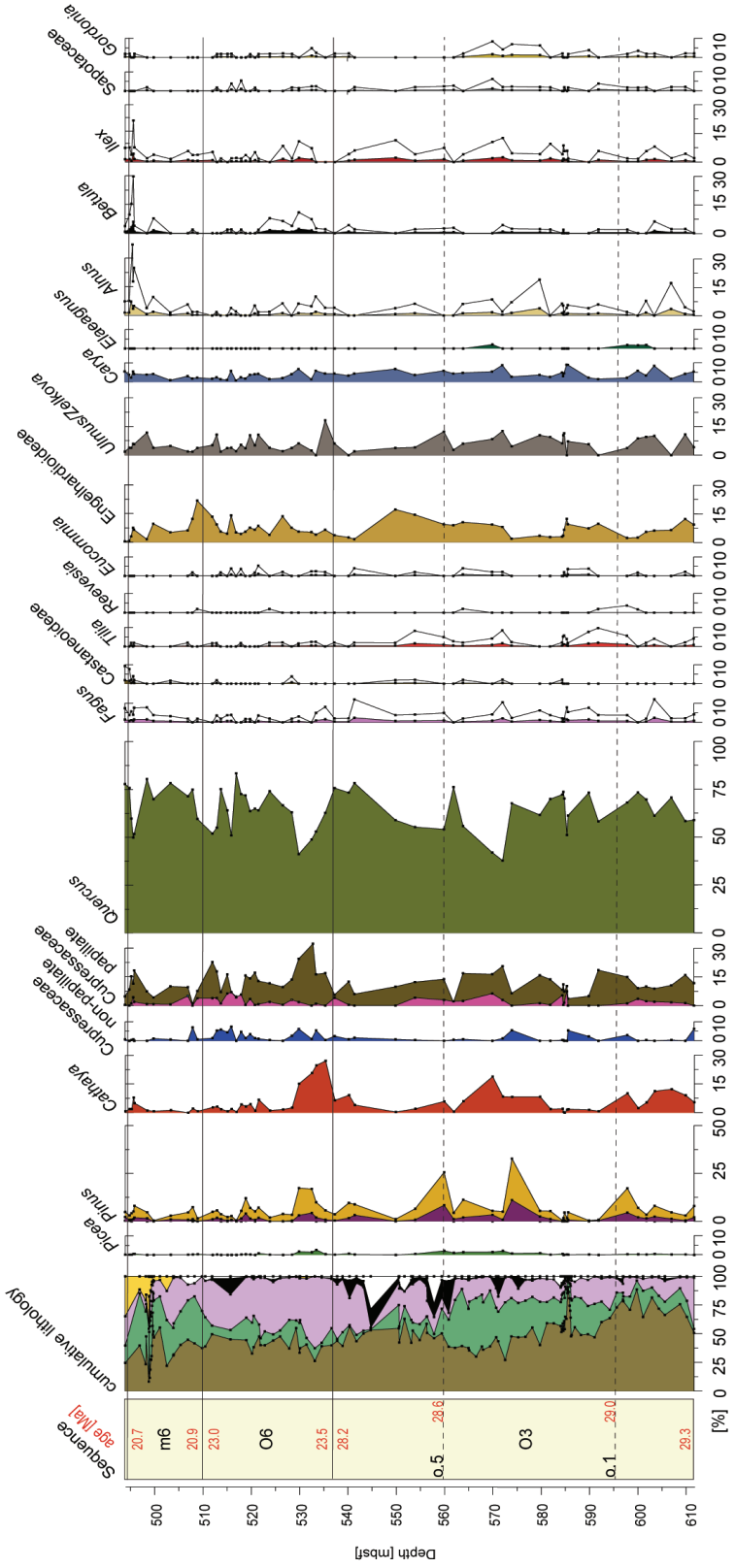

Figure 4.2 Relative abundances of selected pollen grain taxa for Site M0027A plotted against depth (pollen sum excluding bisaccates). Transparent areas in plots of *Fagus*, *Tilia*, *Betula*, *Alnus*, *Ilex*, Sapotaceae, *Reevesia*, *Elaeagnus*, *Eucommia*, *Gordonia* denote 5x exaggerated values. *Pinus* subg. *Strobus*: violet; *Pinus* subg. *Pinus* and unidentifiable *Pinus* pollen grains: yellow. Cupressaceae non-papillate type: blue; Cupressaceae presumably with papilla: pink; Cupressaceae with a papilla: brown. Sequence boundaries and age model after Browning et al. (2013) and Miller et al. (2013a, 2013b) with dashed lines indicating intrasequences. Cumulative lithology after Miller et al. (2013a): brown: clay and silt; green: glauconite; violet: quartz sand; yellow: medium and coarser quartz sand; black: carbonate; white: mica and other.

4.4 Discussion

4.4.1 Taphonomy of terrestrial palynomorphs

Deposition of terrestrial palynomorphs in marine sediments depends on multiple factors (e.g. pollen production, transport mechanisms, shoreline distance; van der Kaars, 2001). Studies concerning deposition of pollen and spores in neritic marine sediments (Mudie and McCarthy, 1994; van der Kaars, 2001) indicate a reliable comparability of the microfloristic assemblage in marine sediments with the contemporary onshore vegetation. Because the palaeo-shelf break only transgressed the Site M0027 during the early Miocene (McCarthy et al., 2013) dominance of bisaccate grains is expected, reflecting their preferential transport in wind and water (McCarthy et al., 2003).

Today the most important transport mechanism of pollen and spores into the marine realm along the North American coast are the westerlies (Mudie and McCarthy, 1994). Prevailing westerly winds were probably already established since the middle Oligocene. A further, but subordinate transport mechanism is pollen input via rivers and streams into the NJSS. Fluvial influence has been identified based on the sedimentological record (Miller et al., 2013a) for the NJSS. Downslope mass transport is not expected to be a major factor at Site M0027 prior to the transgression of the shelf break within sedimentary Unit 6/sequence m5.8 (Fig. 4.5), except during glacioeustatic lowstands – then the ratio of terrestrial vs. marine palynomorphs ("P:D") helps identify resedimentation (McCarthy et al., 2013).

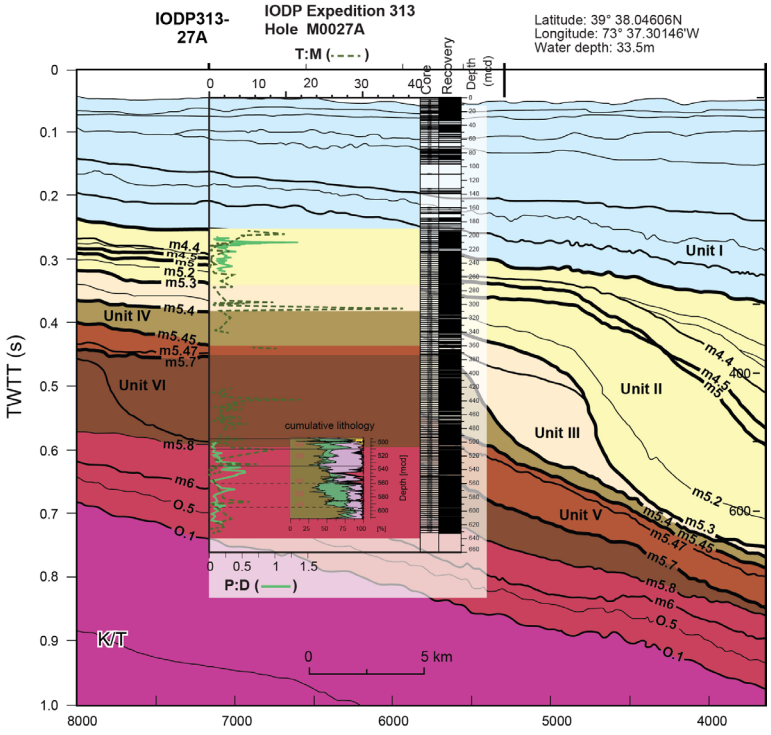

Figure 4.5 Seismic profile through Site M0027 including T:M (terrestrial versus marine palynomorphs after McCarthy et al., 2013), P:D (pollen versus dinoflagellate cyst; this study: Oligocene to early Miocene; late Mid-Miocene after Prader et al., 2017) and cumulative lithology after Miller et al. (2013a). Rapid aggradation (vertical accumulation of sediment at times of sea level rise and high sedimentation rate) and progradation (displacement of coastline and clinoform) across the New Jersey margin is evident in the interpreted seismic record, particularly in the thick Unit VI/ sequence m5.8. The P:D ratio reflects shifts in shoreline distance and major peaks in T:M record pulses of downslope mass wasting associated with glacioeustatic lowstands (Mudie and McCarthy, 1998). Mcd: meters composite depth corresponds with mbsf (meter below seafloor), K/T: Cretaceous-Tertiary boundary. Cumulative lithology: brown: clay and silt; green: glauconite; violet: fine quartz sand; yellow: medium and coarser quartz sand; black: carbonate; white: mica and other.

4.4.2 Palaeoforest composition of the New Jersey hinterland

Our results indicate that the Oligocene hinterland of the NJSS was covered by dense forests, with mesophytic forest growing on dry soils being the most widespread and diverse forest type on areas of low relief. Topographic higher elevations, and/or drier areas were probably inhabited by conifers such as Pinaceae. Oaks (*Quercus* spp.) are the main element dominating the mesophytic forest of eastern North America in the past and at present (Abrams, 1992). Today ~90 different *Quercus* species are found in North America of which ~35 species are present in eastern North America (eFloras, 2008). *Quercus* probably appeared during the early Eocene (Grímsson et al., 2016b and references therein).

A late Eocene to early Oligocene palynofloristic record from southern Mississippi and Alabama (Oboh and Reeves Morris, 1994; Oboh et al., 1996) revealed that oaks became dominant at the Eocene-Oligocene boundary in the southeastern USA, probably indicating a vegetation shift triggered by cooling, as already suggested by Frederiksen (1991b). In North America, the fossil record of *Quercus* implies that four infrageneric groups had existed during the Cenozoic (Denk et al., 2010 and references therein). Three of them persist in the modern North American vegetation, and two of these (Group Lobatae and Quercus) exist east of the Cordillera (eFloras, 2008). The analysed *Quercus* pollen grain sculptures from our study have affinities with Group Quercus (white oaks; Plate 4-III, C-D), Quercus/ Lobatae (white/ red oaks; Plate 4-III, E-H) and aff. Group Protobalanus (golden-cup oaks; Plate 4-III, I-J). These findings suggest the presence of a diverse *Quercus* population at subgeneric level during the Oligocene. Alternatively, the pollen ornamentation of Group Protobalanus may also indicate an ancestral lineage of the Protobalanus-Quercus-Lobatae clade (Grímsson et al., 2015).

The NJSS microfloristic assemblage also suggests the presence of *Eotrigonobalanus* (Plate 4-III, K- L), an extinct Fagaceae lineage. *Eotrigonobalanus* was a typical member of evergreen forests of the Palaeogene and flourished in different ecological habitats (Walther, 2000). The fossil record of *Eotrigonbalanus* in North America is very fragmentary (Grímsson et al., 2016b). In Europe, *Eotrigonobalanus* was an accessory element within the evergreen forest and became dominant during the late Eocene (Walther, 2000). In situ pollen grains from Texas referred to as *Amentoplexipollenites* (late Rupelian to Chattian; Crepet and Nixon, 1989) are very similar with those of our investigation as well as with *Eotrigonobalanus* pollen grains of Central Europe (Denk et al., 2012). After Grímsson et al. (2016) a main characteristic difference between *Amentoplexipollenites* (Crepet and Nixon, 1989) and pollen grains of *Eotrigonobalanus* from British Columbia (Eocene) and Wyoming (Cretaceous) is the much thinner nexine of the latter. Evidence for the existence of *Triogobalanopsis*, another extinct Fagaceae lineage in North America, is known from British Columbia (Eocene; Grímsson et al., 2016b). All analysed pollen grains encountered in this study belonged to *Eotrigonobalanus*, however, we cannot rule out that this extinct lineage flourished in the New Jersey hinterland too.

Oaks are relatively persistent floristic elements within the mesophytic forest when comparing the Oligocene and late Mid-Miocene (Prader et al., 2017); however, significant floristic shifts within the mesophytic forest occurred. Relative abundances of pollen grains of Engelhardioideae or *Carya* in our investigation reveal similar values when compared to data from the eastern coast of the Gulf of Mexico and South Carolina for the late Eocene/early Oligocene (Frederiksen, 1991b; Oboh and Reeves Morris, 1994; Oboh et al., 1996). The recorded

pollen percentages differ significantly from the values revealed for the late Mid-Miocene (Prader et al., 2017).

The Engelhardioideae (Juglandaceae) might have had a greater ecological range in the Oligo-Miocene than reflected by their living representatives (Kvaček, 2007). However, the decreasing relative abundance of Engelhardioideae pollen in the long-term trend from the middle Oligocene to the late Miocene reveals that this group was not as competitive as other taxa concerning environmental changes. Accordingly, this group is not prominent any more in the pollen record of the late Mid-Miocene (Prader et al., 2017). If the drop of relative abundances of the Engelhardioideae was temperature-dependent, subsequent cooling events after the Mi-1 inception were probably necessary to induce the disappearance of the taxon (Prader et al., 2017). In comparison, other tree taxa like *Fagus* or *Liquidambar* were more constant elements of the mesophytic forest of the Miocene (Prader et al., 2017) than during the Oligocene. The fossil records of *Fagus* (Denk and Grimm, 2009) and *Liquidambar* (Manchester, 1999) for the Oligocene are fragmentary. These genera were also not prevalent in the New Jersey hinterland during the analysed time interval.

Fagus appeared the first time in the fossil record during the late early Eocene in western North America (Manchester and Dillhoff, 2005) and was continuously widespread during the late Oligocene in the western part of the continent and Europe (Kvaček and Walther, 1991). Its radiation and diversification led to a first occurrence peak in the Miocene (Denk and Grimm 2009). Our investigations indicate that *Fagus* was only a minor vegetation element in the hinterland of the NJSS during the early Miocene, but was a persistent component during the Mid-Miocene (Prader et al., 2017). Like today, the east coast of North America was never a centre of biodiversity of beeches.
Contrary to *Fagus* and its spatiotemporal distribution, the Atlantic east coast is currently a hot spot of biodiversity of the genus *Carya* (Wen, 1999). In our record, the relative occurrences of this genus were as low as those of *Fagus*. *Carya* first appeared in the Palaeocene in North America (Manchester, 1987) and the first radiation began in the early Miocene (Zhang et al., 2013). Zhang et al. (2013) suggest that the Appalachian uplift phases created new habitats, which led to a diversification of the genus. This might explain the increase of the pollen grain counts of *Carya* in the Mid-Miocene where *Carya* became the prevalent genus of the Juglandaceae (Prader et al., 2017).

4.4.3 Terrestrial ecosystem responses to glacial events of the Mid-Oligocene to the early Miocene.

The entire Oligocene epoch is characterized by periodic climate oscillations associated with orbital insolation changes (Pälike et al., 2006). These orbital climate changes triggered the built-up and decay of Antarctic Ice Sheets, leading to substantial glacioeustatic sea level oscillations (Pekar et al., 2002, 2006; Wade and Pälike, 2004, Pälike et al., 2006).
Reconstructions of bottom water temperatures in the equatorial Pacific (Mg/Ca temperature records of Site 1218) indicate low temperature variations for the Oligocene (on average 3.7 °C ± 1.5 °C; Lear et al., 2004). However, rapid cooling of 2 °C is associated with isotope events Oi-2b and Mi-1 (Lear et al., 2004). Although the limited temporal resolution of our record from

the NJSS inhibits the evaluation of vegetation responses to periodic orbital changes, it may be used to test the potential impacts of particularly strong Oligocene climate shifts. Specifically, fluctuations of the relative abundances of vegetation units can be interpreted in terms of possible movement signals.

However, the indications of such signals within the terrestrial palynomorph signature are weak. Possibly distinct marine influence hampered the regional impact by moderating the global climate changes.

Our reconstructed palaeoclimate shows humid-warm temperate conditions under which only little altitudinal shifts took place. One example for a altitudinal movement signal could be the first peak of the meso- and microthermal Pinaceae (Fig. 4.4) at 29.3 -29.0 Ma. The most plausible explanation for this peak might be the impact of the unnamed $\delta^{18}O$ excursion at ~ 29.1 in the records from New Jersey (Pekar et al., 2002) and from the tropical Pacific (Site 1218: Wade and Pälike, 2004). However, relative pollen abundances of Vegetation Unit 4 remained relative stable (Fig. 4.3), indicating that either the amplitude of climatic factors (e.g. cooling) was too small to induce a strong reduction of the mesophytic forest or the regional vegetation units had a high degree of resilience to the climate forcing.

The first noteworthy reduction of Vegetation Unit 4 and a simultaneous increase of bisaccate Pinaceae probably coincide with the Oi2-a event at ~28.3 Ma (Pekar et al., 2002) and/or the ~28.5-Ma-$\delta^{18}O$ increase (Pekar et al., 2002). The conifers spread into the lowland and partly replaced Vegetation Unit 4 (Fig. 4.3). The idea of downward movement of the conifers is reinforced by the negatively correlating P:D ratio, which indicates an increasing shoreline vicinity and thus only a low chance of transport-induced increase in bisaccate pollen percentages.

Differing to the placing of the Mi-1 event at 23.03 Ma based on orbital tuning (Liebrand et al., 2011), it was placed at 23.8 Ma at the New Jersey margin by Pekar et al. (2002), who postulate an apparent sea-level drop of 56 m connected to the Mi-1 event. A definitive placement of the Mi-1 event is however difficult for Site M0027, since it probably corresponded with a strong sea-level lowstand creating the sequence boundary of Sequence O6 (Browning et al., 2013). The increased input of bisaccate pollen at the beginning of Sequence O6 (probably around the OMB) is consistent with findings of Kotthoff et al. (2014) which indicate that abiotic factors ameliorated the expansion of conifers (Vegetation Units 1 and 2) and led to a relative decrease of Vegetation Unit 4 (mesophytic forest, Fig. 4.3).

A temperature drop might be visible within all parameters at ~530 mbsf in our data, with a stepwise MAT-decline of ~3°C. It probably matches with the MAT-drop of ~4°C described by Kotthoff et al. (2014) at the same depth. A coeval increase of Vegetation Unit 7 (coastal), probably reflecting dryer and cooler conditions, is also consistent with Kotthoff et al. (2014). However, MAP does not decrease around this time interval, the dataset rather suggests an average overall stable trend in precipitation suggesting more occupation of coastal plain. A further decline of Unit 4 occurred within Sequence m6 (~20.9-20.7 Ma; Fig. 4.3), probably reflecting a late Aquitanian vegetation change provoked by the unnamed $\delta^{18}O$ increase at ~20.8 Ma (Browning et al., 2013).

The generally fluctuating patterns of Vegetation Units 3 and 4 and of the (H*(s)*)-Index represent indirect confirmation of climate change in the hinterland of the NJSS in phase with depositional changes of the Oligocene and early Miocene sediment succession at Site M0027. Peaks of Vegetation Units 5 and 3 coincide with all regression phases (glacial phases) discussed above, which exposed shallow shelf areas allowing for the spreading of substrate-depending forest

formations (Fig. 4.3). The simultaneous expansion of Vegetation Units 3 and 5 percentages and concomitant increase of the (H*(s)*)-Index indicate a quite diverse low elevation forest and thus a decreasing distance to the shoreline, facilitating pollen grain input during regression phases and/or a larger altitudinal gradient.

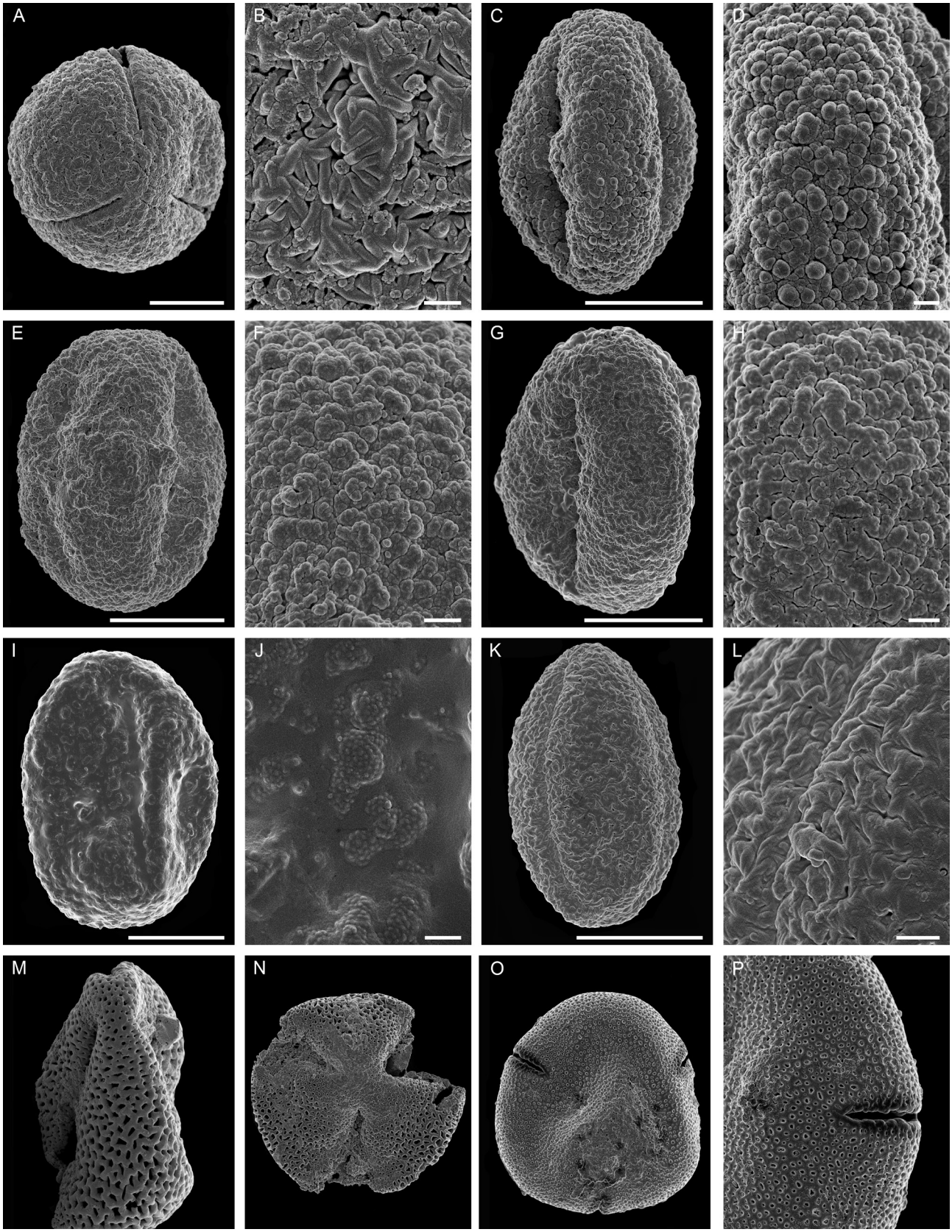

Plate 4-III SEM images of selected pollen grains of Site M0027A (574.05 mbsf). Overview (A, C, E, G, I, K, M, N O) and detail (B, D, F, H, J, L, P). A-B: Fagus; C-D: *Quercus* Group Quercus; E-H: *Quercus* Group Quercus/ Lobatae; I-J: *Quercus* aff. Group Protobalanus; K-L: *Eotrigonobalanus*: M-N: *Gordonia*; O-P: *Tilia*.
Scale bar 10µm (A, C, E, G, I, K, M, N O), 1µm (B, D, F, H, J, L, P).

Orbitally-driven palaeovegetation changes in the New Jersey hinterland during a short time interval (300.000 yrs) of the Burdigalian

5.1 Introduction

Climate variability with its glacial and interglacial changes has been assigned to the interaction of Earth's orbital parameters and is documented in a variety of proxy records such as marine stable-isotope data (e.g. Zachos et al, 2001b, Abels et al., 2005; Wade and Pälike 2004; Pälike et al., 2006; Holbourn et al., 2007, 2015; Liebrand et al., 2011, 2016, 2017). Earth's orbital parameters, comprising eccentricity (100 kyr, 400 ky), obliquity (41 kyr) and precession (19–23 kyr), control solar insolation across the latitudes (Kerr, 1978) and cause biotic responses to perseverative climatic and environmental changes (e.g. Bartlein and Prentice, 1989; Huntly and Webb, 1989; Tzedakis et al., 2003; van Dam et al., 2006; Jiménez-Moreno et al., 2007; Joannin et al., 2011; Barke et al., 2011; Egger et al., 2018).

The Miocene is characterized by a generally warm climate period during the early to middle Miocene (18–14 Ma) and a subsequent cooling and glaciation period during the middle to late Miocene (14–5 Ma; Mudelsee et al., 2014). Different forcing processes are responsible for climate change. For example, the uplift of the Tibetan plateau and the related weathering of silicats contributed to the cooling in the Cenozoic (Raymo and Ruddiman, 1992). The orbital configuration, which determined the Miocene climatic dynamic and the waxing and waning of Antarctic ice sheets, was coupled to long-term (400 kyr) and short-term (100 kyr) eccentricity cycles minima (Zachos et al, 2001b, Abels et al., 2005; Pälike et al., 2006; Holbourn et al., 2007; Liebrand et al., 2011, 2016, 2017).

Information about episodic vegetation responses during the Miocene related to specific orbital configuration derived for example from Spain, where the spreading of thermophilous elements and a contemporaneous retreat of mesothermic-riparian elements are coupled to obliquity variations (Jiménez-Moreno et al., 2007).

The observed downward-directed movement of a conifer forest of the mid latitudes of Europe however, were most likely dominated by short-term eccentricity minima (Jiménez-Moreno et al., 2009), whereas the palynological signature of Antarctica corresponds to long-term eccentricity, in which increased terrestrial palynomorph input matches with long-term eccentricity maxima reflecting warmer conditions and associated plant growth (Griener et al., 2015). The most pronounced Miocene glacial events, like the Mi-1 (23.03 Ma), the Mi-3a (14.2 Ma) or the Mi-2b (13.8 Ma), occurred during comparable orbital configurations, in which eccentricity cycles minima coincided with maxima of long-term (~1.2 Myr) obliquity modulations (Zachos et al, 2001b; Abels et al., 2005; Pälike et al., 2006; Holbourn et al., 2007; Liebrand et al., 2011). Obliquity strongly influenced the seasonality in high latitudes resulting in significant reduction of insolation and low seasonality during obliquity maxima, which pushed the waxing of Antarctic ice sheets (Zachos et al., 2001b).

Core sediments of IODP Expedition 313 to the New Jersey Shallow Shelf (NJSS) bear diverse and very well preserved assemblages of marine (e.g. Katz et al., 2013; McCarthy et al., 2013) and terrestrial microfossils (Fang et al., 2013, Kotthoff et al., 2013; Prader et al., 2017; Prader

et al., 2018), allowing the reconstruction of near-coastal Cenozoic palaeoenvironments. The existing chronostratigraphic framework (Browning et al., 2013) permits the study of long-term and orbital-scale vegetation and climate dynamics of eastern North America and evaluation of links to the global climatic evolution during the Cenozoic.

Earlier investigations of core sediments of IODP Expedition 313 and the reconstruction of terrestrial environmental conditions in the New Jersey hinterland increased the understanding of the terrestrial ecosystem and floristic composition through selected time intervals (Kotthoff et al., 2013: overview; Prader et al., 2017: late middle Miocene; Prader et al., 2018: middle Oligocene to early Miocene). The natural scenery in the hinterland was characterized by a complex palaeovegetation along a topographic gradient. The warm-temperate humid conditions led to the expansion of a diverse mixture of temperate broad-leaved deciduous trees, which formed the zonal vegetation (Prader et al., 2017; Prader et al., 2018).

However, the orbital-scale waxing and waning of Antarctic ice sheets and associated glacioeustatic lowerings affected the Atlantic coastal plain leading to sequence boundaries or hiatuses in the Cenozoic sedimentary record (Browning et al., 2013).

In addition, the expansion and/or restriction in the range of palaeovegetation units during the Middle Oligocene to early Miocene can be related to global cooling events (Prader et al., 2018). The limited temporal resolution of these investigations prevented the evaluation of vegetation responses to periodic orbital changes (Prader et al., 2018).

Periodic orbital-scale variations are visible within various sequences such as the early Langhian at Site M0029, and have also been inferred from relative sea-level reconstructions (McCarthy et al., 2013). To date, further information on the influence of orbital climate variability on the Miocene palaeoenvironments of the New Jersey region is not available.

Accordingly, we have analysed sediments of Site M0027 (IODP Exp. 313) in a relative high-temporal resolution to identify orbital-scale palaeovegetation changes in the hinterland of the North American Atlantic coastal plain during the Burdigalian (18.0 Ma to 17.7 Ma). We present a record with a temporal resolution of ~4600 yrs (65 samples per 300 000 yrs) allowing for a relatively detailed reconstruction of the palaeovegetation and regional climate of the New Jersey hinterland during the Burdigalian, which is characterized by relatively warm and stable global boundary conditions (Liebrand et al., 2017).

5.2 Material and Methods

5.2.1 Study site

Core sediments investigated in this study were derived from IODP Site M0027, recovered during IODP Expedition 313 on the New Jersey Shallow Shelf (NJSS). This site is located 45 km (Fig. 1.4) off the New Jersey margin at 39°38.046'N and 73°37.301'W at 33.5 m water depth (Expedition 313 Scientist, 2010). The position of the research area was ~2° further south during the Miocene and drifted northwards to between 39° and 40°N during the Pliocene (Scotese et al., 1988).

The combination of different age model proxies (calcareous nannofossils, dinoflagellate cysts, planktic diatoms, Sr isotopes, and sequence stratigraphy) reveals an estimated age of 17.7 to 18.0 Ma (± 0.25–0.5 Ma) for the analysed sequence m5.45 (Browning et al., 2013). Lithologically, sequence m5.45 consists mostly of silt and very fine sand (Expedition 313 Scientists, 2010b).

5.2.2 Data analysis

Sample preparation and palynological investigations

A total of 65 samples were processed at Brock University (Canada) following the hydrogen fluoride (HF) protocol described in McCarthy et al., (2013), but using a 10µm Nixon mesh for sieving. The material was then mounted in glycerine jelly and the residual material was used for acetolysis (Erdtman, 1960).

We counted and identified 300–400 terrestrial palynomorphs per sample using the acetolyzed material. Accurate Pollen grain identification was performed with a scanning electron microscope at the Biocenter Grindel (University of Hamburg) using the single-grain technique (Hesse et al., 2009). Bisaccate pollen grains, which are characteristic for many members of the Pinaceae, tend to be overrepresented within marine sediments and were thus excluded from the reference sum (Mudie and McCarthy, 1994).

To calculate the pollen-dinoflagellate index (P:D), 300 marine and terrestrial palynomorphs were additionally counted using the HF-treated (not acetolyzed) material due to the sensitiveness of gonyaulacoid (autotrophic) dinoflagellate cyst and most of the thin-walled protoperidinoid (heterotroph) dinocysts to acetolysis (following Mudie and McCarthy, 2006). The P:D index indicates the shoreline distance and allows inferences about taphonomic transport mechanisms (Mudie and McCarthy, 1994; McCarthy et al., 2013).

Short-term ecosystem dynamics

Plant communities do not migrate as a response to environmental changes as units but as single species (Williams and Jackson, 2007). Nonetheless, the assignment of taxa to different palaeovegetation units (PVU) allows an adjustment to possible palaeovegetation formations.

Accordingly, identified terrestrial palynomorphs were grouped into seven palaeovegetation units following Prader et al. (2017, 2018): PVU-1: high-altitude conifer forest; PVU-2: mid–altitude conifer forest; PVU-3: Cupressaceae; PVU-4: mesophytic forest growing on well-drained soils; PVU-5: mesophytic forest growing on moist/wet soils; PVU-6: mesophytic understorey; PVU-7: plant community associated to coastal environments, growing on sun-exposed sandbanks. In addition, the Shannon-Wiener-Index ($H(s)$) (Spellerberg and Fedor, 2003) was calculated in order to assess changes in biodiversity.

Palaeoclimatic analysis

For quantitative palaeoclimatic estimates, the bioclimatic analysis after Greenwood et al. (2005) and Prebble et al. (2017) was performed on the identified terrestrial palynomorphs. This method is based on the nearest-living-relative concept (NLR: Chaloner and Creber, 1990). Aspects in which the coexistence approach (CA: Mosbrugger and Utescher, 1997; Utescher et al., 2014) differs from the applied bioclimatic analysis are discussed in detail in Prebble et al. (2017). The main differences is the calculation of the climatic borders and the definition and treatment of outliners. In the bioclimatic analysis the border of the climatic overlapping zone of all taxa identified within a sample is calculated by the 10th (lower) percentile and the 90th (upper) percentile, which determine and exclude outliners (Greenwood et al., 2005). Whereas in the CA the lower climatic border is equal, the minimum value of one single taxon and the exclusion of outliners are subjective (Utescher et al., 2014).

Mean annual temperature (MAT), mean temperature of the coldest month (CMMT) and warmest moth (WMMT), and mean annual precipitation (MAP) were calculated in order to describe the palaeo-environmental conditions.

For affiliated taxa of an identified palynomorph, which still grow in North America, the climatic profiles of Thomson et al. (2000a; 2000b) were used. For Chinese taxa, climate profile data of Fang et al. (2011) were used. Further, climate information was taken from Natural Resources Canada (NRC), and the Global Biodiversity Information Facility (GBIF) using WorldClim. Table 5.1 summarizes all identified taxa with the used NLRs together with the climate source. The inclusion/exclusion of identified taxa follows as described in Prader et al. (2018, Appendix material).

To quantify changes in the seasonality, the Seasonality Index C (Schrepfer, 1925; after Pross and Klotz, 2002) was calculated.

Spectral analysis

To evaluate periodic changes within the relative abundances of PVUs, P:D ratio and Seasonality-Index, Blackman-Tukey spectral analyses, and a high pass filtering through a Gaussian band pass filter were performed using the AnalySeries software package, version 2.0 (Paillard et al., 1996). The error estimated at 80 % confidence level on the power spectra of all analysed datasets were $0.622 < \Delta Power / Power < 2.079$.

a: Fang et al. (2011), b Thomson et al. (1999, 2000a, 2000b), c NRC, d GBIF+WorldCLIM

1 high-altitude conifer forest; 2 mid-high-altitude conifer forest. 3 Cupressaceae 4 mesophytic forest growing on well-drained soils; 5 mesophytic forest growing on moist/wet soils; 6 mesophytic understorey; 7 plant community associated to coastal environments, growing on sun-exposed sandbanks.

Table 5.1 Summary of identified taxa in Sequence m5.45 of Site M0027 together with sources of climatic range and assignments to palaeovegetation units (PVU1-7), alphabetically ordered.

Taxon	Climate source	NLR used	PVU
Gymnosperms			
Abies	-		1
Cathaya	a	*C. argyrophylla*	2
Cedrus	b		2
Cupressaceae	-		3
Ephedra	-		7
Larix	-		1
Picea	-		1
Pinus subg. *Pinus*	-		2
Pinus subg. *Strobus*	-		2
Sciadopitys	d	*S. verticillata*	2
Tsuga canadensis	b	*T. canadensis*	4
Tsuga caroliana	b	*T. caroliniana*	4
Tsuga aff. heterophylla	b	*T. heterophylla*	2
Angiosperms			
Acer	b	*Acer* spp. (NA)	4
Alnus	-		5
Anacardiaceae	-		4
Apiaceae	-		6
Araliaceae cf.			-
Arctheubium	-		4
Asteraceae tubuliflorae	-		6
Betula	-		5
Carpinus/ Ostrya	b	*Carpinus* and *Ostrya* spp. (NA)	4
Carya	b	*Carya* spp. (NA)	5
Castaneoideae	b	*Castanea* spp. / *Castanopsis chrysophylla*/ *Lithocarpus densiflorus*	4
Cedrelospermum	-		extinct
Celtis	b	*Celtis* spp. (NA)	4
Chenopodiaceae/ Amaranthaceae	-		7
Clethra	-		4
Cornus	b	*Cornus spp.* (woody, NA)	4
Cornus aff. *sanguinea*	b	*Cornus spp.* (woody, NA)	4
Corylus	b	*Corylus* spp. (NA)	4
Cyperaceae	-		6
Diospyros		*Diospyros* spp. (NA)	4
Elaegnus	-		4
Engelhardioideae	-		4
Eotrigonobalanus/ Trigonobalanopsis	-		extinct

Ericaceae	-		4
Eucommia	a	*E. ulmoides*	4
Fabaceae	-		6
Fagus	b	*F. grandifolia*	4
Fraxinus	b	*Fraxinus* spp. (NA)	5
Gordonia	b	*G. lasianthus*	4
Hamameliadaceae	-		4
Humulus	-		5
Ilex	a	*Ilex* spp. (NA)	5
Itea	b	*I. virginica*	5
Jugalns	b	*Juglans* spp. (NA)	5
Juglandaceae	-		4
Liliaceae	-		5
Liqudambar	b	*L. styraciflua*	5
Liriodendron	b	*L. tulipifera*	4
Lonicera	-		4
Loranthus	-		4
Magnolia	b	*Magnolia* spp. (NA)	4
Myrica/ *Morella*	a	*Morella* spp. (NA)	5
Nuphar	c	*Nuphar* spp. (NA)	6
Nymphaea	c	*Nymphea* spp. (NA)	6
Nyssa	b	*Nyssa* spp. (NA)	5
Oleaceae	-		4
Ostrya	b	*Ostrya* spp. (NA)	4
Pachysandra	-		6
Persicaria	-		6
Parthenocissus	c	*Parthenocissus* spp. (NA)	4
Platanus	b	*Platanus* spp. (NA)	4
Platycarya	a	*Platycarya strobilacea*	5
Poaceae	-		6
Polygonum	-		6
Prunus	-		4
Pterocarya	a	*Pterocarya* spp. (China)	4
Quercus	b	*Quercus* spp. (NA)	4
Reevesia	a	*Reevesia* spp. (China)	4
Rhamnaceae	-		5
Rhododendron			4
Rosaceae	-		4
Salix	-		5
Sanguisorba		*S. canadensis*	6
Sapotoideae	-		5
Sapotaceae	-		5
Symplocos	a	*S. tinctoria*	5
Tetracentron		*T. sinense*	4
Tilia	b	*Tilia spp.* (NA)	4

Table 5.1 Continued

Ulmus	b	*Ulmus spp.* (NA)	5
Viburnum	b	*Viburnum spp.* (NA)	4
Vitaceae	-		5
Vitis	-		5
Zelkova	a	*Zelkova* spp. (China)	5
Pteridophytes			
Equisetum	-		5
Lycopodium	-		5
Osmunda	c	*Osmunda* s.l. (NA)	5
Polypodiaceae	-		5
Dryopteris cf.	-		5

5.3 Results

5.4.1 Terrestrial composition

In total, 92 taxa were identified and are summarized in Table 5.1. Light microscopic images (LM Plate 5-I and 5-II) and scanning electronic images (SEM Plate 5-III to 5-V) illustrate a selection of identified terrestrial palynomorphs.

In addition, several relative abundances of important taxa like pollen grains of *Quercus* comprising 55.2 % (min: 39.8 %; max: 68.1 %) through the entire Sequence m5.45, followed by *Carya* with an average quantity of 9.2 % (min: 3.5 %; max: 20.2 %) and *Fagus* (average: 5.2 %; min: 0.4 %; max: 11.5 %) are shown in Figure 5.1.

The calculated Shannon-Wiener Index H(*(s)*) is generally low (Fig. 5.2), however increased several times above 2. H(*(s)*) values persist around ~331 mbsf to ~323 mbsf and from ~318 mbsf to ~308 mbsf above 2.

5.4.2 Palaeovegetation units

PVU-4 (mesophytic forest growing on dry soils) is the dominant vegetation type in the hinterland (Fig. 5.2). This unit reflects mainly broad-leaved deciduous hardwood genera, which differ highly in their relative abundances: e.g., *Quercus* (Plate 5-III, I-P; Plate 5-V, I-P; Fig. 5.1), *Eucommia* (Plate 5-II, A-B; Plate 5-IV, A-B; Fig. 5.1), *Fagus* (Plate 5-III, G-H; Plate 5-V, G-H; Fig. 5.1) or *Reevesia* (Plate 5-III, Ee-Ff; Plate 5-IV, M-N; Fig. 5.1). Additional, several genera like *Diospyros* (Plate 5-II, K; Plate 5-IV, G-K) or *Tetracentron* (Plate 5-IV, K-L) occur in this group, but were only represented by single pollen grains. The relative abundance of this vegetation unit is almost constant through the time interval analyzed, and with exception of the section between 318.85 mbsf and 311.08 mbsf, it is always above 50%. The decrease of the PUV-4 during the above mentioned interval below 50% coincides with the highest relative pollen grain abundance of PVU-3 (Cupressaceae; > 30%). PVU-5 (mesophytic forest growing on moist soils) fluctuates between 11.3 and 29.6 %, however without significant peaks. The conifer forests on mid- (PVU-2) and high-altitudes (PVU-1) show a general trend towards lower relative abundances (Fig. 5.2) over time, starting with respective values >30% and >10% in the lower

part of the sequence and a declining to > 7% and > 2% in the upper part of the sequence. The P:D ratio is lower than 0.5 over the analysed interval, but shows a slight increase through time and distinct fluctuations (Fig. 5.2), which are most pronounced at ~331.49 mbsf and ~324.7 mbsf (Fig. 5.2).

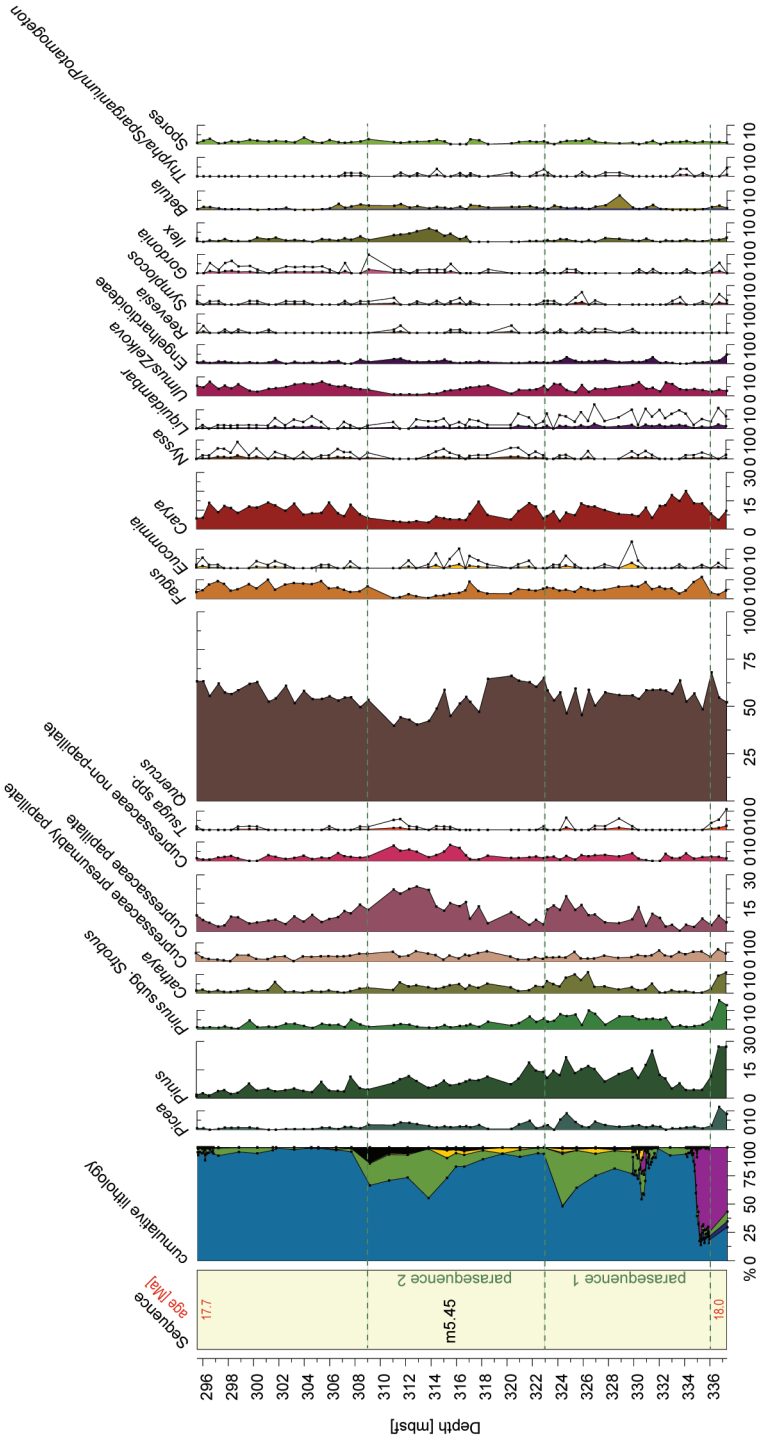

Figure 5.1 Relative pollen abundances of selected taxa (pollen sum excluding bisaccates) identified in core sediments of sequence m5.45 plotted against depth (white areas: 5x exaggeration). Parasequence boundaries (dashed lines) and cumulative lithology after Miller et al. (2013a): blue: clay and silt; dark blue: glauconite; green: fine quartz and medium coarser quartz sand: yellow: mica; magenta: carbonate; black: other. Sequence boundaries and their ages after Browning et al. (2013).

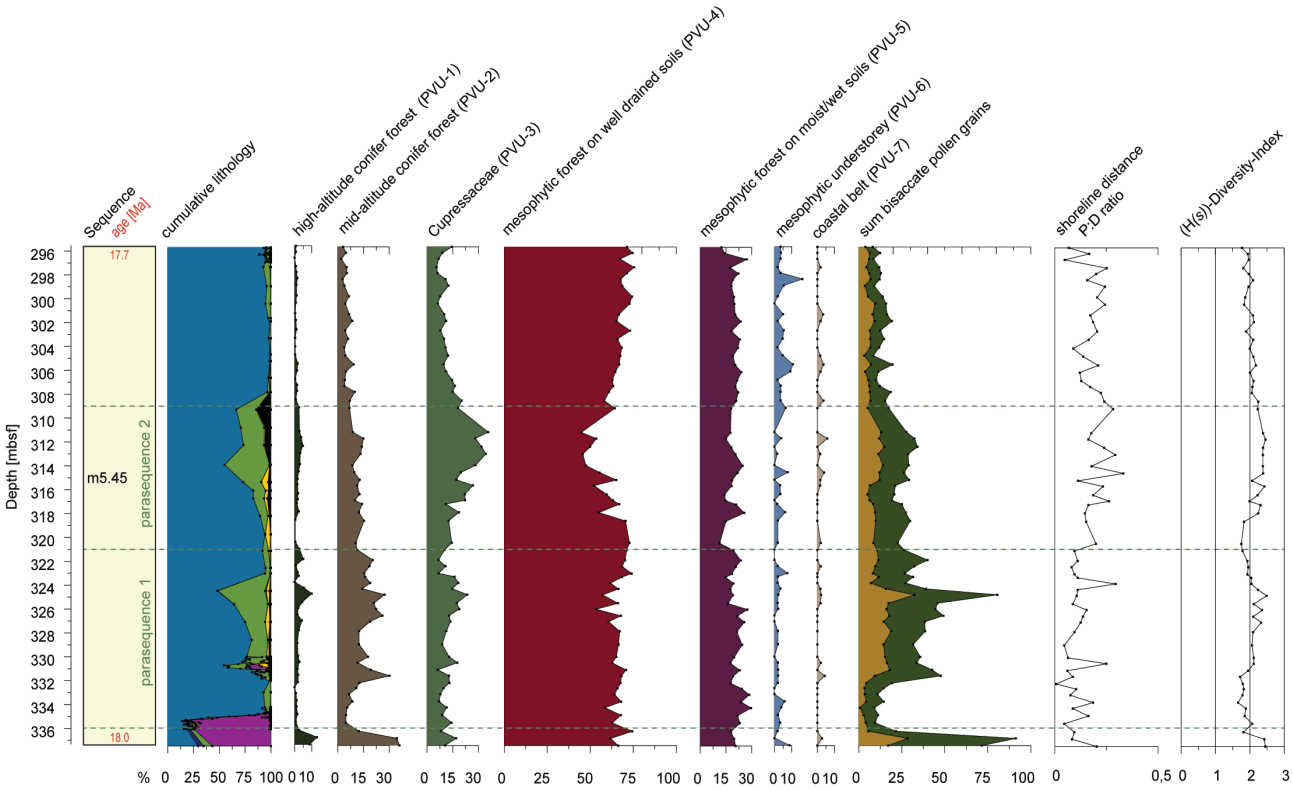

Figure 5.2 The New Jersey hinterlands Vegetation Units (PVU 1-7), P:D ratio and (H*(s)*)-Index of Sequence m5.45 plotted against depth. Taxa are pooled to a vegetation unit as denoted in Table 5.1. PUV-6 and PUV-7 5x exaggeration. Sequence boundaries and their ages after Browning et al. (2013), parasequence boundaries (dashed lines)and cumulative lithology after Miller et al. (2013a): blue: clay and silt; dark blue: glauconite; green: fine quartz; medium coarser quartz sand: yellow: mica; magenta: carbonate; black: other.

Plate 5-I LM images of selected pollen grains of identified taxa of Site M0027 during the Burdigalian. A. *Cathaya* (336.73 mbsf); B. *Cathaya* (323.2 mbsf) same pollen grain as in Plate 5-III; A-B; C. *Pinus* subg. *Strobus* (311.08 mbsf); D. *Pinus* subg. *Pinus* (298.8 mbsf); E. *Pinus* (331.49 mbsf); F. *Abies* (336.73 mbsf); G. *Picea* (309.635 mbsf); H. *Picea* (326.95 mbsf); I. *Tsuga canadensis* (299.7 mbsf); J. *Tsuga caroliniana* (309.635 mbsf); K. *Larix* (326.45 mbsf); L. *Sciadopitys* (307.2 mbsf); M. *Ephedra* (305.4 mbsf); N. Cupressaceae papillate morphotype (315.54 mbsf); O. Cupressaceae (295.55 mbsf); P. Cupressaceae non-papillate morphotype (311.08 mbsf); Q. Polypodiaceae (301.76 mbsf); same spore as in Plate III E-F; R. Polypodiaceae cf. *Dryopteris* (307.2 mbsf); S. *Equisetum* (303.98 mbsf); T. *Lycopodium* (298.26 mbsf) HF-sample; U. *Osmunda* (306 mbsf); V. Trilete spore indet. (299.7 mbsf); W. Trilete spore indet. (303.25 mbsf); X. Poaceae (298.26 mbsf); Y. Apiaceae (296.55 mbsf); Z. Chenopodiaceae/Amaranthaceae (304.66 mbsf); Aa. *Polygonum* (323.2 mbsf); Bb. Onagraceae (301.76 mbsf). Scale bar = 10µm.

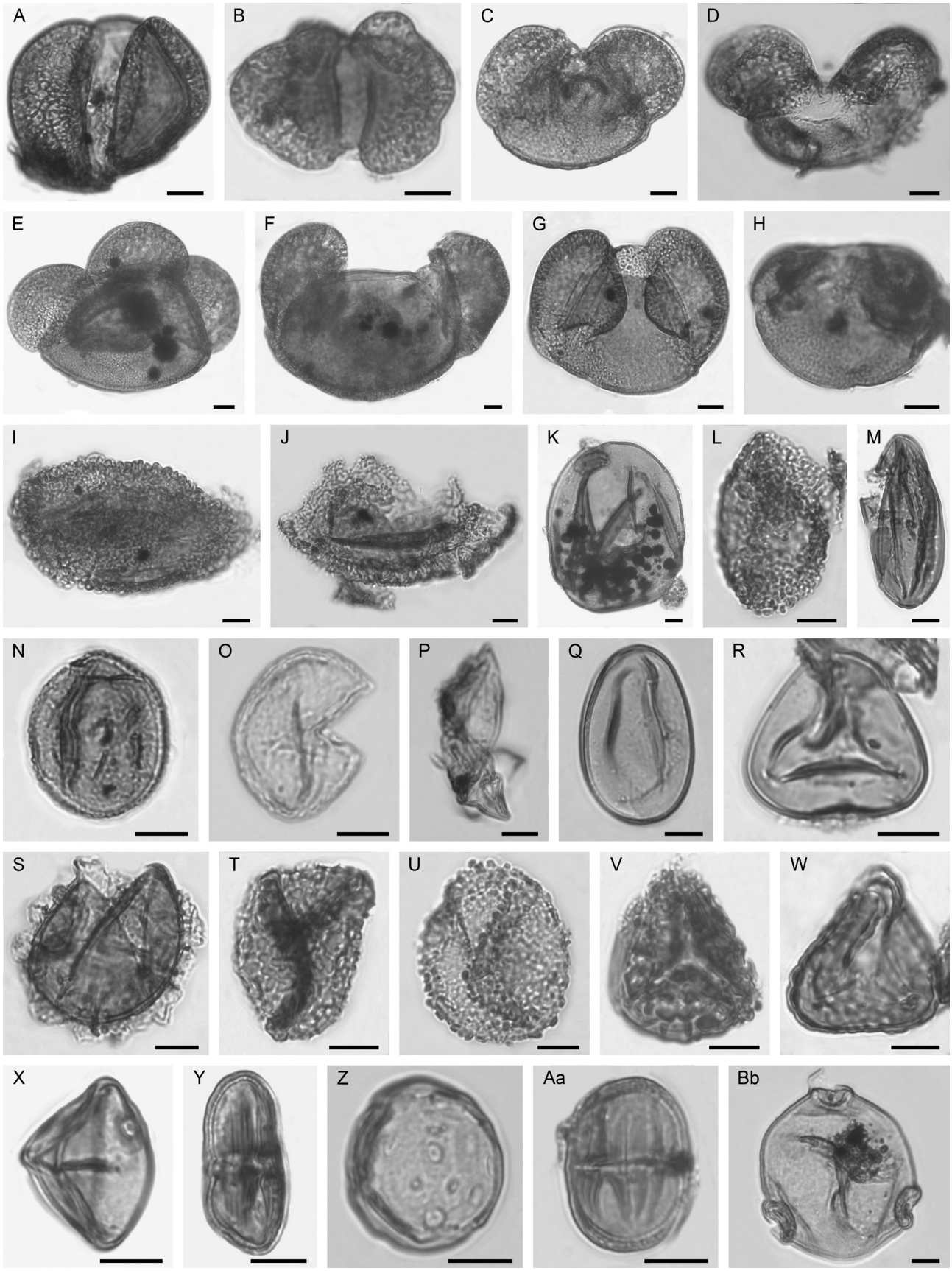

Plate 5-I

5.4.3 Bioclimatic estimations

Humid, warm-temperate climate conditions are indicated for the sequence. Average estimated MAT was 14.5°C ± 4.0°C (Fig. 5.4). Average winter temperatures (CMMT) were 4.8°C ± 5.2°C and average summer temperatures (WMMT) 23.8 °C ± 3.2 °C. MAP shows an average annual amount of 1325.5 mm ± 279.1 mm. The Schrepfer Seasonality Index C fluctuates between 35.9 at 314.45 mbsf and 53.8 at 298.26 mbsf, indicating weak seasonal temperature differences. (Fig. 5.4). On average 17.7 climatic profiles (NLR; min: 9 NLR at 332.09 mbsf; max: 21 NRL at 315.54 mbsf) were used to calculate the climatic palaeoparameters.

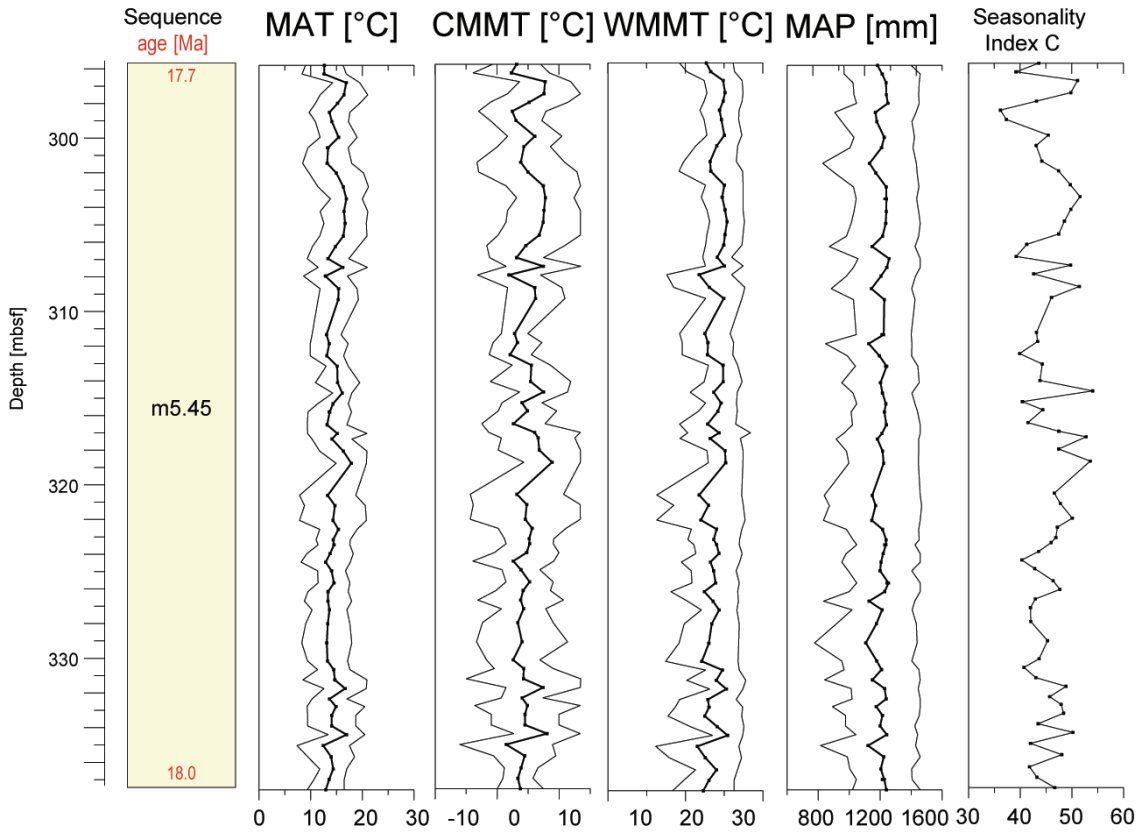

Figure 5.4 Calculated palaeoenvironmental parameters (pollen based palaeotemperatures and palaeoprecipitation). MAT: mean annual temperature, CMMT and WMMT mean annual temperature of the coldest and warmest month, MAP: mean annual precipitation and Seasonality Index C of the New Jersey hinterland during the Burdigalian. Outer lines: error of estimated values. Ages and sequence boundaries after Browning et al. (2013).

5.4.4 Orbital variability

Spectral analyses revealed clear orbital variability with strong power in the obliquity and short-term eccentricity domains (Fig. 5.5a, b). The PVU-5 (mesophytic forest on moist/wet soils) and the Schrepfer Seasonality Index C reveal a strong coherence in the obliquity band (Fig. 5.5d, f). A strong response to short-term eccentricity is observed in PVU-1 (Fig. 5.5c) and a weaker response in the Schrepfer Seasonality Index C (Fig. 5.5e).

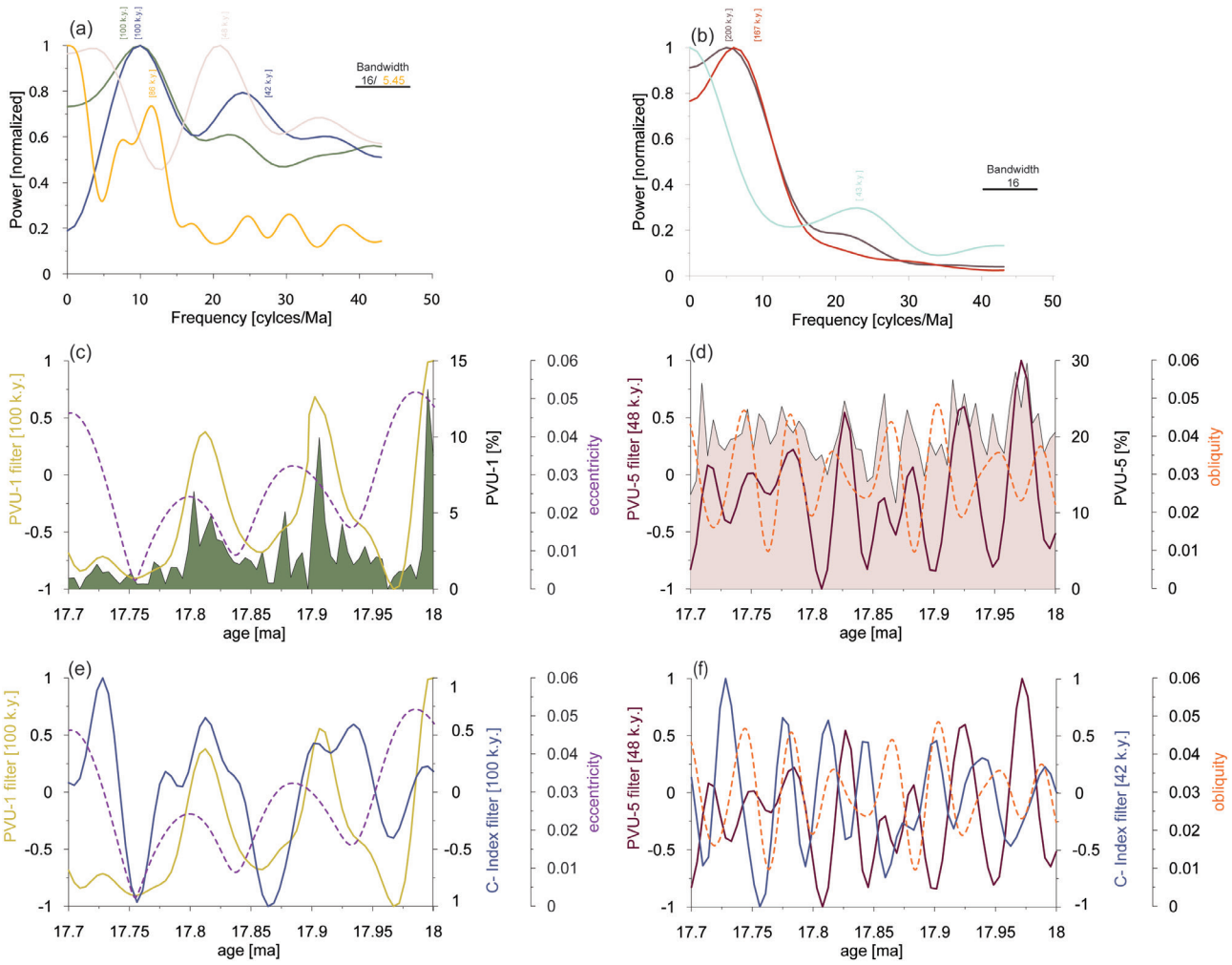

Figure 5.5 (a, b) Normalized Blackman-Tukey power spectra of the New Jersey palaeovegetation units, Seasonality Index C and benthic $\delta^{18}O$ values after Liebrand et al. (2016), (c) relative abundances of PVU-1 with Gaussian band pass filter and standard eccentricity, (d) relative abundances of PVU-5 with Gaussian band pass filter and standard obliquity (e) Gaussian band pass filter of PVU-1, standard eccentricity and Gaussian band pass filter of Seasonality Index C, (f) Gaussian band pass filter of PVU-5, standard obliquity and Gaussian band pass filter of Schrepfer Seasonality Index C, All datasets are plotted against interpolated age. Standard eccentricity and obliquity after Laskar et al. (2004).

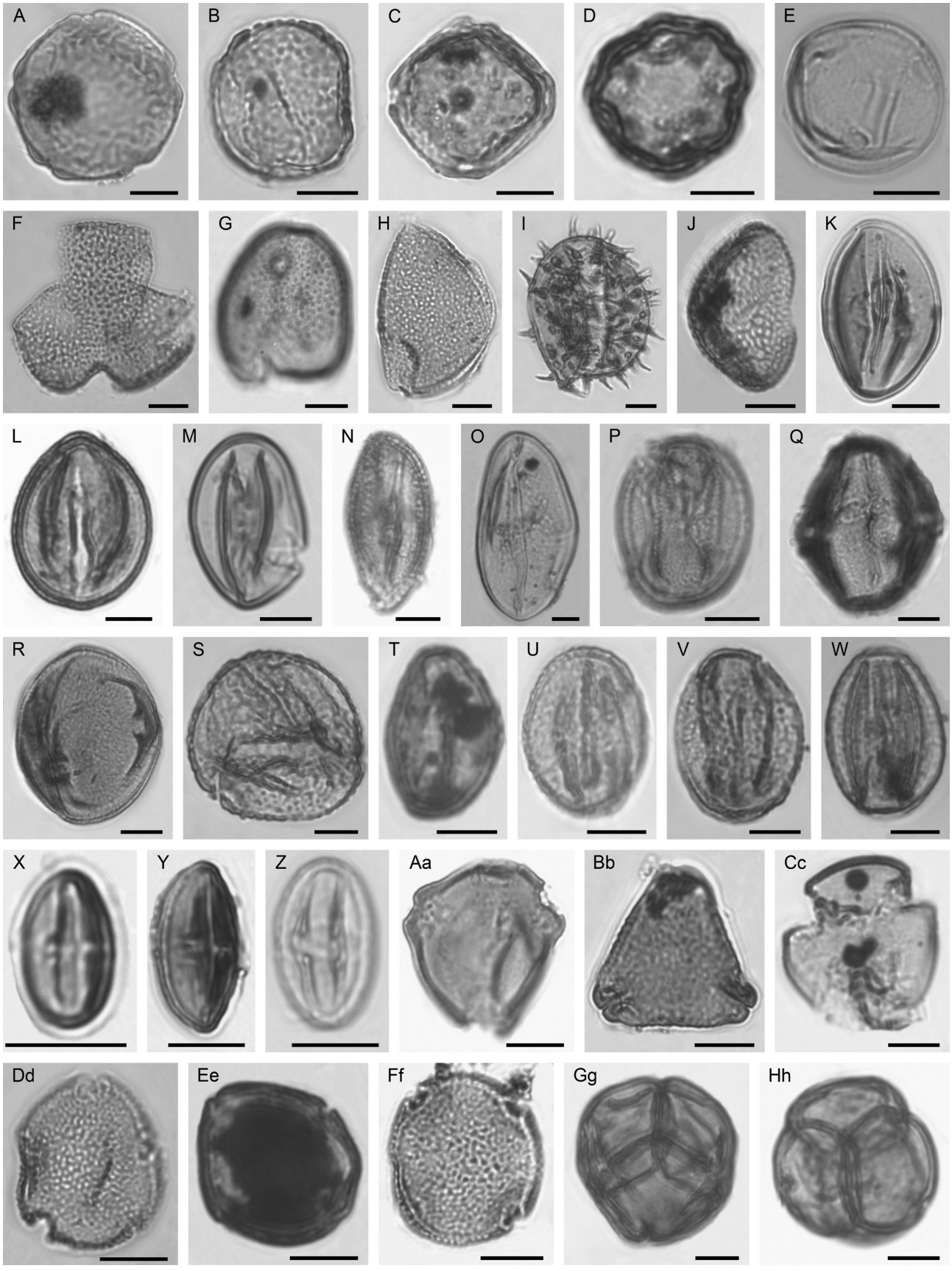

Plate 5-II

5.5 Discussion

5.5.1 Vegetation response of the New Jersey hinterland to shelf exposure and habitat changes

The palynological data series suggest orbital-scale palaeoenvironmental changes of PVU-1–4 between 18.0 and 17.7 Ma, which might be related to identified parasequences at 336–323 mbsf and 323–309 mbsf (Miller et al., 2013a; Fig. 5.1, 5.2). These parasequences represent high-order relative sea-level oscillations and are lithologically expressed by a characteristic stacking pattern of a coarsening-upward trend, indicating relatively shallower conditions (Miller et al., 2013). These alternations of transgression and regression might have triggered regional landscape modifications in the New Jersey hinterland by exposing shallow shelf areas, accompanied by a characteristic vegetation response. For example, the repetitive regressions phases coincide with cyclic oscillations of relative pollen grain abundances of Cupressaceae (Fig. 5.2). This indicates that several members of Cupressaceae (e.g., *Taxodium* forms pneumatophores in wet substrates: Farjon, 2010) gradually expanded/contracted their populations in association to successive modified coastal settings, formed by the prograding/retrograding shoreline. The inferred vegetation expansion patterns are probably similar to those observed during regression phases of the Middle Oligocene and early Miocene (Prader et al., 2018).

Changing temporal environmental conditions during the parasequences correspond to periodic changes of the relative abundance of PVU-4 (e.g., *Quercus*, *Fagus*, *Celtis*, *Liriodendron*, *Magnolia*, *Pterocarya*). This may imply a successive vegetation change caused by expansion of wetland areas during regression phases. However, the increased input of Cupressaceae pollen grains during regression phases is rather caused by the proximity of extended swampy environments to the shoreline, and thus to Site M0027, than by a successive replacement of well-drained lowland areas (PVU-4; Fig. 5.2). The fluctuations in the relative abundance of PVU-4 might be a signal of repetitive changes in environmental conditions further inland and may also reflect a replacement of PVU-4 by downslope spreading of conifer taxa such as *Picea*, *Pinus* or *Cathaya*, which most likely grew on topographically higher elevated areas (PVU-1 and 2 in Fig. 5.2). The periodic cooling phases controlled and shifted the altitudinal distribution of PVU's further inland by pushing higher elevated palaeovegetation units into lower topographic areas. Under cooler environmental conditions, the selective pressure probably favoured the distribution of conifers over arborescent deciduous angiosperms.

Plate 5-II LM images of selected pollen grains of identified taxa of Site M0027 during the Burdigalian. A. *Ulmus* (297.74 mbsf); B. *Cedrelospermum* (295.55 mbsf); C. *Zelkova* (296.55 mbsf); D. *Liquidambar* (297.74 mbsf); E. *Celtis* (304.66 mbsf); F. *Gordonia* (314.45 mbsf); G. sulcate pollen grain of a monocot (330.4 mbsf); H. sulcate pollen grain of a monocot cf. Liliaceae (302.56 mbsf); I. *Nuphar* (297.74 mbsf) same pollen grain as in Plate 5-III, G-H; J. sulcate pollen grain of a monocot cf. Liliaceae (301.76 mbsf); K. *Diospyros* (296.55 mbsf); L. *Acer* (297.74 mbsf); same pollen grain as in Plate 5-IV, E-F; M. *Eucommia* (316.78 mbsf) same pollen grain as in Plate IV, A-B; N. *Parthenocissus* (309.635 mbsf); O. *Magnolia* (311.08 mbsf) same pollen grain as in Plate 5-III, K-L; P. Hamamelidaceae (335.43 mbsf); Q. *Cornus* aff. *sanguinea* (313.85 mbsf); R. *Nyssa* (297.74 mbsf); same pollen grain as in Plate 5-V, E-F; S. *Fagus* (297.74 mbsf) same pollen grain as in Plate 5-V, G-H; T. *Quercus* (323.2 mbsf) same pollen grain as in Plate 5-V, I-J; U. *Quercus* (323.2 mbsf) same pollen grain as in Plate 5-V, O-P; V. *Quercus* (297.74 mbsf) same pollen grain as in Plate 5-V, M-N; W. *Quercus* (297.74 mbsf) same pollen grain as in Plate 5-V, K-L; X. Castaneoideae (317.1 mbsf); Y. *Eotrigonobalanus* ? (325.9 mbsf); Z. *Decodon?* (296.05 mbsf); Aa. *Myrica*/*Morella* (298.26 mbsf); Bb. *Symplocos* (315.54 mbsf); Cc. *Platanus* (311.08 mbsf) same pollen grain as in Plate 5-IV, I-J; Dd. *Reevesia* (296.05 mbsf); Ee. *Reevesia* (316.78 mbsf) same pollen grain as in Plate 5-IV, M-N; Ff. *Reevesia* (315.54 mbsf); Gg. *Rhododendron* (297.74 mbsf) same pollen grain as in Plate 5-III, M-N; Hh. Ericaceae (316.78 mbsf) same pollen grain as in Plate 5-III, O-P. Scale bar = 10µm.

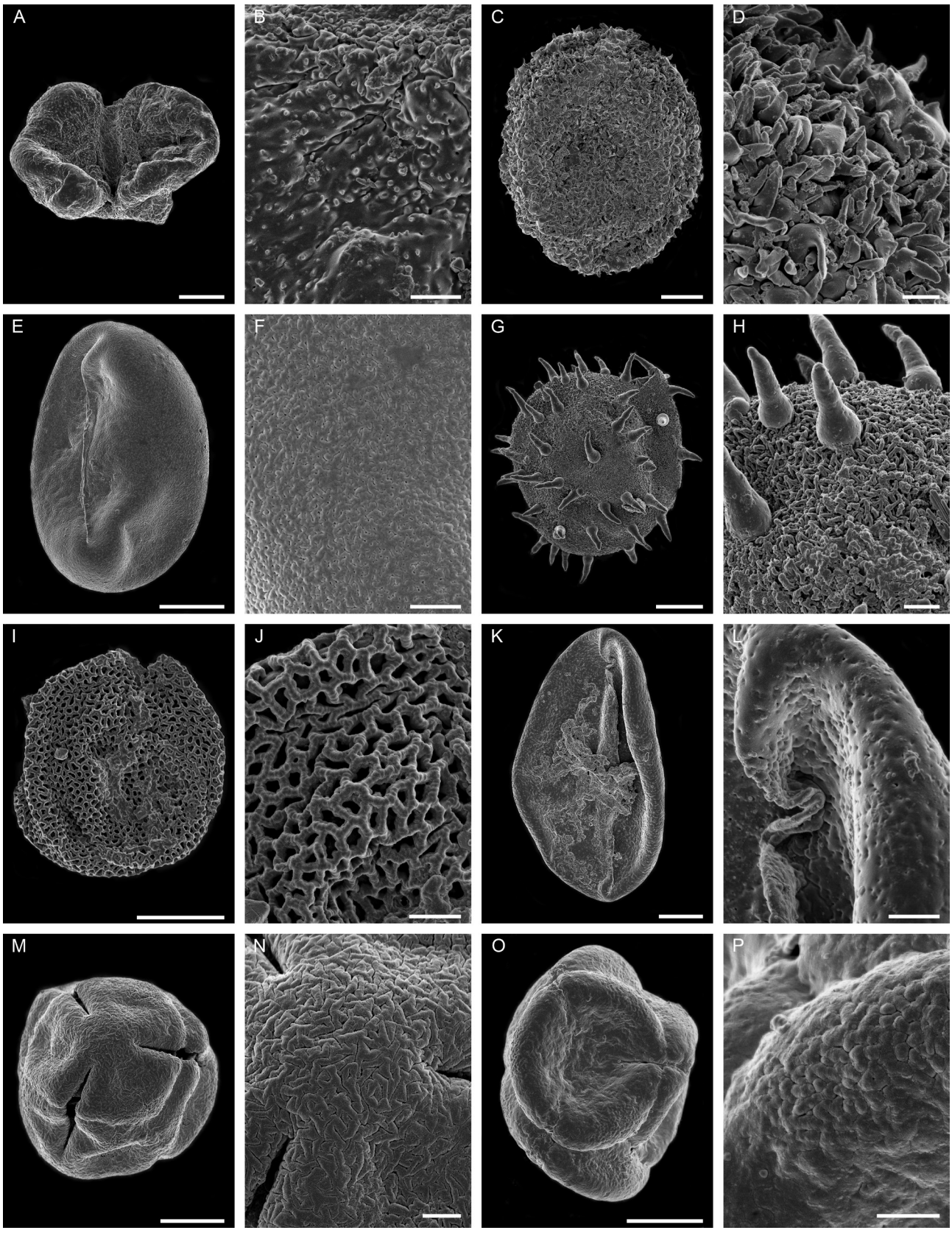

Plate 5-III

The observed changes in pollen grain abundances of bisaccate conifers during the studied time interval do not solely correlate to taphonomic transport processes as suggested by the P:D ratio, and thus most likely represent a clear palaeovegetation signal (Fig. 5.2). This underlines the interpretation that a gradual replacement of PVU-4 in higher elevated areas occurred during cooler conditions. Conifers with bisaccate pollen grains were continuously observed in the sequence, indicating that this group of taxa formed a permanent component in the hinterland. However, the general decreasing trend probably suggests a gradual loss of suitable habitats for conifer growth probably on intra-mountainous areas.

Responding to palaeoenvironmental changes of the Burdigalian, extensive habitats were repetitively developed and colonized. The recurrent habitat changes are also inferred from pollen diversity, exhibiting comparable changes (Fig. 5.2). This is particular expressed in the second deposited cycle (323–309 mbsf, Fig. 5.2) when a regression phase created a wide variety of vertical ecological (e.g., substrate-depending; microclimatic) habitats, which contributed to an increased plant diversity in the hinterland.

5.4.2 Orbital-scale climate influence on short-term vegetation variability in the New Jersey hinterland

Taking the uncertainties of the age model of Sequence m5.45 into account (Browning et al., 2013), the PVU's exhibit orbital-scale periodic variations (Laskar et al., 2004), suggesting a direct climate forcing of New Jersey palaeoenvironments and palaeovegetation during the Burdigalian. The conifer forest, dominating the high-altitudes (PVU-1), is strongly coherent with the short-term eccentricity cycle (Laskar et al., 2004; Fig. 5.5c, e). Relative PVU-1 abundance maxima are associated with short-term eccentricity minima (Fig. 5.5c) and are consistent with early Miocene glacial phases, which are strongly associated with short-term (110 kyr) eccentricity minima (Liebrand et al., 2016, 2017). This suggests that shifts in the abiotic palaeoenvironmental conditions forced the vertical migration of PVU-1 to lower altitudes during glacial periods. Such short-term eccentricity-related changes during the early Miocene are also observed for mid- and high-altitude conifer forests of Croatia (Jiménez-Moreno et al., 2009). The cooler phases of the Neogene are consistent with episodic latitudinal southward shifts of the entire Pinaceae family (Millar, 1998), which is related to the high resistance of frost-induced embolism of conifers and associated competitive advances of conifers over angiosperms (Pitterman and Sperry 2006; Brodribb et al., 2012). Significant oscillations in the vegetation patterns of higher altitudes in south-west Romania during the early Pliocene were also eccentricity-controlled, showing a dominance of taxa such as *Picea*, *Cathaya*, *Pinus* or *Cedrus* during eccentricity maxima (Popescu et al., 2006).

Plate 5-III SEM images of selected pollen grains of identified taxa of Site M0027A during the Burdigalian. A-B. *Cathaya* (323.2 mbsf); C-D. *Tsuga caroliniana* (311.08 mbsf); E-F. Polypodiaceae (311.08 mbsf); G-H: *Nuphar* (297.74 mbsf); I-J: *Typha* (323.2 mbsf); K-L. *Magnolia* (311.08 mbsf); M-N. *Rhododendron* (297.74 mbsf); O-P. Ericaceae (316.78 mbsf). Scale bar: 10µm: overview (A; C; E; G; I; K; M; O); 1µm: detail (B; D; F; H; J; L; N; P).

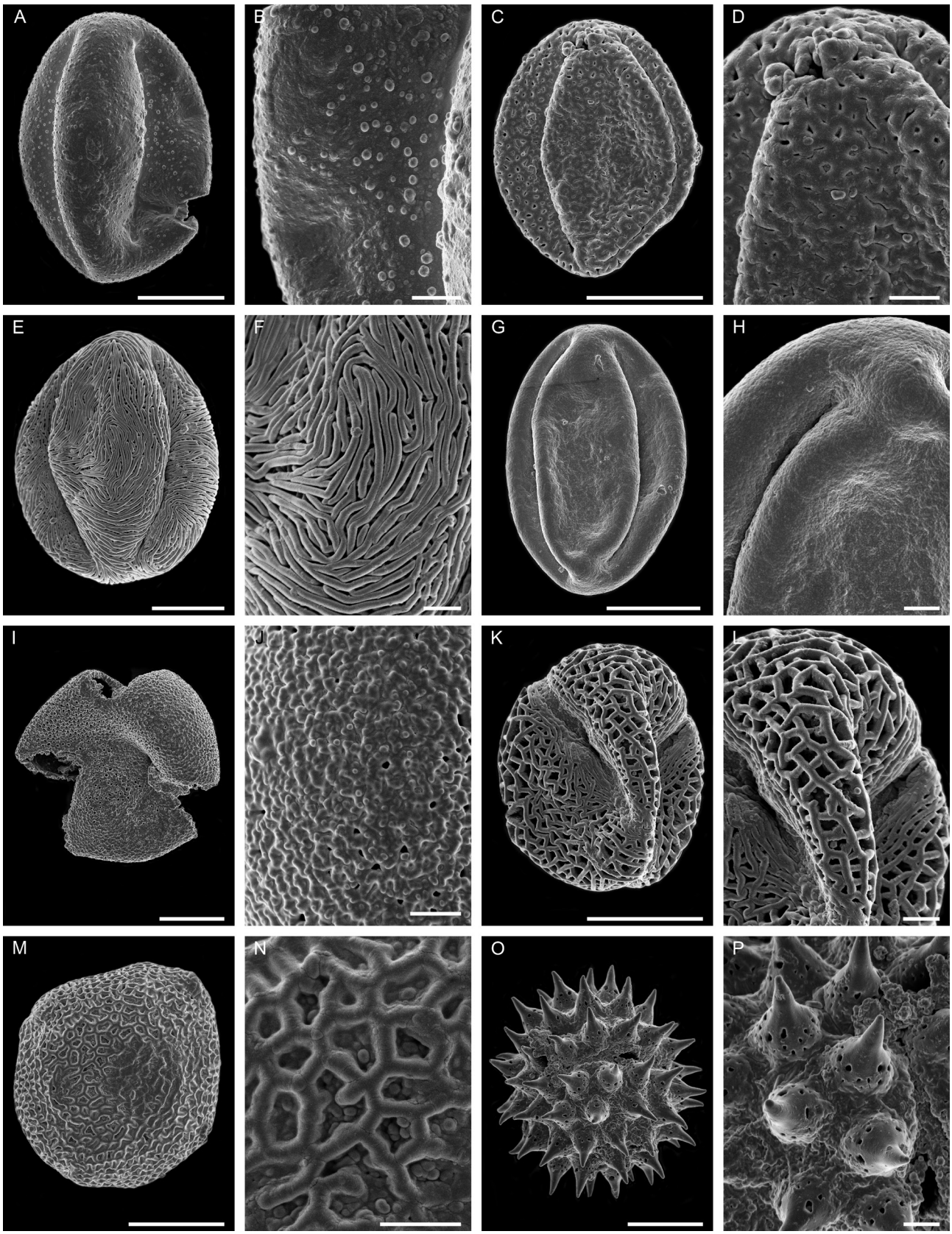

Plate 5-IV

We observed strong obliquity-related changes in the mesophytic forest growing on moist/wet soils (PVU-5; Fig. 5.5d). Similar obliquity-related vegetation changes occurred during the early Miocene of north-east Spain, indicated by shifts in the dominance of thermophilous taxa such as *Symplocos* (Jiménez-Moreno et al., 2007).

5.4.3 Characterization of the palaeoclimate in the New Jersey hinterland during the Burdigalian

During the investigated time period, the climate in the New Jersey hinterland was humid warm-temperate (i.e., a Cfa climate; Kottek et al., 2006), as reflected by the identified microfloristic assemblages. The estimated mean annual temperatures prevailed around 13°C most of the time, with several maximum values above 14°C (Fig. 5.4). The very low MAT oscillations during the Burdigalian supported the growth of a diverse mixture of deciduous broad-leaved forests in the lowlands of the mid-latitudes of eastern North America. In particular, reconstructed summer temperatures remained constant above ~20°C, and calculated precipitation values revealed fairly moist conditions, always prevailing above 1000 mm. Estimated winter temperatures suggest generally mild conditions with an average around 5°C, however, when considering the uncertainty range of ± 5.2 °C, freezing cannot be excluded (Fig. 5.4). The temperate zone is characterized by a strong seasonality, which regularly changes the resource availability though the year (Lieth, 1974). In addition, to this typical temperate seasonality, calculated Seasonality Index C reflects small temperature seasonality variation (Fig. 5.4). The weak temperature seasonality is modulated by orbital parameters of which seasonality maxima correspond to obliquity maxima (Fig. 5.5f). Taking into account the response of PVU′s to orbital climate changes, an interaction of the calculated Seasonality Index C with the mesophytic forest growing on moist/wet soils (PVU-5) is most likely possible (Fig. 5.5f). PVU-5 abundance minima seem to be associated to seasonality maxima, probably indicating a vegetation response to seasonality variations through the analysed Burdigalian time interval. Similarly to the conditions in the New Jersey hinterland, periodic alternations of thermophilous taxa (e.g., *Symplocos*, *Nyssa*) occurred in north-east Spain during the early Miocene matching obliquity-forced changes in precipitation and temperature (Jiménez-Moreno et al., 2007). In the New Jersey hinterland, the observed decrease in the dominance of PVU-5 during obliquity minima was likely induced by temperature rather than precipitation changes, which is consistent with the effect of specific temperature thresholds on the phenology of plants growing in the temperate zone (Kramer et al., 2000). The obliquity triggers the season and the variability in the obliquity regulates the contrast of the seasons (Kerr, 1978). The strong seasonal contrasts during the Oligocene and early Miocene correlate with glacial maxima and are in phase with obliquity maxima (Zachos et al., 2001b; Pälike et al., 2006). The observed different effect of the calculated temperature seasonality on the mesophytic forests (PVU-4 vs. PVU-5) might correlate to different phenological responses of deciduous tree species, regulating plant productivity and competition (Kramer et al., 2000).

Plate 5-IV SEM images of selected pollen grains of identified taxa of Site M0027A during the Burdigalian. A-B. *Eucommia* (316.78 mbsf); C-D. *Gordonia* (316.78 mbsf); E-F. *Acer* (297.74 mbsf); G-H. *Diospyros* (297.74 mbsf); I-J. *Platanus* (311.08 mbsf); K-L. *Tetracentron* (297.74 mbsf): M-N. *Reevesia* (316.78 mbsf); O-P. Asteraceae (301.76 mbsf).Scale bar: 10µm: overview (A; C; E; G; I; K; M; O); 1µm: detail (B; D; F; H; J; L; N; P). (A; C; E; G; I; K; M; O) and (B; D; F; H; J; L; N; P).

Plate 5-V SEM images of selected pollen grains of identified taxa of Site M0027A during the Burdigalian. A-B. Rosaceae aff. *Prunus* (316.78 mbsf); C-D. Sapotoideae (297.74 mbsf); E-F. *Nyssa* (297.74 mbsf); G-H. *Fagus* (297.74 mbsf); I-J. *Quercus* Group Lobatae (323.2 mbsf); K-L. *Quercus* Group Quercus (297.74 mbsf): M-N. *Quercus* Group Protobalanus (297.74 mbsf); O-P. *Quercus* Group Quercus/ Lobatae (323.2 mbsf).
Scale bar: 10µm: overview (A; C; E; G; I; K; M; O); 1µm: detail (B; D; F; H; J; L; N; P). (A; C; E; G; I; K; M; O) and (B; D; F; H; J; L; N; P).

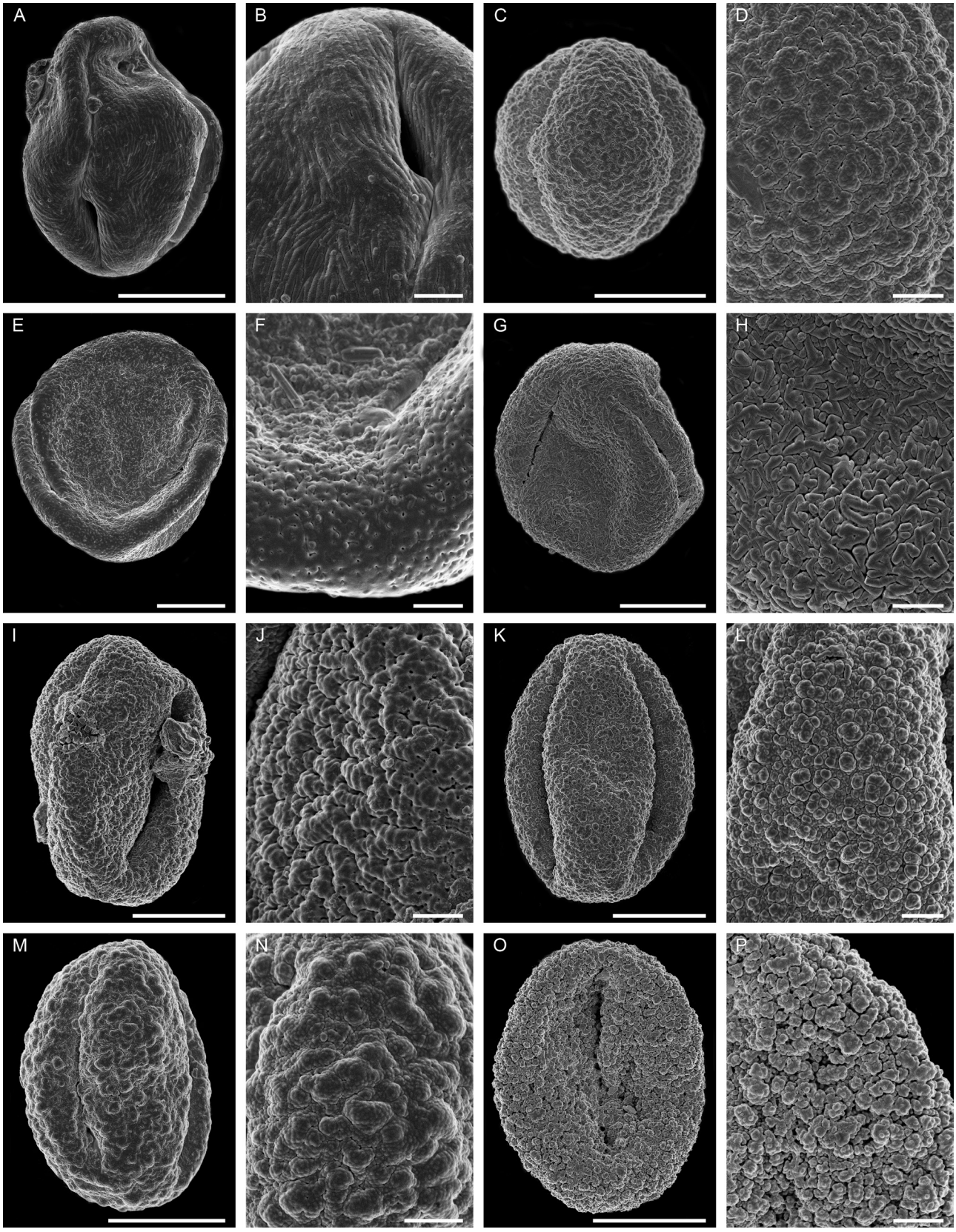

Plate 5-V

General discussion, conclusion and future perspective

6.1 Floristic composition across the Oligocene and Miocene in eastern North America

Floristic information inferred from the terrestrial palynomorph assemblages of Site M0027 document a diverse terrestrial flora and confirms that the overall microfloristic composition is generally congruent to compositions documented in earlier studies for eastern North America (e.g. Greller and Rachele, 1983; Traverse, 1994; Pazzaglia et al., 1997; Ochoa et al., 2012). Nevertheless, as emphasized by the present thesis, the hinterland of the Atlantic coastal plains was even more diverse than previously thought (Chapter 3, 4, 5). The sporadic occurrence of several new identified pollen grains e.g. *Diospyros*, *Tetracentron* or *Reevesia*, besides the identification of extinct genera *Eotrigonobalanus* (Fagaceae) and *Cedrelospermum* (Ulmaceae) in the New Jersey hinterland, widens the understanding of their distribution pattern in the Northern Hemisphere during the Cenozoic.
The relatively high abundance of *Quercus* pollen grains emphasises the dominance and significance of this taxon. Moreover, the intensive use of the SEM allowed identifying different pollen grain sculptures within the genus *Quercus*, suggesting a diverse *Quercus* population at subgeneric level during the analysed time intervals (Chapter 4 and 5).
The comparison of the recorded pollen percentages from the middle Oligocene (Chapter, 4) with percentages from the late Mid-Miocene values (Chapter 3) revealed a contrasting spatiotemporal distribution of mesic taxa in the New Jersey hinterland, probably caused by changing environmental conditions, which in the long-term trend led to an enhanced floristic turnover.

Several floristic elements reported in earlier studies (Chapter 1) as *Cyathea* or *Podopcarpus* could not be confirmed in the framework of the present thesis. Moreover, the present thesis demonstrates that occurring pollen grains similar to *Podocarpus* and *Pinus* subg. *Strobus* in closer analyses turned out to be *Cathaya* (Chapter 1, 2, 3, 5). The "Arecaceae problem" discussed in detail in Chapter 2 still needs further investigations. The identification of sulcate pollen grains of monocotyledons (e.g. Arecaceae) in the fossil record is often particularly complex, even in combination with the SEM (R. Zetter personal communication). The sulcate reticulate pollen grains encountered in the framework of the studies presented in Chapters 3–5 turned out to have more in common with sulcate reticulate Liliaceae pollen grains. A more detailed pollen grain analysis would also be needed for *Trigonobalanopsis* (Chapter 4).
Nevertheless, this study increased the knowledge of the floristic composition of eastern North America during the Oligocene and Miocene, but reveals as well that the floristic diversity in the New Jersey hinterland during the Cenozoic still needs more research. Future work should include a rigorous pollen grain evaluation via SEM providing a more detailed picture of the floristic diversity in the New Jersey hinterland and therefore of eastern North America. These important microfossil information would benefit palaeobiogeographic research for a number of plant genera and families.

6.2 Long-term vegetation evolution and their factors leading to vegetation changes through time

Regarding the poor and fragmentary palaeobotanical records of eastern North America (Wing, 1998; Graham, 1999; Chapter 1) this thesis reveals insights into the terrestrial vegetation evolution. In order to assess comprehensive continental palaeoecological changes, the identified taxa were grouped to palaeovegetation units, which might have existed throughout the entire analysed time intervals. The microfloristic assemblages indicate that the landscape was covered by a complex regional vertical onshore vegetation and signalize a variety of ecological conditions. Throughout the analysed Oligocene and Miocene time intervals mixed mesophytic forest represents the zonal vegetation.

Nevertheless, several small but significant vegetation changes in response to varying Cenozoic environmental conditions could be identified and confirm one of the main findings of this thesis. Factors leading to vegetation changes through time were of regional and global origin. During the middle Oligocene to early Miocene weak fluctuations signals demonstrate possible movement signals in terms of periodic climate oscillations.

The lack of information about continental floristic events according to changed environmental conditions during the Oligocene and early Miocene in eastern North America (compare chapter 1) emphasizes the importance of Chapter 4 and parts of Chapter 2. The observed movement signals during the middle Oligocene and early Miocene of different intensions are probably best reflected within peaks of meso- and microthermal Pinaceae, probably corresponding to the unnamed $\delta^{18}O$ excursion at ~29.1, the Oi2-a event at ~28.3 Ma and/or the ~28.5-Ma-$\delta^{18}O$ increase and to the Mi-1 event at ~23.8 Ma (Pekar et al., 2002). Moreover, regression phases (glacial phases) exposed shallow shelf areas and allowed the spreading of substrate-depending forest formations. The spreading of Palaeovegetation Units 3 (Cupressaceae) and 4 (mesophytic forest growing on dry soils) during glacial phases represents thus an indirect confirmation of climate change.

The limited temporal resolution of the pollen record presented in Chapter 4 inhibited, however, the evaluation of vegetation responses to periodic orbital changes of the Oligocene and early Miocene. Nonetheless, orbitally driven changes could be identified by studying Burdigalian sediment cores in a relative high temporal resolution (Chapter 5). The observed regional changes in the palaeovegetation in the New Jersey hinterland confirm the influence of orbital parameters during the Burdigalian corresponding to determined orbital parameters of the Burdigalian time interval (Laskar et al., 2004). Our results indicate that eccentricity and obliquity induced the reorganisation of the PVU-1 (high-altitude conifer forest) and 5 (mesophytic forest growing on moist/wet soils). Both eccentricity and obliquity operated in different altitudes and most likely modified specific threshold values, which regulated regional plant productivity and their competition. According to this, the small but significant continental palaeovegetation changes documented during a relatively warm time period with only modest amplitude of climatic variability (Liebrand et al., 2017) emphasises that the palaeovegetation of the New Jersey hinterland was not stable, in opposition to what various climate models indicate (von der Heydt and Dijkstra, 2006; Herold et al., 2011; 2012). This was also shown in Chapter 4.

Several pronounced hiatuses occur during the investigated Cenozoic time intervals formed during glacial phases (Browning et al., 2013) and hindered the examination of the global cooling events Mi3-a and Mi3-b, around ~14.2 Ma and ~13.8 Ma (Miller et al., 1996; Abels et al., 2005;

Chapter 2, 3). However, the fluctuation behaviour of several palaeovegetation types during selected Oligocene and Miocene time intervals (Chapter 4, 5) demonstrates plant movement according to cooling events. This implies that if sediments would have been deposited during the MMCT (Chapter 2, 3), pollen grain analysis would allow showing some significant signals according to this event. To resolve the hiatus problem and to receive information about plant movements during pronounced cooling events, the analysis of core sediments retrieved during previous drilling campaigns to the New Jersey margin (Chapter 1) could be a possibility.
The terrestrial palynomorph signature of the second half of the MMCO (Chapter 3) allowed the interpretation of vegetation changes linked to regional landscape modifications, which caused several vegetation units to spread or retreat. A trigger factor leading to a spreading of Cupressaceae between ~15.0 and ~14.8 Ma was edaphically induced, probably by an elevated soil moisture content, whereas the spreading of the conifer forest between ~15.8 and ~15.6 Ma was probably triggered by the Appalachian mountain uplift (Gallen et al., 2013; Liu, 2014), creating shallow immature soils (Carey et al., 2005).
In conclusion, through the selected Oligocene and Miocene time intervals, the evolution of palaeovegetation of the New Jersey hinterland reacts specifically to a variety of regional and global environmental conditions.

6.3 Climate history in the hinterland of New Jersey and the bioclimatic analysis

The regional climate evolution of the New Jersey hinterland during the late Palaeogene to the early middle Neogene reveals a general relative climatic stability, reflecting stable humid warm-temperate macroclimatic conditions. This climatic stability in the long-term trend is also expressed by the constant persistence of mesic taxa. Altogether, the macroclimatic conditions did not react as sensitively and would correspond to climate models of the geological time interval (von der Heydt and Dijkstra, 2006; Herold et al., 2011; 2012). However, since the analysed sediment cores along the analysed geological time scale were deposited during warmer Cenozoic intervals, in which several major marine isotopic stadia correspond to sequence boundaries (Browning et al., 2013), the analysis of time intervals with pronounced cooling (e.g. MMCT; Chapter 2, 3) was hindered, and thus only limited climatic changes could be identified.
The small, but stepwise weak cooling signal, which might correspond to the Mi-1 event (Chapter 2, 4), is reflected in calculated MAT, WMMT and CMMT (MAT and WMMT ~ –3°C; CMMT ~ –5°C). The observed differences in the calculated Schrepfer seasonality Index C (Chapter 5) show a strong coherence to the obliquity domain. In addition, it was shown that PVU-5 abundance minima are likely to be associated to seasonality maxima, which might indicate that seasonality variation triggered the variation of relative PVU-5 abundances.
Furthermore, the small vegetation changes in the hinterland through the analysed time intervals strongly emphasize a topographic climate gradient (mentioned in Chapter 2 and visible in all other Chapters). To what degree, however, is still unresolved because the applied method is not primarily developed to calculate topographic climate gradients.
Nevertheless, data providing a terrestrial topographic climate gradient are available for the Eocene of Wilkes Land (Antarctica), which were calculated with the same bioclimatic analysis as used in this thesis (Pross et al., 2012). The possible difference between the abovementioned study (Pross et al., 2012) and the present investigations for the New Jersey hinterland is that

the high- and mid-altitudes during the Oligocene and Miocene time interval were covered by conifer forest, whereas the palaeovegetation reconstruction for Wilkes Land during the Eocene revealed a temperate rainforest for higher elevated areas (Pross et al., 2012; Contreras et al., 2013). Genera like *Pinus*, *Picea* and *Abies* are – like in our investigations – often excluded from the generated climate estimates because the range of values of generated palaeoclimatic estimates would increase, resulting in less reliable generated estimates.
In any case further investigations relating to the topographic climate gradient in the New Jersey hinterland are required. Considering the discussion concerning the differentiation of Cupressaceae pollen grains, this thesis offered climate reconstructions including and excluding different Cupressaceae types (Chapter 3). The inclusion of thermophilous members of Cupressaceae reduces the large ranges of temperature values.
Taking all together, calculated pollen-based climatic reconstructions in the long-term trend reveal slight climatic changes within the humid warm temperate regional climate conditions of the New Jersey hinterland.

6.4 Data combination with other research fields

Moreover, the framework of IOPD Exp. 313 offers the prospect to investigate a combination with other research fields to receive a comprehensive reconstruction of the palaeoenvironmetal conditions not only from the continental hinterland but as well from the marine realm during the selective time intervals.
The integration of organic-walled dinoflagellate cyst, which are suitable for the reconstruction of marine palaeoenvironmental conditions like sea-surface temperature and productivity changes, would offer a correlation of the palaeoenvironmental conditions in the marine realm with those in the New Jersey hinterland. This could be realized, when samples would be analyzed using the identical samples as in the present thesis. This would offer a direct land-sea correlation for the selected time intervals. In addition, data sets of TEX-86 – a proxy for palaeotemperature reconstruction based on lipids derived of archaea – could be generated and could be used to correlate the temperature reconstructions generated during phases of this thesis.

Appendix Material

The raw dataset of Chapter 2-5 are on the attached compact disc.

References

Abels, H.A., Hilgen, F.J., Krijgsman, W., Kruk, R.W., Raffi, I., Turco, E., Zachariasse, W.J., 2005. Long-period orbital control on middle Miocene global cooling: Integrated stratigraphy and astronomical tuning of the Blue Clay Formation on Malta. Paleoceanography 20, PA4012, doi:10.1029/2004PA001129.

Abrams, M.D.,1992. Fire and the development of oak forests. BioScience 42, 346-353.

Alexander, M., 1973. Nonbiodegradable and other racalcitrant molecules. Biotechnology and Bioengineering 15, 611-647.

Axelrod, D.I., 1995. The Miocene Purple Mountain flora of western Nevada. University of California Publications, Geological Science 139, 1-62.

Barke, J., Abels, H.A., Sangiorgi, F., Greenwood, D.R., Sweet, A.R., Donders, T., Reichart, G.-J., Lotter, A.F., Brinkhuis, H., 2011. Orbitally forced Azolla blooms and Middle Eocene Arctic hydrology: Clues from palynology. Geology 39, 427-430.

Bartlein, P.J., Prentice, I.C., 1989. Orbital variations, climate and paleoecology. Trends in Ecology and Evolution 4, 195-199.

Bates, C.D., Coxon, P., Gibbard, P.L., 1978. A new method for the preparation of clay-rich sediment samples for palynological investigation. The New Phytologist 81, 459-463.

Beug, H.J., 2004. Leitfaden der Pollenbestimmung für Mitteleuropa und angrenzende Gebiete. Verlag Dr. Friedrich Pfeil, München, 542 pp.

Böhme, M., Bruch, A.A., Selmeier, A., 2007. The reconstruction of Early and Middle Miocene climate and vegetation in southern Germany as determined from the fossil wood flora. Palaeogeography, Palaeoclimatology, Palaeoecology 253, 91-114.

Bouchal, J., Zetter R., Grímsson, F., Denk, T., 2014. Evolutionary trends and ecological differentiation in early Cenozoic Fagaceae of western North America. American Journal of Botany 101, 1-18.

Box, E.O., 2015. Warm-temperate deciduous forest of Eastern North America. In: Box, E.O., Fujiwara, K., (Eds.). Warm-temperate Deciduos Forest around the Northern Hemisphere. Geobotany Studies, Springer International Publishing, Swizerland, pp. 225-255.

Boyce, C.K., Lee, J.-E., 2017. Plant evolution and climate over geological timescales. Annual Review of Earth and Planetary Sciences 45, 61-87.

Braun, E.L., 1950. Deciduous forest of eastern North America. Philadelphia, Blakiston Co, 596 pp.

Brodribb, T.J., Pittermann, J., Coomes, D.A., 2012. Elegance versus speed: Examining the competition between conifer and angiosperm trees. International Journal of Plant Sciences 173, 673-694.

Browning, J.V., Miller, K.G., Sugarman, P.J., Barron, J., McCarthy, F.M.G., Kulhanek, D.K., Katz, M.E., Feigenson, M.D., 2013. Chronology of Eocene-Miocene sequences on the New Jersey shallow shelf: Implications for regional, interregional, and global correlations. Geosphere 9, 1434-1456.

Bryson, R.A., Hare, F.K., 1974. Climates of North America (World Survey of Climatology, volume 11), Elsevier, Amsterdam, 420 pp.

Bůzek, Č., Kvaček, Z., Manchester, S.R. 1989. Sapindaceous affinities of the *Pteleaecarpum* Fruits from the Tertiary of Eurasia and North America. Botanical Gazette 150, 477-489.

Carey, A.E., Lyons, W.B., Owen, J.S., 2005. Significance of landscape age, uplift, and weathering rates to ecosystem development. Aquatic Geochemistry 11, 215-239.

Chaloner, W.G., Creber, G.T., 1990. Do fossil plants give a climatic signal? Journal of the Geological Society 147, 343-350.

Chen, S.T., Smith, S.Y., Sheldon, N.D., Strömberg, C.A., 2015. Regional-scale variability in the spread of grasslands in the late Miocene. Palaeogeography, Palaeoclimatology, Palaeoecology 437, 42-52.

Conner, W.H., Brody, M., 1989. Rising water levels and the future of southeastern Louisiana swamp forests. Estuaries 12, 318-323.

Contreras, L., Pross, J., Bijl, P.K., Koutsodendris, A., Raine, J.I., van de Schootbrugge, B., Brinkhuis, H., 2013. Early to middle Eocene vegetation dynamics at the Wilkes Land Margin (East Antarctica). Review of Palaeobotany and Palynology 197, 119-142.

Coates, A.G., Obando, J.A., 1996. The geologic evolution of the Central American Isthmus. In: Jackson, J.B.C., Budd, A.F., Coates, A.G., (Eds.), Evolution of Environments in Tropical America. University of Chicago Press, Chicago and London, pp. 21-56.

Coxall, H.K., Wilson, P.A., Palike, H., Lear, C.H. Backman, J., 2005. Rapid stepwise onset of Antarctic glaciation and deeper calcite compensation in the Pacific Ocean. Nature 433, 53-57.

Cramer, B.S., Toggweiler, J.R., Wright, D., Katz, M.E., Miller, K.G., 2009. Ocean overturning since the Late Cretaceous: Inferences from a new benthic foraminiferal isotope compilation. Paleoceanography 24, 1-14.

Crepet, W.L., Nixon, K.C.,1989. Extinct transitional Fagaceae from the Oligocene and their phylogenetic implications. American Journal of Botany 76, 1493-1505.

Csanady, G.T., Hamilton. P., 1988. Circulation of slopewater. Continental Shelf Research 8, 568-624.

Davis, R.B., Webb, T., 1975. The contemporary distribution of pollen in eastern North America: a comparison with the vegetation. Quaternary Research 5, 395-434.

Davis, O.K., Ellis, B., 2010. Early occurrence of sagebrush steppe, Miocene (12 Ma) on the Snake River Plain. Review of Palaeobotany and Palynology 160, 172-180.

DeConto, R.M., Pollard, D., Wilson, P.A., Pälike, H., Lear, C.H., Pagani, M., 2008. Thresholds for Cenozoic bipolar glaciation. Nature 455, 652-657.

Delcourt, P. A., Delcourt, H. R., Webb III, T., 1984. Atlas of Mapped Distribution of Dominance and Modern Pollen Percentages for Important Tree Taxa of Eastern North America, AASP Contribution 14, 131 pp.

Denk, T. & Grimm, G.W., 2009. The biogeographic history of beech trees. Review of Palaeobotany and Palynology 158, 83-100.

Denk, T., Grímsson, F., Zetter, R., 2010. Episodic migration of oaks to Iceland: Evidence for a North Atlantic "land bridge" in the latest Miocene. American Journal of Botany 97, 276-287.

Denk, T., Grímsson, F., Zetter, R., 2012. Fagaceae from the early Oligocene of Central Europe: Persisting new world and emerging old world biogeographic links. Review of Palaeobotany and Palynology 169, 7-20.

Denk, T., Grimm, G.W., Grímsson, F., Zetter, R., 2013. Evidence from „Köppen signatures" of fossil plant assemblages for effective heat transport of Gulf Stream to subarctic North Atlantic during Miocene cooling. Biogeosciences 10, 7927-7942.

Dicke, S.G., Toliver, J.R., 1990. Growth and development of bald-cypress/water-tupelo stands under continuous versus seasonal flooding. Forest Ecology and Management 33, 523-530.

Donders, T.H., Wagner, F., Dilcher, D.L., Visscher, H., 2005. Mid- to late-Holocene El Niño-Southern Oscillation dynamics reflected in the subtropical terrestrial realm. Proceedings of the National Academy of Sciences of the United States of America 102, 10904-10908.

Donders, T.H., Weijers, J.W.H., Munsterman, D.K., Kloosterboer-van Hoeve, M.L., Buckles, L.K., Pancost, R.D., Schouten,

S., Sinninghe Damsté, J.S. Brinkhuis, H., 2009. Strong climate coupling of terrestrial and marin environments in the Miocene of northwestern Europe. Earth and Planetary Science Letters 281, 215-225.

Dyer, J.M., 2006. Revisiting the deciduous forests of eastern North America. BioScience 56, 341-352.

eFloras. 2008. Flora of North America. http://www.efloras.org; accessed February–June 2016, March–June 2017.

Eldrett, J.S., Greenwood, D.R., Harding, I.C., Huber, M., 2009. Increased seasonality through the Eocene to Oligocene transition in northern high latitudes. Nature 459, 969-973.

Eldrett, J.S., Greenwood, D.R., Polling, M., Brinkhuis, H., Sluijs, A., 2014. A seasonality trigger for carbon injection at the Paleocene-Eocene Thermal Maximum. Climate of the Past 10, 759-769.

Egger, L.M., Bahr, A., Friedrich, O., Wilson, P.A., Norris, R.D., van Peer, T.E., Lippert, P.C., Liebrand, D., Pross, J., 2018. Sea-level and surface-water change in the western North Atlantic across the Oligocene-Miocene Transition: A palynological perspective from IODP Site U1406 (Newfoundland margin). Marine Micropaleontology 139, 57-71.

Expedition 313 Scientists, 2010a. Expedition 313 Summary. In Mountain, G., Proust, J.-N., McInroy, D., Cotterill, C., and the Expedition 313 Scientists (Eds.) Proceedings of the Integrated Ocean Drilling Program. Expedition 313: Tokyo (Integrated Ocean Drilling Program Management International, Inc.), 40 pp.

Expedition 313 Scientists, 2010b. Site M0027A. In: Mountain, G., Proust, J.-N., McInroy, D., Cotterill, C., and the Expedition 313 Scientists (Eds.), Proceedings of the Integrated Ocean Drilling Program. Expedition 313: Tokyo (Integrated Ocean Drilling Program Management International, Inc.), 148 pp.

Erdei, B., Hably, L., Kázmér, M., Utescher, T., Bruch, A.A., 2007. Neogene flora and vegetation development of the Pannonian domain in relation to palaeoclimate and palaeogeography. Palaeogeography, Palaeoclimatology, Palaeoecology 253, 115-140.

Erdtman, G., 1960. The acetolysis method. A revised description. Svensk Botanisk Tidskrift 54, 561-564.

Fang, J., Wang, Z., Tang, Z., 2011. Atlas of Woody Plants in China: Distribution and Climate. Higher Education Press, Beijing and Springer Verlag, Berlin, 1972 pp.

Fang, L., Bjerrum, C.J., Hesselbo, S.P., Kotthoff, U., McCarthy, F.M., Huang, B., Ditchfield, P.W., 2013. Carbon-isotope stratigraphy from terrestrial organic matter through the Monterey event, Miocene, New Jersey margin (IODP Expedition 313). Geosphere 9, 1303-1318.

Farjon, A., 2010. A Handbook of the World's Conifers. Volumes 1 and 2. Leiden: E. J. Brill.

Farjon, A., Filer, D., 2013. An Atlas of the World´s Conifers. An Analysis of their Distribution, Biogeography, Diversity and Conservation Status. Leiden, Boston: E. J. Brill, 512 pp.

Fauquette, S., Guiot, J., Suc, J.-P., 1998. A method for climatic reconstruction of the Mediterranean Pliocene using pollen data. Palaeogeography, Palaeoclimatology, Palaeoecology 144, 183-201.

Fauquette, S., Suc, J.-P., Bertini, A., Popescu, S.-M., Warny, S., Bachiri Taoufiq, N., Perez Villa, M.-J., Chikhi, H., Feddi, N., Subally, D., Clauzon, G., Ferrier, J., 2006. How much did climate force the Messinian salinity crisis? Quantified climatic conditions from pollen records in the Mediterranean region. Palaeogeography, Palaeoclimatology, Palaeoecology 238, 281-301.

Feng, C.-M., Manchester, S.R., Xiang, Q.-Y., 2009. Phylogeny and biogeography of Alangiaceae (Cornales) inferred from DNA

sequences, morphology, and fossils. Molecular Phylogenetics and Evolution 51, 201-214.

Flower, B.P., Kennett, J.P., 1994. Cenozoic climate and paleogeographic changes in the Pacific region the middle Miocene climatic transition: East Antarctic ice sheet development, deep ocean circulation and global carbon cycling. Palaeogeography, Palaeoclimatology, Palaeoecology 108, 537-555.

Fraser, W.T., Scott, A.C., Forbes, A.E.S., Glasspool, I.J., Plotnick, R.E., Kenig, F., Lomax, B.H., 2012. Evolutionary stasis of sporopollenin biochemistry revealed by unaltered Pennsylvanian spores. New Phytologist 196, 397-401.

Frederiksen, N.O., 1979. Paleogene sporomorph biostratigraphy, northeastern Virginia. Palynology 3, 129-167.

Frederiksen, N.O., 1980. Sporomorphs from the Jackson Group (Upper Eocene) and adjacent strata of Mississippi and western Alabama. U.S. Geological Survey, Reston, VA. Professional Paper 1084, 75 pp.

Frederiksen, N.O., 1991a. Midwayan (Paleocene) pollen correlations in the Eastern United States. Micropaleontology 37, 101-123.

Frederiksen, N.O., 1991b. Pulses of middle Eocene to earliest Oligocene climatic deterioration in Southern California and the Gulf Coast. PALAIOS 6, 564-571.

Frederiksen, N.O., 1984. Stratigraphic, paleoclimatic, and paleobiogeographic significance of Tertiary sporomorphs from Massachusetts. Geological Survey Professional Paper, 1308, United States Government Printing Office, Washington, 25 pp.

Gallen, S.F., Wegmann, K.W., Bohnenstiehl, D., 2013. Miocene rejuvenation of topographic relief in the southern Appalachians. Geological Society of America Today 23, 4-10.

Global Biodiversity Information Facility (GBF). http://www.gbif.org, last access: May, 2012.

Graham, A., 1999. Late Cretaceous History of North America Vegetation, North of Mexico. Oxford University Press New York, 338 pp.

Gray, J., 1960. Temperate pollen genera in the Eocene (Claiborne) flora, Alabama. Science 132, 808-810.

Greenwood, D.R., Moss, P.T., Rowett, A.I., Vadala, A.J., Keefe, R.L., 2003. Plant communities and climate change in southeastern Australia during the early Paleogene, Special Papers-Geological Society of America, 365-380.

Greenwood, D.R., Archibald, S.B., Mathewes, R.W., Moss, P.T., 2005. Fossil biotas from the Okanagan Highlands, southern British Columbia and northeastern Washington State: climates and ecosystems across an Eocene landscape. Canadian Journal of Earth Sciences 42, 167-185.

Greenwood, D.R., Hill, C.R., Conran, J.G., 2013. *Prumnopitys anglica* sp. nov. (Podocarpaceae) from the Eocene of England. Taxon 62, 565-580.

Grega, L., Anderson, S., Cheetham, M., Clemente, M., Colletti, A., Moy, W., Talarico, D., Thatcher, S.L., Osborn, J.M., 2013. Aerodynamic characteristics of saccate pollen grains. International Journal of Plant Sciences 174, 499-510.

Greller, A.M., Rachele, L.D., 1984. Climatic limits of exotic genera in the Legler palynoflora, Miocene, New Jersey, U.S.A.. Review of Palaeobotany and Palynology 40, 149-163.

Greller, A.M., 1988. Deciduous forest. In: Barbour, M.G., Billings, W.D. (Eds.). North America Terrestial Vegetation. Cambrigde University Press, pp. 287-316.

Griener, K.W., Warny, S., Askin, R., Acton, G., 2015. Early to middle Miocene vegetation history of Antarctica supports eccentricity-paced warming intervals during the Ant-

arctic icehouse phase. Global and Planetary Change 127, 67-78.

Grimm, G.W., Denk, T., 2012. Reliability and resolution of the Coexistence approach - A revalidation using modern-day data. Review of Palaeobotany and Palynology 172, 33-47.

Grimm, G., Denk, T., Bouchal, J.M., Potts, A.J., 2015. Fables and foibles: a critical analysis of the Palaeoflora database and the Coexistence approach for palaeoclimate reconstruction. Review of Palaeobotany and Palynology 233, 216-235.

Grimm, G.W., Potts, A.J., 2016. Fallacies and fantasies: the theoretical underpinnings of the Coexistence Approach for palaeoclimate reconstruction. Climate of the Past 12, 611-622.

Grímsson, F., Zetter, R., 2011. Combined LM and SEM study of the Middle Miocene (Sarmatian) palynoflora from the Lavanttal Basin, Austria: Part II. Pinophyta (Cupressaceae, Pinaceae and Sciadopityaceae). Grana 50, 262-310.

Grímsson, F., Zetter, R., Grimm, G.W., Pedersen, G.K., Pedersen, A.K., Denk, T., 2015. Fagaceae pollen from the early Cenozoic of West Greenland: revisiting Engler's and Chaney's Arcto-Tertiary hypotheses. Plant Systematics and Evolution 301, 809-832.

Grímsson, F., Grimm, G.W., Meller, B., Bouchal, J.M., Zetter, R., 2016a. Combined LM and SEM study of the middle Miocene (Sarmatian) palynoflora from the Lavanttal Basin, Austria: part IV. Magnoliophyta 2 - Fagales to Rosales. Grana 55, 101-163.

Grímsson, F., Grimm G.W., Zetter, R., Denk, T., 2016b. Cretaceous and Paleogene Fagaceae from North America and Greenland: evidence for a Late Cretaceous split between Fagus and the remaining Fagaceae. Acta Palaeobotanica 56, 247-305.

Groot, J.J., 1991. Palynological evidence for Late Miocene, Pliocene and Early Pleistocene climate changes in the middle U.S. Atlantic Coastal Plain. Quaternary Science Reviews 10, 147-162.

Groot, J.J., 1992. Plant microfossils of the Calvert Formation of Delaware, Newark, DE. Delaware Geological Survey, University of Delaware 50, 13 pp.

Hably, L., Kvaček, Z., Manchester, S.R., 2000. Shared taxa of land plants in the Oligocene of Europe and North America in context of Holarctic Phytogeography. Acta Universitatis Carolinae Geologica 44, 59-74.

Hansen, B.C.S., Grimm, E.C., Watts, W. A., 2001. Palynology of the Peace Creek site, Polk County, Florida. Geological Society of American Bulletin 113, 682-692.

Harley, M.M, Baker, W.J., 2001. Pollen aperture morphology in Arecaceae: application within phylogenetic analyses, and a summary of the fossil record of palm-like pollen. Grana 40, 45-77.

Havill, N.P., Campbell, C.S., Vining, T.F., LePage, B., Bayer, R.J., Donoghue, M.J., 2008. Phylogeny and biogeography of *Tsuga* (Pinaceae) inferred from nuclear ribosomal ITS and chloroplast DNA sequence data. Systematic Botany 33, 478-489.

Herbert, J., 2005. Systematics and biogeography of Myricaceae. PhD thesis, University of St. Andrews, St. Andrews, UK, 244 pp.

Herold, N., You, Y., Müller, R.D., Seton, M., 2009. Climate model sensitivity to changes in Miocene paleotopography. Australian Journal of Earth Sciences 56, 1049-1059.

Herold, N., Huber, M., Müller, R.D., 2011. Modeling the Miocene Climatic Optimum: Part 1 Land and Atmosphere, Journal of Climate 24, 6353-6372.

Grimes, S.T., Hooker, J.J., Collinson, M.E., Mattey, D.P., 2005. Summer temperatures of late Eocene to early Oligocene freshwaters. Geology 33, 189-192.

Herold, N., Huber, M., Müller, R.D., Seton, M., 2012. Modeling the Miocene Climatic Optimum: Ocean circulation, Paleoceanography 27, PA1209, doi:10.1029/2010PA002041.

Hesse, M., Blackmore, S., 2013. Preface to the special focus manuscripts. Plant Systematics and Evolution 299, 1011-1012.

Hesse, M., Halbritter, H., Zetter, R., Weber, M., Buchner, R., Frosch-Radivo, A., Ulrich, S., 2009. Pollen terminology. An illustrated handbook, Springer, New York, Wien, 261 pp.

Heusser, L.E., Shackleton, N., 1979. Direct marine-continental correlation: 150,000-Year oxygen isotope pollen record from the North Pacific. Science 204, 837-838.

Heusser, L.E., 1983. Pollen distribution in the bottom sediments of the western North Atlantic Ocean. Marine Micropaleontology 8, 77-88.

Heusser, L.E., 1988. Pollen distribution in marine sediments on the continental margin off northern California. Marine Geology 80, 131-147.

Hofmann, C.-C., Zetter, R., 2005. Reconstruction of different wetland plant habitats of the Pannonian Basin System (Neogene, Eastern Austria). Palaios 20, 266-279.

Hooghiemstra, H., Agwu, C.O.C., 1986. Distribution of palynomorphs in marine sediments: A record for seasonal wind patterns over NW Africa and adjacent Atlantic. Geologische Rundschau 75, 81-95.

Hooghiemstra, H., 1988. Palynological records from Northwest African marine sediments: a general outline of the interpretation of the pollen signal. Philosophical Transactions of the Royal Society of London, Series B, Biological Sciences 318, 431-449.

Hopkins, J.A. and McCarthy, F.M.G., 2002. Postdepositional palynomorph degradation in Quaternary shelf sediments: a laboratory experiment studying the effects of progressive oxidation. Palynology 26, 167-184.

Holbourn, A., Kuhnt, W., Schulz, M., Flores, J.-A., Andersen, N., 2007. Orbitally-paced climate evolution during the middle Miocene "Monterey" carbon-isotope excursion. Earth and Planetary Science Letters 261, 534-550.

Holbourn, A., Kuhnt, W., Kochhann, K.G.D., Andersen, N., Meier, K.J.S., 2015. Global perturbation of the carbon cycle at the onset of the Miocene Climatic Optimum. Geology 43, 123-126.

Huntley, B., Webb, T., 1989. Migration: Species' response to climatic variations caused by changes in the Earth's orbit. Journal of Biogeography 16, 5-19.

Jacobs, B.F., Kingston, J.D., Jacobs, L.L., 1999. The origin of grass dominated ecosystems. Annals of the Missouri Botanical Garden 86, 590-644.

Janis, C.M., 1993. Tertiary mammal evolution in the context of changing climates, vegetation and tectonic events. Annual Review of Ecology, Evolution and Systematics 24, 467-500.

Jarzen, D.M., Dilcher, D.L., 2006. Middle Eocene terrestrial palynomorphs from the Dolime Minerals and Gulf Hammock Quarries, Florida, USA. Palynology 30, 89-110.

Jarzen, D.M., Corbett, S.L., Manchester, S.R., 2010. Palynology and paleoecology of the Middle Miocene Alum Bluff Flora, Liberty. Palynology 34, 261-286.

Jiménez-Moreno, G., Rodriguez, F.J., Pardo-Iguzquiza, E., Fauquette, S., Suc, J., Muller, P., 2005. High resolution palynological analysis in late early-middle Miocene core from the Pannonian Basin, Hungary: Climate changes, astronomical forcing and eustatic fluctuations in the Central Paratethys. Palaeogeography, Palaeoclimatology, Palaeoecology 216, 73-97.

Jiménez-Moreno, G., Fauquette, S., Fauquette, S., Suc, J., Aziz, H.A., 2007. Early Miocene repetitive vegetation and climatic changes in the lacustrine deposits of the Rubielos de Mora Basin (Teruel, NE Spain). Palaeogeography, Palaeoclimatology, Palaeoecology 250, 103-113.

Jiménez-Moreno, G., de Leeuw, A., Mandic, O., Harzhauser, M., Pavelić, D., Krijgs-

man, W., Vranjković, A., 2009. Integrated stratigraphy of the Early Miocene lacustrine deposits of Pag Island (SW Croatia): Palaeovegetation and environmental changes in the Dinaride Lake System. Palaeogeography, Palaeoclimatology, Palaeoecology 280, 193-206.

Jiménez-Moreno, G., Fauquette, S., Suc, J.-P., 2010. Miocene to Pliocene vegetation reconstruction and climate estimates in the Iberian Peninsula from pollen data. Review of Palaeobotany and Palynology 162, 403-415.

Joannin, S., Bassinot, F., Nebout, N.C., Peyron, O., Beaudouin, C., 2011. Vegetation response to obliquity and precession forcing during the Mid-Pleistocene Transition in Western Mediterranean region (ODP site 976). Quaternary Science Reviews 30, 280-297.

Kaneps, A.G., 1979. Gulf Stream: velocity fluctuations during the late Cenozoic. Science 204, 297-301.

Katz, M.E., Miller, K.G., Wright, J.D., Wade, B.S., Browning, J.V., Cramer, B.S., Rosenthal, Y., 2008. Stepwise transition from the Eocene greenhouse to the Oligocene icehouse. Nature Geoscience 1, 329-334.

Katz, M.E., Browning, J.V., Miller, K.G., Monteverde, D., Mountain, G.S., Williams, R.H., 2013. Paleobathymetry and sequence stratigraphic interpretations from benthic foraminifera: Insights on New Jersey shelf architecture, IODP Expedition 313: Geosphere 9, 1488-1513.

Kerr, R.A., 1978. Climate control: How large a role for orbital variations? Science 201, 144-146.

Kmenta, M., Zetter, R., 2013. Combined LM and SEM study of the upper Oligocene/lower Miocene palynoflora from Altmittweida (Saxony): Providing new insights into Cenozoic vegetation evolution of Central Europe. Review of Palaeobotany and Palynology 195, 1-18.

Kottek, M., Grieser, J., Beck, C., Rudolf, B., Rubel, F., 2006. World map of the Köppen-Geiger climate classification updated. Meteorologische Zeitschrift 15, 259-263.

Kotthoff, U., Müller, U.C., Pross, J., Schmiedl, G., Lawson, I.T., van de Schootbrugge, B., Schulz, H., 2008a. Late Glacial and Holocene vegetation dynamics in the Aegean region: An integrated view based on pollen data from marine and terrestrial archives. Holocene 18, 1019-1032.

Kotthoff, U., Pross, J., Müller, U.C., Peyron, O., Schmiedl, G., Schulz, H., Bordon, A., 2008b. Timing and characteristics of terrestrial vegetation change in the NE Mediterranean region associated with the formation of marine Sapropel S1: A land-sea correlation. Quaternary Science Review 27, 832-845.

Kotthoff, U., Müller, U.C., Pross, J., Schmiedl, G., Lawson, I.T., van de Schootbrugge, B., Schulz, H., 2008c. Late Glazial and Holocene vegetation dynamics in the Aegean region: an integrated view based on pollen data from the marine and terrestrial archives. Holocene 18, 1019-1032.

Kotthoff, U., Greenwood, D., McCarthy, F., Müller-Navarra, K., Prader, S., Hesselbo, S., 2014. Late Eocene to middle Miocene (33 to 13 million years ago) vegetation and climate development on the North American Atlantic Coastal Plain (IODP Expedition 313, Site M0027). Climate of the Past 10, 1523-1539.

Kovar-Eder, J., 2016. Early Oligocene plant diversity along the Upper Rhine Graben: The fossil flora of Rauenberg, Germany. Acta Palaeobotanica 56, 329-440.

Kramer, K., Leinonen, I., Loustau, D., 2000. The importance of phenology for the evaluation of impact of climate change on growth of boreal, temperate and Mediterranean forests ecosystems: an overview. International Journal of Biometeorology 44, 67-75.

Krutzsch, W., 1963a. Atlas der mittel- und

jungtertiären dispersen Sporen- und Pollen- sowie der Mikroplanktonformen des nördlichen Mitteleuropa, Lieferung II. VEB Deutscher Verlag der Wissenschaften, Berlin, 141 pp.

Krutzsch, W., 1963b. Atlas der mittel- und jungtertiären dispersen Sporen- und Pollen- sowie der Mikroplanktonformen des nördlichen Mitteleuropa, Lieferung III. VEB Deutscher Verlag der Wissenschaften, Berlin, 128 pp.

Krutzsch, W., 1967. Atlas der mittel- und jungtertiären dispersen Sporen- und Pollen- sowie der Mikroplanktonformen des nördlichen Mitteleuropa, Lieferung IV und V. VEB Deutscher Verlag der Wissenschaften, Berlin, 232 pp.

Krutzsch, W., 1970. Atlas der mittel- und jungtertiären dispersen Sporen- und Pollen- sowie der Mikroplanktonformen des nördlichen Mitteleuropa, Lieferung VII. VEB Deutscher Verlag der Wissenschaften, Berlin, 175 pp.

Krutzsch, W., 1971. Atlas der mittel- und jungtertiären dispersen Sporen- und Pollen- sowie der Mikroplanktonformen des nördlichen Mitteleuropa, Lieferung VI. VEB Deutscher Verlag der Wissenschaften, Berlin, 234 pp.

Kvaček, Z., Walther H., 1991. Revision der mitteleuropäischen tertiären Fagaceen nach blattepidermalen Charakteristiken. IV. Teil *Fagus* Linné. Feddes Repertorium 102, 471-534.

Kvaček, Z., 2007. Do extant nearest relatives of thermophile European Cenozoic plant elements reliably reflect climatic signal? Palaeogeography, Palaeoclimatology, Palaeoecology 253, 32-40.

Kvaček, Z., Rember, W.C., 2000. Shared Miocene conifers of the Clarkia flora and Europe. Acta Universitatis Carolinae Geologica 44, 74-86.

Kvaček, Z., Manchester, S.R., Zetter, R., Pingen, M., 2002. Fruits and seeds of *Craigia bronnii* (Malvaceae - Tilioideae) and associated flower buds from the late Miocene Inden Formation, Lower Rhine Basin, Germany. Review of Palaeobotany and Palynology 119, 311-324.

Kvaček, Z., Walther, H., 2004. Oligocene flora of Bechlejovice at Děčín from the neovolcanic area of the České středohoří Mountains, Czech Republic. Acta Musei Nationalis Pragae, Series B, Natural History 60, 9-60.

Lacourse, T., Mathewes, R.W., Fedje, D.W., 2003. Paleoecology of late-glacial terrestrial deposits with in situ conifers from the submerged continental shelf of western Canada. Quaternary Research 60, 180-188.

Larcher, W., 2005. Climatic constraints drive the evolution of low temperature resistance in woody plants. Journal of Agricultural Meteorology 61, 189-202.

Larsson, L.M., Vajda, V., Dybkjær, K., 2010. Vegetation and climate in the latest Oligocene-earliest Miocene in Jylland, Denmark. Review of Palaeobotany and Palynology 159, 166-176.

Larsson, L.M., Dybkjær, K., Rasmussen, E.S., Piasecki, S., Utescher, T., Vajda, V., 2011. Miocene climate evolution of northern Europe: A palynological investigation from Denmark. Palaeogeography, Palaeoclimatology, Palaeoecology 309, 161-175.

Laskar, J., Robutel, P., Joutel, F., Gastineau, M., Correia, A.C.M., Levrard, B., 2004. A long term numerical solution for the insolation quantities of the Earth. Astronomy and Astrophysics 428, 261-285.

Lear, C.H., Rosenthal, Y., Coxall, H.K., Wilson, P.A., 2004. Late Eocene to early Miocene ice sheet dynamics and the global carbon cycle. Paleoceanography 19, PA4015, doi:10.1029/2004PA001039.

Lelono, E.B., Morley, R.J., 2011. Oligocene palynological succession from the East Java Sea. Geological Society, London, Special Publications 355, 333-345.

Leopold, E.B., Liu, G., Clay-Poole, S., 1992. Low-biomass vegetation in the Oligocene?. In: Prothero, D. A., Bergren, W.A., (Eds.). Eocene-Oligocene Climatic and Biotic Evolution. Princeton University Press, Princeton, NJ, 399-420.

Leopold, E.B., Liu, G., 1994. A long pollen sequence of Neogene age, Alaska range. Quaternary International 22-23, 103-140.

Liebrand, D., Lourens, L.J., Hodell, D.A., de Boer, B., van de Wal, R.S.W., Pälike, H., 2011. Antarctic ice sheet and oceanographic response to eccentricity forcing during the early Miocene. Climate of the Past 7, 869-880.

Liebrand, D., Beddow, H.M., Lourens, L.J., Pälike, H., Raffi, I., Bohaty, S.M., Hilgen, F.J., Saes, M.J.M., Wilson, P.A., van Dijk, A.E., Hodell, D.A., Kroon, D., Huck, C.E., Batenburg, S.J., 2016. Cyclostratigraphy and eccentricity tuning of the early Oligocene through early Miocene (30.1-17.1 Ma): *Cibicides mundulus* stable oxygen and carbon isotope records from Walvis Ridge Site 1264. Earth and Planetary Science Letters 450, 392-405.

Liebrand, D., de Bakker, A.T.M., Beddow, H.M., Wilson, P.A., Bohaty, S.M., Ruessink, G., Pälike, H., Batenburg, S.J., Hilgen, F.J., Hodell, D.A., Huck, C.E., Kroon, D., Raffi, I., Saes, M.J.M., van Dijk, A.E., Lourens, L.J., 2017. Evolution of the early Antarctic ice ages. Proceedings of the National Academy of Sciences 114, 3867-3872.

Lieth, H., 1974. Introduction to phenology and modeling of seasonality. In: Lieth, H., (Ed.), Phenology and Seasonality Modeling Ecological Studies. Springer Sciene and Business Media LLC, pp. 3-23.

Lieth, H., Berlekamp, J., Fuest, S., Riediger, S., 1999. Climate Diagram World Atlas. Backhuys Leiden.

Liu, G., Leopold, E.B., 1992. Paleoecology of a Miocene flora from the Shanwang formation, Shandong Province, northern east China. Palynology 16, 187-212.

Liu, G., Leopold, E.B., 1994. Cenozoic climate and paleogeographic changes in the Pacific region - climatic comparison of Miocene pollen floras from northern East-China and south-central Alaska, USA. Palaeogeography, Palaeoclimatology, Palaeoecology 108, 217-228.

Liu, L., 2014. Rejuvenation of Appalachian topography caused by subsidence-induced differential erosion. Nature Geoscience 7, 518-523.

Liu, Y.S., Basinger, J.F., 2000. Fossil *Cathaya* (Pinaceae) pollen from the Canadian High Arctic. International Journal of Plant Sciences 161, 829-847.

Liu, Z., Pagani, M., Zinniker, D., DeConto, R., Huber, M., Brinkhuis, H., Shah, S.R., Leckie, R.M., Pearson, A., 2009. Global cooling during the Eocene-Oligocene climate transition. Science 323, 1187-1190.

Lourens, L.J., Sluijs, A., Kroon, D., Zachos, J.C., Thomas, E., Röhl, U., Bowles, J., Raffi, I., 2005. Astronomical pacing of late Palaeocene to early Eocene global warming events. Nature 435, 1083.

Lyons, W.B., Carey, A.E., Hicks, D.M., Nezat, C.A., 2005. Chemical weathering in high-sediment-yielding watersheds, New Zealand. Journal of Geophysical Research, 110, F01008, doi:10.1029/2003/JF000088.

Manchester, S.R., 1987. The fossil history of the Juglandaceae. Monographs in Systematic Botany 21, 1-137.

Manchester, S.R., 1999. Biogeographical relationships of North American Tertiary floras. Annals of the Missouri Botanical Garden 86, 472-522.

Manchester, S.R., Dillhoff, R.M., 2005. *Fagus* (Fagaceae) fruits, foliage, and pollen from the Middle Eocene of Pacific northwestern North America. Canadian Journal of Botany 82, 1509-1517.

Manchester, S.R., Chen, Z.-D., Lu, A.-M., Uemura, K., 2009. Eastern Asian endemic seed

plant genera and their paleogeographic history throughout the Northern Hemisphere. Journal of Systematics and Evolution 47, 1-42.

Meyer, H.W., Manchester, S.R., 1997. The Oligocene Bridge Creek Flora of the John Day Formation, Oregon. In: Awramik, S.W., Barnosky, A., Doyle, J.A., Droser, M.L., Sadler, P.M., (Eds.). University of California Publications in Geological Sciences. University of California Press Berkeley, Los Angeles, London, 197 pp.

Manos, P.S., Meireles, J.E., 2015. Biogeographic analysis of the woody plants of the Southern Appalachians: Implications for the origins of a regional flora. American Journal of Botany 102, 1-25.

Marret, F., 1993. Les effets de l'acétolyse sur les assemblages de kystes de dinoflagellés. Palynosciences 2, 267-272.

McAndrews, J.H., Berti, A.A., Norris, G., 1973. Key to the Quaternary Pollen and Spores of the Great Lakes Region. Life Science Miscellaneous Publications, Royal Ontario Museum, Toronto, 65 pp.

McCartan, L., Tiffney, B.H., Wolfe, J.A., Ager, T.A., Wing, S.L., Sirkin, L.A., Ward, L.W., Brooks, J., 1990. Late Tertiary floral assemblage from upland gravel deposits of the southern Maryland Coastal Plain. Geology 18, 311-314.

McCarthy, F.M.G., Mudie, P.J., 1998. Oceanic pollen transport and pollen:dinocyst ratios as markers of late cenozoic sea level change and sediment transport. Palaeogeography, Palaeoclimatology, Palaeoecology 138, 187-206.

McCarthy, F.M.G., Gostlin, K.E., 2000. Correlating Pleistocene sequences across the New Jersey margin, Sedimentary Geology 134, 181-196.

McCarthy, F.M.G., Gostlin, K.E., Mudie, P.J., Scott, D.B., 2000. Synchronous palynological changes in early Pleistocene sediments off New Jersey and Iberia, and a possible paleoceanographic explanation. Palynology 24, 63-77.

McCarthy, F.M.G., Gostlin, K.E., Mudie, P.J., Hopkins, J.A., 2003. Terrestrial and marine palynomorphs as sea-level proxies: an example from Quaternary sediments on the New Jersey margin. Society for Sedimentary Geology Special Publications 75, 119-129.

McCarthy, F.M.G., Gostlin, K.E., Mudie, P.J., Pedersen, R.O., 2004. The palynological record of terrigenous flux to the deep sea: late Pliocene-Recent examples from 41N in the abyssal Atlantic and Pacific oceans. Review of Palaeobotany and Palynology 128, 81-95.

McCarthy, F.M.G., Katz, M.E., Kotthoff, U., Browning, J.V., Miller, K.G., Zanatta, R., Williams, R.H., Drljepan, M., Hesselbo, S.P., Bjerrum, C.J., Mountain, G.S., 2013. Sea-level control of New Jersey margin architecture: Palynological evidence from Integrated Ocean Drilling Program Expedition 313. Geosphere 9, 1457-1487.

Millar, C.I.,1998. Early evolution of pines. In: Richardson, D.M., (Ed.). Ecology and Biogeography of *Pinus*. Cambridge University Press, Cambridge, pp.69-94.

Miller, K.G., Fairbanks, R.G., Mountain, G.S., 1987. Tertiary oxygen isotope synthesis, sea level history, and continental margin erosion. Paleoceanography 2, 1-19.

Miller, K.G., Wright, J.D., Fairbanks, R.G., 1991. Unlocking the Ice House: Oligocene-Miocene oxygen isotopes, eustasy, and margin erosion. Journal of Geophysical Research: Solid Earth 96, 6829-6848.

Miller, K.G., Mountain, G.S., 1994. Global sea-level change and the New Jersey margin. In: Mountain, G.S., Miller, K.G., Blum, P., et al., (Eds.). Proceedings of the Ocean Drilling Program, Initial Repports 150. College Station, TX (Ocean Drilling Program), 11-20.

Miller, K.G., Sugarman, P.J., 1995. Correlat-

ing Miocene sequences in onshore New Jersey boreholes (IODP Leg 150X) with global $\delta^{18}O$ and Maryland outcrops. Geology 23, 747-750.

Miller, K.G., Mountain, G.S., the Leg 150 Shipboard Party Members of the New Jersey Coastal Plain Drilling Project, 1996. Drilling and Dating New Jersey Oligocene-Miocene Sequences: Ice volume, global sea level, and Exxon Records. Science 27, 1092-1095.

Miller, K.G., Mountain, G.S., Browning, J.V., Kominz, M., Sugarman, P.J., Christie-Blick, N., Katz, M.E., Wright, J.D., 1998. Cenozoic global sea level, sequences, and the New Jersey Transect: Results from coastal plain and continental slope drilling. Reviews of Geophysics 36, 569-601.

Miller, K.G., Kominz, M.A., Browning, J.V., Wright, J.D., Mountain, G.S., Katz, M.E., Sugerman, P.J., Cramer, B.S., Christie-Blick, N., Pekar, S.F., 2005. The Phanerozoic record of global sea-level change. Science 310, 1293-1298.

Miller, K.G., Mountain, G.S., Wright, J.D., Browning, J.V., 2011. A 180-million-year record of sea level and ice volume variations from continental margin and deep-sea isotopic records.Oceanography 24, 40-53.

Miller, K.G., Browning, J.V., Mountain, G.S., Bassetti, M.A., Monteverde, D., Katz, M.E., Inwood, J., Lofi, J., Proust, J.-N., 2013a. Sequence boundaries are impedance contrasts: Core-seismic-log integration of Oligocene-Miocene sequences, New Jersey shallow shelf. Geosphere 9, 1257-1285.

Miller, K.G., Mountain, G.S., Browning, J.V., Katz, M.E., Monteverde, D., Sugarman, P.J., Ando, H., Bassetti, M.A., Bjerrum, C.J., Hodgson, D., Hesselbo, S., Karakaya, S., Proust, J.-N., Rabineau, M., 2013b. Testing sequence stratigraphic models by drilling Miocene foresets on the New Jersey shallow shelf. Geosphere 9, 1236-1256.

Milne, R.I., Abbott, R.J., 2002. The origin and evolution of tertiary relict floras, Advances in Botanical Research Academic Press, 281-314.

Montade, V., Nebout, N.C., Kissel, C., Mulsow, S., 2011. Pollen distribution in marine surface sediments from Chilean Patagonia. Marine Geology 282, 161-168.

Moran, K., Backman, J., Brinkhuis, H., Clemens, S.C., Cronin, T., Dickens, G.R., Eynaud, F., Gattacceca, J., Jakobsson, M., Jordan, R.W., Kaminski, M., King, J., Koc, N., Krylov, A., Martinez, N., Matthiessen, J., McInroy, D., Moore, T.C., Onodera, J., O'Regan, M., Pälike, H., Rea, B., Rio, D., Sakamoto, T., Smith, D.C., Stein, R., St John, K., Suto, I., Suzuki, N., Takahashi, K., Watanabe, M., Yamamoto, M., Farrell, J., Frank, M., Kubik, P., Jokat, W., Kristoffersen, Y., 2006. The Cenozoic palaeoenvironment of the Arctic Ocean. Nature 441, 601-605.

Mountain, G., Proust, J.-N., the Expedition 313 Scientists, 2010a. The New Jersey margin scientific drilling project (IOPD Expedition 313): Untangling the record of global and local sea-level changes. Progress Report, Scientific Drilling, 10, 26-34.

Mountain, G., Proust, J.-N., McInroy, D., Cotterill, C., the Expedition 313 Scientists, 2010b. Proceedings of the Integrated Ocean Drilling Program. Expedition 313: Tokyo (Integrated Ocean Drilling Program Management International, Inc.) doi:10.2204/iodp.proc.313.101.2010, 40 pp.

Mosbrugger, V., Utescher, T., 1997. The Coexistence approach - a method for quantitative reconstructions of Tertiary terrestrial palaeoclimate data using plant fossils. Palaeogeography, Palaeoclimatology, Palaeoecology 134, 61-86.

Mosbrugger, V., Utescher, T., Dilcher, D.L., 2005. Cenozoic continental climatic evolution of Central Europe. Proceedings of the National Academy of Sciences of the United States of America 102, 14964-14969.

Mudelsee, M., Bickert, T., Lear, C.H., Lohmann, G., 2014. Cenozoic climate changes: A review based on time series analysis of marine benthic $\delta^{18}O$ records. Reviews of Geophysics 52, 333-374.

Mudie, P.J., 1982. Pollen distribution in recent marine sediments, eastern Canada. Canadian Journal of Earth Science 19, 729-747.

Mudie, P.J., McCarthy, F.M.G., 1994. Late Quaternary pollen transport processes, western North Atlantic: Data from box models, cross-margin and N-S transects. Marine Geology 118, 79-105.

Mudie, P.J., McCarthy, F.M.G., 2006. Marine palynology: potentials for onshore-offshore correlation of Pleistocene-Holocene records. Transactions of the Royal Society of South Africa 61, 139-157.

Mullins, H.T., Neumann, A.C., 1979. Geology of the Miami Terrace and its paleo-oceanographic implications. Marine Geology 30, 205-232.

Mullins, H.T., Gardulski, A.F., Wise, S.W., Applegate, J., 1987. Middle Miocene oceanographic event in the eastern Gulf of Mexico: Implications for seismic stratigraphic succession and Loop Current/Gulf Stream circulation. Geological Society of America Bulletin 98, 702-713.

Natural Resources Canada: Climatic Range map (1971-2000scenario)/climatic profile:Canadian Forest Service, Sault Ste. Marie, http.//planthardiness.gc.ca/index.pl?lang=enandm=13anddp=1, last access: May 2012.

Nichols, D.J., 1973. North American and European species of *Momipites* ("*Engelhardtia*") and related genera. Geoscience and Man 7, 103-117.

Nichols D.J., Brown, J.L., 1992. Palynostratigraphy of the Tullock Member lower Paleocene of the Fort Union Formation in the Powder River Basin Montana and Wyoming. Evolution of sedimentary basins Powder River Basin. U.S. Geological Survey Bulletin 1917-F, F1-F35.

Oboh, F.E., Jaramillo, C.A., Reeves Morris, L.M., 1996. Late Eocene-Early Oligocene paleofloristic patterns in southern Mississippi and Alabama, US Gulf Coast. Review of Palaeobotany and Palynology 91, 23-34.

Oboh, F.E., Reeves Morris, L.M., 1994. Early Oligocene palynosequences in the Eastern Gulf Coast, USA. Palynology 18, 213-235.

Ochoa, D., Whitelaw, M., Liu, Y.-S., Zavada, M., 2012. Palynology of Neogene sediments at the Gray Fossil Site, Tennessee, USA: Floristic implications. Review of Palaeobotany and Palynology 184, 36-48.

Owens, J.P., Bybell, L.M., Paulachok, G., Ager, T.A., Gonzalez, V.M., Sugarman, P.J., 1988. Stratigraphy of the Tertiary sediments in a 945-foot-deep corehole near Mays Landing in the southeastern New Jersey coastal plain, USGS Professional Paper 1484, 39 pp.

Pagani, M., Arthur, M.A., Freeman, K.H., 1999. Miocene evolution of atmospheric carbon dioxide. Paleoceanography 14, 273-292.

Pagani, M., Zachos, J.C., Freeman, K.H., Tipple, B., Bohaty, S., 2005. Marked decline in atmospheric carbon dioxide concentrations during the Paleogene. Science 309, 600-603.

Pagani, M., Caldeira, K., Berner, R., Beerling D. J., 2009. The role of terrestrial plants in limiting atmospheric CO2 decline over the past 24 million years. Nature 460, 85-88.

Paillard, D., Labeyrie, L., and Yiou, P., 1996. Macintosh program performs time-series analysis, Eos Transactions of the American Gepohysical Union 77, 379-379.

Pälike, H., Norris, R.D., Herrle, J.O., Wilson, P.A., Coxall, H.K., Lear, C.H., Shackleton, N.J., Tripati, A.K., Wade, B.S., 2006. The heartbeat of the Oligocene climate system. Science 314, 1894-1898.

Pazzaglia, F.J., Brandon, M.T., 1996. Macrogeomorphic evolution of the post-Triassic Appalachian mountains determined

by deconvolution of the offshore basin sedimentary record. Basin Research 8, 255-278.

Pazzaglia, F.J., Robinson, R.A.J., Traverse, A., 1997. Evolution of the Atlantic coastal Plain palynology of the Bryn Mawr Formation (Miocene): Insights on the age and genesis of middle Atlantic margin fluvial deposits. Sedimentary Geology 108, 19-44.

Peet, R.K., 1988. Forest of the Rocky Mountains. In: Barbour, M.G. and Billings, W.D. (Eds.). North American Terrestrial Vegetation. Cambridge University Press, Cambridge, 63-101.

Pekar, S.F., Christie-Blick, N., Kominz, M.A., Miller, K.G., 2001. Evaluating the stratigraphic response to eustasy from Oligocene strata in New Jersey. Geology 29, 55-58.

Pekar, S.F., Christie-Blick, N., 2008. Resolving apparent conflicts between oceanographic and Antarctic climate records and evidence for a decrease in pCO2 during the Oligocene through early Miocene (34-16 Ma). Palaeogeography, Palaeoclimatology, Palaeoecology 260, 41-49.

Pekar, S.F., Christie-Blick, N., Kominz, M.A., Miller, K.G., 2002. Calibration between eustatic estimates from backstripping and oxygen isotopic records for the Oligocene. Geology 30, 903-906.

Pekar, S.F., DeConto, R.M., Harwood, D.M., 2006. Resolving a late Oligocene conundrum: Deep-sea warming and Antarctic glaciation. Palaeogeography, Palaeoclimatology, Palaeoecology 231, 29-40.

Pennington, T.D., 2004. Sapotaceae. In: Kubitzki, K. (Ed.), Flowering Plants. Dicotyledons: Celastrales, Oxalidales, Rosales, Cornales, Ericales. Springer Berlin Heidelberg, Berlin, Heidelberg, 390-421.

Pinet, P.R., Popenoe, P., Nelligan, D.F., 1981. Gulf Stream: reconstruction of Cenozoic flow patterns over the Blake Plateau. Geology 9, 266-270.

Pittermann, J., Sperry, J.S., 2006. Analysis of freeze-thaw embolism in Conifers. The interaction between cavitation pressure and tracheid size. Plant Physiology 140, 374-382.

Poag, C.W., Sevon, W.D., 1989. A record of Appalachian denudation in postrift Mesozoic and Cenozoic sedimentary deposits of the U.S. Middle Atlantic Continental Margin. Geomorphology 2, 119-157.

Popescu, S.-M., Suc, J.-P., Loutre, M.-F., 2006. Early Pliocene vegetation changes forced by eccentricity-precession. Example from southwestern Romania. Palaeogeography, Palaeoclimatology, Palaeoecology 238, 340-348.

Potter, P.E., Szatmari, P., 2009. Global Miocene tectonics and the modern world. Earth-Science Reviews 96, 279-295.

Prader, S., Kotthoff, U., McCarthy, F.M.G., Schmiedl, G., Donders, T.H., Greenwood, D.R., 2017. Vegetation and climate development of the New Jersey hinterland during the late Middle Miocene (IODP Expedition 313 Site M0027). Palaeogeography, Palaeoclimatology, Palaeoecology 485, 854-868.

Prader, S., Kotthoff, U., McCarthy, F.M.G., Schmiedl, G., Donders, T.H., Greenwood, D.R., 2018. Plants in movement - Floristic and climatic characterization of the New Jersey hinterland during the Palaeogene-Neogene transition in relation to major glaciation events. Biogeosciences Discussions. doi.org/10.5194/bg-2017-511.

Prebble, J.G., Reichgelt, T., Mildenhall, D.C., Greenwood, D.R., Raine, J.I., Kennedy, E.M., Seebeck, H.C., 2017. Terrestrial climate evolution in the southwest Pacific over the past 30 million years. Earth and Planetary Science Letters 459, 136-144.

Prentice, I.C., Cramer, W., Harrison, S.P., Leemans, R., Monserud, R.A., Solomon, A.M., 1992. Special Paper: A global Biome model based on plant physiology and dominance, soil properties and climate. Journal of Biogeography 19, 117-134.

Price, L.W., Harden, C.P., 2013. Mountain

soils. In: Price, M.F., Byers, A.C., Friend, D.A., Kohler, T., Price, L.W. (Eds.). Mountain Geography - Physical and Human Dimensions. University of California Press, Berkley and Los Angelse 167-182.

Pross, J., Klotz, S., Mosbrugger, V., 2000. Reconstructing palaeotemperatures for the Early and Middle Pleistocene using the mutual climatic range method based on plant fossils. Quaternary Science Reviews 19, 1785-1799.

Pross, J., Klotz, S., 2002. Palaeotemperature calculations from the Praetiglian/Tiglian (Plio-Pleistocene) pollen record of Lieth, northern Germany: Implications for the climatic evolution of NW Europe. Global and Planetary Change 34, 253-267.

Pross, J., Contreras, L., Bijl, P.K., Greenwood, D.R., Bohaty, S.M., Schouten, S., Bendle, J.A., Rohl, U., Tauxe, L., Raine, J.I., Huck, C.E., van de Flierdt, T., Jamieson, S.S.R., Stickley, C.E., van de Schootbrugge, B., Escutia, C., Brinkhuis, H., 2012. Persistent near-tropical warmth on the Antarctic continent during the early Eocene epoch. Nature 488, 73-77.

Prothero, D.R., Heaton, T.H., 1996. Faunal stability during the early Oligocene climatic crash. Palaeogeography, Palaeoclimatology, Palaeoecology 127, 257-283.

Quijtaal, W., Donders, T.H., Persico, D., Louwye, S., 2014. Characterising the middle Eocene Mi-events in the Eastern North Atlantic realm: A first high-resolution marine palynological record from the Porcupine Basin. Palaeogeography, Palaeoclimatology, Palaeoecology 399, 140-159.

Rachele, L.D., 1976. Palynology of the legler lignite: A deposit in the Tertiary Cohansey Formation of New Jersey, USA. Review of Palaeobotany and Palynology 22, 225-252.

Reichgelt, T., Kennedy, E. M., Mildenhall, D.C., Conran, J G., Greenwood, D.R., Lee, D.E., 2013. Quantitative palaeoclimate estimates for Early Miocene southern New Zealand: evidence from Foulden Maar, Palaeogeography, Palaeoclimatology, Palaeoecology 378, 36-44.

Retallack, G.J., Orr, W.N., Prothero, D.R., Duncan, R.A., Kester, P.R., Ambers, C.P., 2004. Eocene-Oligocene extinction and paleoclimatic change near Eugene, Oregon. Geological Society of America Bulletin 116, 817-839.

Rich, F.J., Pirkle, F.L., Arenberg E., 2002. Palynology and paleoecology of strata associated with the Ohoopee River dune field, Emanuel County, Georgia. Palynology 26, 239-256.

Roth-Nebelsick, A., Oehm, C., Grein, M., Utescher, T., Kunzmann, L., Friedrich, J.-P., Konrad W., 2014. Stomatal density and index data of *Platanus neptuni* leaf fossils and their evaluation as a CO_2 proxy for the Oligocene. Review of Palaeobotany and Palynology 206, 1-9.

Scher, H.D., Martin, E.E., 2006. Timing and climatic consequences of the opening of Drake Passage. Science 312, 428-430.

Schlitzer, R., 2011. Ocean Data View, http://odv.awi.de.

Scotese, C.R., Gahagan, L.M., Larson, R.L., 1988. Plate tectonic reconstructions of the Cretaceous and Cenozoic ocean basins. Tectonophysics 155, 27-48.

Shackleton, N.J., Kennett, J.P., 1975. Paleotemperature history oft he Cenozoic and initiation of Antarctic glaciation: Oxygen and carbon isotopic analyses in DSDP sites 277, 279, and 281. In: Kennet, J.P., Houtz, R.E., et al., (Eds.). Initial reports of the Deep Sea Drilling Project 29. Washington, D.C., U.S. Government Printing Office, 743-755.

Shevenell, A.E., Kennett, J.P., Lea, D.W., 2004. Middle Miocene Southern Ocean cooling and Antarctic cryosphere expansion. Science 305, 1766-1770.

Shevenell, A.E., Kennett, J.P., Lea, D.W., 2008. Middle Miocene ice sheet dynamics, deep-sea temperatures, and carbon cycling:

A Southern Ocean perspective. Geochemistry, Geophysics, Geosystems 9, Q02006, doi:10.1029/2007GC001736.

Schrepfer, H., 1925. Die Kontinentalität des deutschen Klimas. Petermanns Geographische Mitteilungen 71, 49-51.

Spellerberg, I.F., Fedor, P.J., 2003. A tribute to Claude Shannon (1916-2001) and a plea for more rigorous use of species richness, species diversity and the 'Shannon-Wiener' Index. Global Ecology and Biogeography 12, 177-179.

Sperry, J.S., Hacke, U.G., Pittermann, J., 2006. Size and function in conifer tracheids and angiosperm vessels. American Journal of Botany 93, 1490-1500.

Spicer, R.A., Chapman, J.L., 1990. Climate change and the evolution of high-latitude terrestrial vegetation and floras. Trends in Ecology and Evolution 5, 279-284.

Stockmarr, J., 1971. Tablets with spores used in absolute pollen analysis. Pollen et Spores 13, 615-621.

Strömberg, C.A.E., 2005. Decoupled taxonomic radiation and ecological expansion of open-habitat grasses in the Cenozoic of North America. Proceeding of the National Academy of Sciene 102, 11980-11984.

Stults, D.Z., Axsmith, B.J., Liu, Y.-S., 2010. Evidence of white pine (*Pinus* subgenus *Strobus*) dominance from the Pliocene northeastern Gulf of Mexico coastal plain. Palaeogeography, Palaeoclimatology, Palaeoecology 287, 95-100.

Sun, Q.-G., Collinson, M.E., Li, C.-S., Wang, Y.-F., Beerling, D.J., 2002. Quantitative reconstruction of palaeoclimate from the Middle Miocene Shanwang flora, eastern China. Palaeogeography, Palaeoclimatology, Palaeoecology 180, 315-329.

Taylor, L.L., Leake, J.R., Quirk, J., Hardy, K., Banwart, S.A., Beerling, D.J., 2009. Biological weathering and the long-term carbon cycle: Integrating mycorrhizal evolution and function into the current paradigm. Geobiology 7, 171-191.

Thompson, R.S., Anderson, K.H., Bartlein, P.J., Smith, S.A., 1999. Atlas of relations between climatic parameters and distributions of important trees and shrubs in North America. U.S. Geological Survey Professional Paper 1650 A and B. http://pubs.usgs.gov/pp/p1650-a/; last access: December 1999.

Thompson, R.S., Anderson, K.H., Bartlein, P.J., 2000a. Atlas of relations between climatic parameters and distributions of important trees and shrubs in North America: Hardwoods. U.S. Geological Survey Professional Paper 1650 B, 423 pp.

Thompson, R.S., Anderson, K.H., Bartlein, P.J., Smith, S.A., 2000b. Atlas of relations between climatic parameters and distributions of important trees and shrubs in North America: additional conifers, hardwoods, and monocots. U.S. Geological Survey Professional Paper 1650 C, 386 pp.

Thompson, R.S., Anderson, K.H., Strickland, L.E., Shafer, S.L., Pelltier, R.T., Bartlein, P.J., 2006. Atlas of relations between climatic parameters and distributions of important trees and shrubs in North America-Alaska species and ecoregions. U.S. Geological Survey Professional Paper 1650-D, 342 pp.

Thompson, R.S., Anderson, K.H., Pelltier, R.T., Strickland, L.E., Bartlein, P.J., Shafer, S.L., 2012. Quantitative estimation of climatic parameters from vegetation data in North America by the mutual climatic range technique. Journal of Quaternary Science 51, 18-39.

Tiffney, B.H., 1994. Re-evaluation of the age of the Brandon Lignite (Vermont, USA) based on plant megafossils. Review of Palaeobotany and Palynology 82, 299-315.

Tiffney, B.H., Manchester, S.R., 2001. The use of geological and paleontological evidence in evaluating plant phylogeographic hypotheses in the Northern Hemisphere Tertiary. International Journal of Plant

Sciences 162, 3-17.

Townsend, P.A., Walsh, S.J., 2001. Remote sensing of forested wetlands: Application of multitemporal and multispectral satellite imagery to determine plant community composition and structure in southeastern USA. Plant Ecology 157, 129-149.

Traverse, A., 1994. Palynofloral geochronology of the Brandon Lignite of Vermont, USA. Review of Palaeobotany and Palynology 82, 265-297.

Traverse, A., 2008. Paleopalynology. In: Landman, N.H., Jones, D.S., (Eds.). Topics of Geobiology. 28, Springer, Dordrecht, 813 pp.

Tzedakis, P.C., McManus, J.F., Hooghiemstra, H., Oppo, D.W., Wijmstra, T.A., 2003. Comparison of changes in vegetation in northeast Greece with records of climate variability on orbital and suborbital frequencies over the last 450 000 years. Earth and Planetary Science Letters 212, 197-212.

US Climate Data (2017). https://www.usclimatedata.com; accessed November 2017, January 2018.

Utescher, T., Ivanov, D., Harzhauser, M., Bozukov, V., Ashraf, A.R., Rolf, C., Urbat, M., Mosbrugger, V., 2009. Cyclic climate and vegetation change in the Late Miocene of Western Bulgaria. Palaeogeography, Palaeoclimatology, Palaeoecology 272, 99-114.

Utescher, T., Djordjevic-Milutinovic, D., Bruch, A., Mosbrugger, V., 2007. Palaeoclimate and vegetation change in Serbia during the last 30 Ma. Palaeogeography, Palaeoclimatology, Palaeoecology 253, 141-152.

Utescher, T., Bruch, A.A., Erdei, B., François, L., Ivanov, D., Jacques, F.M.B., Kern, A.K., Liu, Y.S., Mosbrugger, V., Spicer, R.A., 2014. The Coexistence Approach-Theoretical background and practical considerations of using plant fossils for climate quantification. Palaeogeography, Palaeoclimatology, Palaeoecology 410, 58-73.

Utescher, T., Bondarenko, O. V., Mosbrugger, V., 2015. The Cenozoic Cooling - continental signals from the Atlantic and Pacific side of Eurasia. Earth Planetary Science Letters 415, 121-133.

van Dam, J.A., Abdul Aziz, H., Ángeles Álvarez Sierra, M., Hilgen, F.J., van den Hoek Ostende, L.W., Lourens, L.J., Mein, P., van der Meulen, A.J., Pelaez-Campomanes, P., 2006. Long-period astronomical forcing of mammal turnover. Nature 443, 687.

van der Kaars, S., 2001. Pollen distribution in marine sediments from the south-eastern Indonesian waters. Palaeogeography, Palaeoclimatology, Palaeoecology 171, 341-361.

Velitzelos, D., Bouchal, J.M., Denk, T., 2014. Review of the Cenozoic floras and vegetation of Greece. Review of Palaeobotany and Palynology 204, 56-117.

van Dam, J.A., Abdul Aziz, H., Ángeles Álvarez Sierra, M., Hilgen, F.J., van den Hoek Ostende, L.W., Lourens, L.J., Mein, P., van der Meulen, A.J., Pelaez-Campomanes, P., 2006. Long-period astronomical forcing of mammal turnover. Nature 443, 687.

von der Heydt, A., Dijkstra, H.A., 2006. Effect of ocean gateways on the global ocean circulation in the late Oligocene and early Miocene. Paleoceanography 21, PA1011, doi:10.1029/2005PA001149.

Wade, B.S., Pälike, H., 2004. Oligocene climate dynamics. Paleoceanography 19, doi:10.1029/2004PA001042.

Walther, H., 2000. Floristic relationship between North and Central America and Europe in the Eocene. Acta Universitatis Carolinae Geologica 44, 51-57.

Wen, J., 1999. Evolution of eastern Asian and eastern North American disjunct distributions in flowering plants. Annual Review of Ecology and Systematics 30, 421-455.

White, J.M., Ager, T.A., Adam, D.P., Leopold, E.B., Liu, G., Jetté, H., Schweger, C.E., 1997. An 18 million year record of vegetation and climate change in northwestern Canada and Alaska: Tectonic and global climatic corre-

lates. Palaeogeography, Palaeoclimatology, Palaeoecology 130, 293-306.

Williams, J.W., Jackson, S.T., 2007. Novel climates, no-analog communities, and ecological surprises. Frontiers in Ecology and the Environment 5, 475-482.

Williams, C.J., Mendell, E.K., Murphy, J., Court, W.M., Johnson, A.H., Richter, S.L., 2008. Paleoenvironmental reconstruction of a Middle Miocene forest from the western Canadian Arctic. Palaeogeography, Palaeoclimatology, Palaeoecology 261, 160-176.

Williams, J.W.B., Shuman, P.J., Bartlein, J., Whitmore, K., Gajewski, M., Sawada, T., Minckley, S., Shafer, A.E., Viau, T., Webb, III, P. M., Anderson, L.B., Brubaker, C., Whitlock, O.K. Davis., 2006. An Atlas of Pollen-Vegetation-Climate Relationships for the United States and Canada. American Association of Stratigraphic Palynologists Foundation, Dallas, Texas, 293 pp.

Willis, K.J., McElwain, J.C., 2002. The Evolution of Plants. Oxford University Press, Oxford-New York, 392 pp.

Wing, S.L., 1998. Tertiary vegetation of North America as a context for mammalian evolution. In: Janis, C.M., Schott, K.M., Jacobs, L.L., (Eds.). Evolution of Tertiary mammals of North America. Cambridge University Press, Cambridge 37-65.

Wolfe, J.A., Schorn, H.E., 1989. Paleoecologic, paleoclimatic, and evolutionary significance of the Oligocene Creede flora, Colorado. Paleobiology 15, 180-198.

Wolfe, J.A., Schorn, H.E., 1990. Taxonomic revision of the Spermatopsida of the Oligocene Creede Flora, Southern Colorado. U.S. Geological Survey Bulletin 1923, 40 pp.

Wolfe, J.A., 1992. Climatic, floristic, and vegetational changes near the Eocene/Oligocene boundary in North America. In: Prothero, D. A., Bergren, W.A., (Eds.). Eocene-Oligocene Climatic and Biotic Evolution. Princeton University Press, Princeton, New Jersey, 421-436.

Wolfe, J.A., 1994. Cenozoic climate and paleogeographic changes in the Pacific region - An analysis of Neogene climates in Beringia. Palaeogeography, Palaeoclimatology, Palaeoecology 108, 207-216.

Worldclim: Global weather stations. http.// www.worldclim.org, last access: May 2012.

Woodward, F.I., Williams, B.G., 1987. Climate and plant distribution at global and local scales. Vegetatio 69, 189-197.

Woodward, F.I., 1990. The impact of low temperatures in controlling the geographical distribution of plants. Philosophical Transactions of the Royal Society of London. B, Biological Sciences 326, 585-593.

Wright, J.D., Miller, K.G., Fairbanks, R.G., 1992. Early and Middle Miocene stable isotopes: Implications for deepwater circulation and climate. Paleoceanography 7, 357-389.

Yang, J., Wang, Y.-F., Spicer, R.A., Mosbrugger, V., Li, C.-S., Sun, Q.-G., 2007. Climatic reconstruction at the Miocene Shanwang basin, China, using leaf margin analysis, CLAMP, coexistence approach, and overlapping distribution analysis. American Journal of Botany 94, 599-608.

Zachos, J., Pagani, M., Sloan, L., Thomas, E., Billups, K., 2001a. Trends, rhythms, and aberrations in global climate 65 Ma to present. Science 292, 686-693.

Zachos, J.C., Shackleton, N.J., Revenaugh, J.S., Pälike, H.B., Flower, B.P., 2001b. Climate response to orbital forcing across the Oligocene-Miocene boundary. Science 292, 274-278.

Zachos, J.C., Dickens, G.R., Zeebe, R.E., 2008. An early Cenozoic perspective on greenhouse warming and carbon-cycle dynamics. Nature 451, 279-283.

Zanazzi, A., Kohn, M.J., MacFadden, B.J., Terry, D.O., 2007. Large temperature drop across the Eocene-Oligocene transition in central North America. Nature 445, 639-642.

Zetter, R., Ferguson, D.K., 2001. Trapaceae pollen in the Cenozoic. Acta Palaeobotanica 41, 321-339.

Zhang, J.-B., Li, R.-Q., Xiang, X.-G., Manchester, S.R., Lin, L., Wang, W., Wen, J., Chen, Z.-D., 2013. Integrated fossil and molecular data reveal the biogeographic diversification of the eastern Asian-eastern North American disjunct Hickory genus (*Carya* Nutt.) Plos One 8, e70449. doi:10.1371/journal.pone.0070449.

Zonneveld, K.A.F., Versteegh, G.J.M., Kasten, S., Eglinton, T.I., Emeis, K.C., Huguet, C., Koch, B.P., de Lange, G.J., de Leeuw, J.W., Middelburg, J.J., Mollenhauer, G., Prahl, F.G., Rethemeyer, J., Wakeham, S.G., 2010. Selective preservation of organic matter in marine environments; processes and impact on the sedimentary record. Biogeosciences 7, 483-511.

Dankeschön

Großen Dank an meinen Supervisor Ulrich Kotthoff für seine Betreuung und das Vertrauen, das er mir schenkte, die vorliegende Arbeit wissenschaftlich zu bearbeiten. Wir führten viele Diskussionen, laute und weniger laute, wissenschaftliche und von privater Natur, rückblickend alle sehr konstruktiv. Vielen Dank!

Meinem Co-Supervisor Gerhard Schmiedl möchte ich ebenfalls für seine Unterstützung und Ratschläge herzlichst danken.

Bedanken möchte ich mich auch bei den gesamten Co-Autoren, die mir mit ihren kritischen Gedanken und ihrer fachlichen Unterstützung tatkräftig zur Seite standen.

Francine McCarthy möchte ich herzlichst für ihre Offenheit danken und dafür, dass sie mich während meiner Aufenthalte in Kanada bewirtet hat. Ich bedanke mich bei ihr sowie auch bei Marin Head, welche mir die sonderbare Welt der Dinoflagellaten näher brachten, bei David Greenwood, der mich die Anwendung seiner Bioklimatischen Analyse lehrte.

Einen besonderen Dank auch an Marc Theodor und Renate Walter für die aufregende und schöne Zeit am REM.
An dieser Stelle möchte ich mich auch ganz herzlich bei Marilena Finotti für ihre fachliche Unterstützung, diese Arbeit in ein vorzeigbares Format zu überführen, bedanken, sowie bei Manuel Irsara und Felix Schneeberger fürs Korrekturlesen.

Die Menschen meines Lebensumfelds wissen, dass ich in den letzten Jahren durch sehr dunkle Täler wanderte. Wenn man selbst nicht so genau weiß, wer man ist, ist es schön Vertrauen und Menschen zu haben, die einem stützend die Hand geben. Ganz besonders möchte ich hier Ole Valk danken, der sich liebevoll und fürsorglich um mich kümmerte und natürlich auch meiner Familie.

Besonders sei auch Fabian Pompecki und Paul Kowalski gedankt, welche mir in einer sehr schwierigen Zeit eine emotionale Stütze waren.

Es sei auch der gesamten mikropaläonthologischen AG herzlichst für ihr Verständnis und ihre Unterstützung gedankt. Die Vogelexkursion war super.
Lydia Baumann danke auch dir.

Ich bedanke mich für die wunderbaren Momente, die ich mit liebgewonnen, neuen und langjährigen Freunden, Arbeitskollegen, meinem Freund und meiner Familie erleben durfte.

Danke für die Schokokuchenstücke, Ulrich!

Eidesstattliche Versicherung

Declaration on oath

Hiermit erkläre ich an Eides statt, dass die vorliegende Dissertationsschrift von mir selbst verfasst wurde und ich keine anderen als die angegebenen Quellen und Hilfsmittel benutzt habe.

I hereby declare, on oath, that I have written the present dissertation by my own and have not usedother than the acknowledged resources and aids.

Hamburg, den